The effect of 1,25-dihydroxyvitamin D_3 on methylation and expression of the human renin gene by

Daniesha Govender

(1102301)

Dissertation

Submitted in fulfilment of the requirements for the degree

Master of Science

in

Molecular and Cell Biology

in the Faculty of Science, University of the Witwatersrand, Johannesburg, South Africa

Supervisor: Dr Vanessa Meyer

June 2022

Declaration

I, **Daniesha Govender (1102301)**, am a student registered for the degree of **Master of Science** in the academic year **2022**.

I hereby declare the following:

- I am aware that plagiarism (the use of someone else's work without their permission and/or without acknowledging the original source) is wrong.
- I confirm that the work submitted for assessment for the above degree is my own unaided work except where explicitly indicated otherwise and acknowledged. In this context, I understand that the use of editing services is considered aided work and must be declared.
- I have not submitted this work before for any other degree or examination at this or any other University.
- The information used in the Dissertation **HAS NOT** been obtained by me while employed by, or working under the aegis of, any person or organisation other than the University.
- I have followed the required conventions in referencing the thoughts and ideas of others.
- I understand that the University of the Witwatersrand may take disciplinary action against me if there is a belief that this is not my own unaided work or that I have failed to acknowledge the source of the ideas or words in my writing.

_____

Daniesha Govender (1102301)

Date: **8 June 2022**

Preface

The renin-angiotensin-aldosterone system (RAAS) is a well-established physiological pathway that regulates blood pressure in humans. The maintenance of this pathway is critical in regulating blood pressure homeostasis as dysregulated and inappropriate expression of proteins in the RAAS can lead to raised blood pressure and subsequent hypertension development. Globally, cardiovascular disease (CVD) accounts for the largest portion of premature death. One of the major risk factors for CVD is hypertension. In a South African context, 54% of the population are diagnosed with the disease, which often goes untreated. Thus, it is a growing public health concern. The rate-limiting factor in the RAAS is renin, which is encoded by the *REN* gene. *REN* was thus selected for analysis as it plays an essential role in blood pressure homeostasis. Renin is an aspartic protease enzyme that facilitates a cleavage reaction that is significant for RAAS signalling. This research is a component of a larger project which aimed to fully annotate *REN* in order to understand the combined effect of both genetic, epigenetic and environmental factors which may be associated with hypertension susceptibility and progression. Research regarding *REN* is largely limited with respect to epigenetics and full characterisation of the gene and its integral regulatory components are incomplete, as most hypertension studies focus on the effector angiotensin II (Ang II) as well as the angiotensin converting enzyme (ACE). Major objectives of the project included a complete annotation and characterisation of *REN* which was done with the use of a bioinformatic workflow which provided an *in sillico* representation of *REN* highlighting genetic and epigenetic regions which may have a functional role in *REN* regulation. The next objective, which was conducted in this study, was to experimentally validate the functional relevance of the annotated regions with an *in vitro* analysis to both validate the bioinformatic workflow, as well as assess the effect of vitamin D on *REN* regulation and subsequent hypertension susceptibility. The bioinformatic workflow and *in sillico* analysis was performed by Lidijia Damjanovic (Table i). Fully defining the genetic and epigenetic overlap in *REN* regulation may inform health and therapeutic treatments to effectively target and treat hypertension, which poses both a health and economic concern in South Africa.

Table i: Techniques performed by Daniesha Govender and Colleagues

Technique	Done by
Execution of bioinformatic workflow	Lidija Damjanović [a]
In silico characterisation and annotation of *REN*	Lidija Damjanović
Development and use of a custom scoring system	Lidija Damjanović
HEK293 culture and vitamin D treatment	Daniesha Govender
VDR knockdown via siRNA transfection	Daniesha Govender
VDR protein quantification via flow-cytometry	Daniesha Govender
DNA extraction and quantification	Daniesha Govender
DNA methylation analysis	Inqaba Biotech[b]
RNA extraction and RT-qPCR	Daniesha Govender
Identification of VDR binding sites in TETs	Daniesha Govender
Identification of TFBS in *REN* CGIs	Lidija Damjanović
Mapping of TFBS in *REN* CGIs	Daniesha Govender

[a]MSc Dissertation (April 2020): *In silico* characterization of the human renin gene for the selection of functionally relevant regions of epigenetic control.
[b]DNA methylation analysis was outsourced to Inqaba Biotech.

Presentations and awards arising from research:

1. 11th annual Cross-faculty Wits Post-graduate symposium on 12th October 2020– *Geneenvironment interaction: Vitamin D, Renin and Hypertension.* Placed 4th in the Gradflash category
2. Wits Molecular Biosciences Research Thrust (MBRT) Virtual Postgraduate Research Day on 9th December 2021 – *The effect of 1,25-dihydroxyvitamin D_3 on methylation and expression of the human renin gene.* Won first prize for the best grad-flash presentation.

Publications arising from research:

Govender, D., Damjanovic, L., Gaza, C. A. and Meyer, V. (2021) Vitamin D decreases silencer methylation to downregulate renin gene expression, *Gene*, 786, p. 145623. doi: 10.1016/j.gene.2021.145623.

Acknowledgments

I would like to acknowledge the National Research Foundation for funding this project via the Thuthuka grant to Vanessa Meyer (Grant No. 118133).

To Dr Meyer, I don't even know where to start. I will forever be grateful for the opportunity you have given me. I remember sitting in presentation room in my Honour's year when you pitched your work to the students. You have always been passionate about your work and that is what drew me to your lab. You were kind enough to allow me to take part in your research and explore the full extent of Vitamin D in all its glory. The past three years have been challenging but it was made easier with your guidance and encouragement. You have shown me that I am capable of achieving anything with just the right amount of effort and support. Never in a million years did I think I would co-author a research publication. I am forever indebted to you for allowing me to see your ideas through and be a part of your Vitamin D journey. The lab techniques are just a small layer of the wealth of knowledge you have given me. In a world of intimidating and often discouraging academic superiors, you are a ray of sunshine! You gave me just enough room to grow but never failed to provide guidance in a way that has always been encouraging and thoughtful. There is not a single time I couldn't count on you as you always make your student's a priority even when you undeniably deserve a break. No words can describe the extent of my appreciation and gratitude for you. You truly are a role model to me. I am continuously in awe of your numerous abilities, a teacher, a mother, a friend and most importantly a mentor. You are a living, breathing wonder woman and I hope to one day achieve as much as you have so early in your life. THANK YOU! For your time, energy, patience, and consideration.

To Dr Gentle, thank you for your brutal but necessary honesty. You push me and everyone in the lab to think differently and most importantly be critical in our research.

To my amazing colleagues in GH514 and FunGenics, you have made this daunting journey fun. To Shuaib, we started this together and by supporting each other through self-doubt and repeated failed RNA extractions, we finally made it! To Darisia, the person who I can always count on to help me with anything at any time, watching all your accomplishments and progress in your work has inspired me to work harder and most importantly push myself to

achieve more. Thank you for all our pep talks and offering me your ears to vent. To Lidijia and Jinsi, thank you for all your work towards this project and offering your expertise at times when I was lost in either literature or lab work. To Kuda, you were the first person I met in the lab and helped me navigate my way around until I was confident enough to tackle experiments on my own. You are such a kind-hearted soul who is always willing and eager to help anyone in need. To my GH514 girls, Suheena, Almaaz and Bronwyn, I am so fortunate to have met you all. You know all too well how frustrated I can get when things go wrong and you have all been there to not only console me but remind me to chill and tackle each problem as it comes. I will always cherish our hilarious moments in the lab. If we can make it through *Mycoplasma* contamination, multiple equipment failures, wild birds and a whole flood, we can make it through anything!

I would like to thank my family for pushing me to further my academic career and offering me the opportunity to not only get a tertiary degree but also further pursue my academic career in research. To my father and brother for driving me back and forth to the lab even on weekends to keep my cells alive and to my mother for always supporting me when I doubted myself. Your encouragement and love have allowed me to reach this point.

Lastly to my dearest Nabeelah, we both started this post-graduate journey together and you have always been supportive of my academic career. Thank you for your reassurance and love.

Table of Contents

List of abbreviations

$1,25(OH)_2D_3$	1,25-dihydroxivitamin D_3
$25(OH)D_3$	25-hydroxivitamin D_3
%KD	Percentage knockdown
ACE	Angiotensin converting enzyme
ACEI	Angiotensin converting enzyme inhibitor
Ang I	Angiotensin one
Ang II	Angiotensin two
ARB	Angiotensin receptor blockers
AT_1	Angiotensin II type 1
AT_2	Angiotensin II type 2
BCa	Breast carcinoma
BLAT	BLAST-Like Alignment Tool
CGI	CpG island
CHIP-seq	chromatin immunoprecipitation sequencing
CpG	Cytosine phosphate Guanine
CREB	cAMP response element binding protein
CTCF	CCCTC-binding factor
CVD	Cardiovascular disease
DAP-seq	DNA affinity purification sequencing
DNA	Deoxyribonucleic acid
DNase	Deoxyribonuclease 1

DMEM	Dulbecco's Modified Eagle Medium
DNMT	DNA methyl transferase
EDTA	Ethylenediaminetetra-acetic acid
ELISA	Enzyme-linked immunosorbent assay
ENCODE	Encyclopaedia of DNA Elements
FI	Fluorescence intensity
HDAC	Histone deacytelase
HDM	Histone demethylase
HEK293	Human embryonic kidney 293
HTSELEX	High-throughput systematic evolution of ligands by exponential enrichment
MALDI-TOF	Matrix-assisted laser desorption/ionisation- time of flight
MS	Mass spectrometry
NCBI	National Center for Biotechnology Information
NCD	Non-communicable disease
PFM	Position frequency matrix
PTH	Parathyroid hormone
qPCR	Quantitative polymerase chain reaction
RAAS	Renin angiotensin aldosterone system
RNA	Ribonucleic acid
RNase	Ribonuclease
RT-qPCR	Reverse transcriptase quantitative polymerase chain reaction
RXR	Retinoic acid X receptor
SAP	Shrimp alkaline phosphatase

SMiLE-seq	Selective microfluidics-based ligand enrichment sequencing
siRNA	Small-interfering RNA
TAD	Topologically associated domain
TET	Ten-eleven translocation dioxygenase
TF	Transcription factor
TFBS	Transcription factor binding site
UCSC	University of California, Santa Cruz
UV	Ultraviolet
UVB	Ultraviolet beta ray
VDR	Vitamin D receptor
VDRE	Vitamin D response element
WHO	World Health Organisation
YY1	Yin Yang 1
ZTRE	Zinc transcriptional regulatory element

List of Figures

List of Tables

Abstract

Blood pressure has long been associated with vitamin D suggesting a link between vitamin D deficiency and hypertension progression. Renin, encoded by the *REN* gene, is an essential enzyme in the renin-angiotensin-aldosterone system (RAAS) which is responsible for the maintenance of blood pressure homeostasis. The active metabolite of vitamin D, 1,25dihydroxyvitamin D_3 ($1,25(OH)_2D_3$) mediates almost all its functions when bound to its nuclear receptor, the vitamin D receptor (VDR). Transcriptional regulation of *REN* has been linked to enhancer-promoter crosstalk, cAMP response element-binding protein (CREB), $1,25(OH)_2D_3$-bound VDR and a less well-characterised intronic silencer element. We therefore hypothesised that differential DNA methylation affects *REN* expression and influenced by $1,25(OH)_2D_3$. A *VDR* $^+$ and *VDR* $^-$ HEK293 cell culture model, which readily expressed *REN*, was established, and used to elucidate the effect of $1,25(OH)_2D_3$ on *REN* methylation and expression, as quantified by matrix-assisted laser desorption ionisation- time of flight mass spectrometry (MALDI-TOF MS) and reverse transcriptase-quantitative polymerase chain reaction (RT-qPCR), respectively. *In vitro* $1,25(OH)_2D_3$ supplementation (10 nM) induced changes in DNA methylation within the *REN* enhancer and silencer regions, which was coupled to a significant reduction in *REN* expression ($P < 0.010$) in the *VDR* $^+$ samples. In addition, $1,25(OH)_2D_3$ increased the expression of *VDR* ($P < 0.050$), and that of the ten-eleven translocation enzyme encoding genes, *TET1* ($P < 0.050$) and *TET2* ($P < 0.050$); responsible for DNA demethylation. The induced expression of both *VDR* and the demethylating agents, *TET1* and *TET2,* suggest that $1,25(OH)_2D_3$ may induce active loci specific demethylation events at the *REN* silencer. Thus, it appears that both the enhancer and silencer elements are regulated by DNA methylation, which is influenced by $1,25(OH)_2D_3$, and play an essential role in regulating *REN* expression.

1.1 Hypertension

The force exerted against the blood vessel walls by blood in circulation is known as blood pressure. Blood pressure values are usually given as a combination of the maximum (systolic) and minimum (diastolic) arterial pressures. Systolic pressure denotes the blood pressure during the heart contraction and the diastolic pressure indicates the blood pressure between two contractions or heart relaxation. Persistently high blood pressure or hypertension is generally characterised as a systolic blood pressure that is greater than 130 mmHg and/or a diastolic blood pressure greater than or equal to 90 mmHg (American Heart Association, 2017). The severity of increased blood pressure is based on the combination of systolic and diastolic blood pressure and can be grouped (Table 1.1). Very often the increase in blood pressure will have detrimental effects on vital organs including the heart (Berkin and Ball, 2001), lungs (Southgate et al., 2020) and kidneys (Bidani et al., 2004), thus leading to severe health complications including hypertrophy of cardiac muscle, stroke, heart failure and premature death (WHO, 2019). Although a major contributor to cardiovascular disease (CVD), hypertension is still a modifiable risk factor. The heterogeneous disease has various aetiologies with several interacting environmental and genetic factors (Patel et al., 2017). Hypertension falls into two categories, primary (essential) and secondary hypertension. Most patients (90 – 95%) fall under the primary hypertension group which has no known underlying cause (Zhang and Moran, 2017). Substantial clinical data has reported significant cardiovascular risks associated with raised blood pressure which are mostly subject to the interplay between genetics and the cellular environment (Biino et al., 2013; Hollenberg, 2001; Kazmi et al., 2020; Knight et al., 2009; Robinson et al., 2005). Over the last several years genome-wide association studies (GWASs) and sequencing methods have identified countless potential blood pressure–associated pathways, however the associations between these related pathways and hypertension are inconsistent and rare (The International Consortium of Blood Pressure (ICBP) 1000G Analyses et al., 2017; Zheng et al., 2015). Hypertension, which is a major preventable risk factor attributing to CVD related premature death, poses a serious global health concern due to its increasing prevalence. The greatest burden of premature deaths as a result of non-communicable diseases (NCDs) is faced by low to middle- income countries like South Africa (World Health Organization, 2018).

Table 1. 1: Blood pressure ranges from normal to hypertensive states with respect to systolic and diastolic pressure.

Low Blood Pressure Range

Systolic pressure (mm Hg)	Diastolic pressure (mm Hg)	Pressure Range
90	60	Borderline Low blood Pressure
60	40	Too Low Blood Pressure
50	33	Dangerously Low Blood Pressure

Normal Blood Pressure Range

Systolic pressure (mm Hg)	Diastolic pressure (mm Hg)	Pressure Range
130	85	High Normal Blood Pressure
120	80	Normal Blood Pressure
110	75	Low Normal Blood Pressure

High Blood Pressure Range

Systolic pressure (mm Hg)	Diastolic pressure (mm Hg)	Stages of High Blood Pressure
210	120	Stage 4
180	110	Stage 3
160	100	Stage 2
140	90	Stage 1

1.2 Prevalence and statistics

Hypertension is the foremost contributing factor of CVD progression. Globally, premature death associated with CVD is approximated to be around 17 million deaths a year which is a third of the total (WHO, 2019). Hypertension accounts for roughly half of the deaths associated with heart disease and stroke (Lloyd-Sherlock et al., 2014). An estimated 1.13 billion people worldwide are diagnosed with hypertension yet only 1 in 5 hypertensives are effectively treated for the disease making it a major cause of premature death (WHO, 2019). A global target for NCDs was set to reduce the prevalence of hypertension by 25% by the year 2025 (2010 Baseline; WHO, 2019). Since the implementation of the Global Hearts Initiative in 2016, up to 24 countries have presented interest in joining the initiative which may be coupled to several notable reductions in CVD related diseases (Martinez et al., .2020). Due to the use of hypertensive medications, global BP levels have either remained constant or decreased however, the prevalence has increased (Mills et al., 2020). In a South African context, blood pressure control is poor. By 2025, it is predicted that the number of hypertensives will rise by roughly 60% to a total of 1.56 billion, mainly in developing countries (Kearney et al., 2005). With respect to SubSaharan Africa, the greatest hypertension prevalence is in South Africa (Gómez-Olivé et al., 2017). It is estimated that only 21% of male and 36% of female South Africans suffering from hypertension take treatment in the form prescription medication to control their blood pressure (Rayner, 2010). In South Africa 91.1% of hypertensive patients go undetected, are not properly diagnosed, and do not control or take treatment for the disease thus creating a serious need for hypertension healthcare (Berry et al., 2017). In response to the increasing affliction of non-communicable diseases, a target was set by the South African government aimed at reducing the prevalence of hypertensive patients by 20% in the year 2020, through improved medical care and lifestyle changes (Wandai et al., 2020).

1.3 Renin-angiotensin-aldosterone system

Physiologically, blood pressure is maintained by the renin-angiotensin-aldosterone system (RAAS). The RAAS (Fig. 1.1) is an essential endocrine system which facilitates blood pressure regulation and fluid balance. The three major hormones in this system are renin, angiotensin II (Ang II) and aldosterone. Renin, which was one of the first proteins within this system to be discovered (Tigerstedt et al., 1898), is produced in the kidney via the juxtaglomerular cells

(JGCs) (Persson, 2003) and catalyses the rate-limiting step in the formation of Ang II. RAAS activation begins with the release of renin into the bloodstream. Granular cells of the renal juxtaglomerular apparatus (JGA) will secrete renin in response to low sodium levels, reduced blood flow to the kidneys and sympathetic stimulation of β_1 adrenoreceptors. Once expressed, renin, an aspartyl protease, facilitates the cleavage of the substrate molecule angiotensinogen forming angiotensin I (Ang I). A carboxypeptidase, angiotensin converting enzyme (ACE), then cleaves Ang I to form angiotensin II (Ang II). Ang II is able to bind to either Ang II type 1 receptor (AT_1) or Ang II type 2 receptors (AT_2) which can signal a multitude of effects (Ferrario, 2016; Table 1.2) and is a highly effective vasoconstrictor with antinatriuretic capability (Sigmund, 2002). Ang II localises its effect on the proximal convoluted tubule of the kidney by triggering both the reabsorption of sodium and stimulating the release of aldosterone. Aldosterone will signal the retention of salt and water by increasing the expression of epithelial sodium channels. The collection of sodium in the kidney tissue will reduce water excretion via osmosis resulting in increased blood volume and thus blood pressure. In contrast, the stretching of the atria stimulates the autonomic nervous system (ANS) triggering the release of atrial natriuretic peptide (ANP) which will inhibit renin release. ANP will reduce blood pressure by stimulating excretion of water and sodium by the kidneys resulting in reduced blood volume. ANP triggers the dilation of the afferent arteriole of the glomerulus which will increase glomerular flow rate (GFR) and blood flow thus reducing blood pressure. Although baroreceptors respond to changes in blood pressure, they cannot regulate blood pressure in the long-term which is where the RAAS pathway comes into play. Irregular activation of the RAAS is associated with the development of CVD including hypertension, hypertrophy of cardiac muscle and eventual heart failure (Steckelings et al., 2009).

Renin encoded by the *REN* gene, plays an integral role in this system as it catalyses the rate limiting step in the formation of Ang II. Thus, tight transcriptional control of *REN* is important in understanding hypertension progression and treatment. Despite the immense research and data obtained around RAAS regulation and hypertension, the aetiology of the disease is still not well understood with most studies focusing on Ang II and its receptors excluding the role of renin.

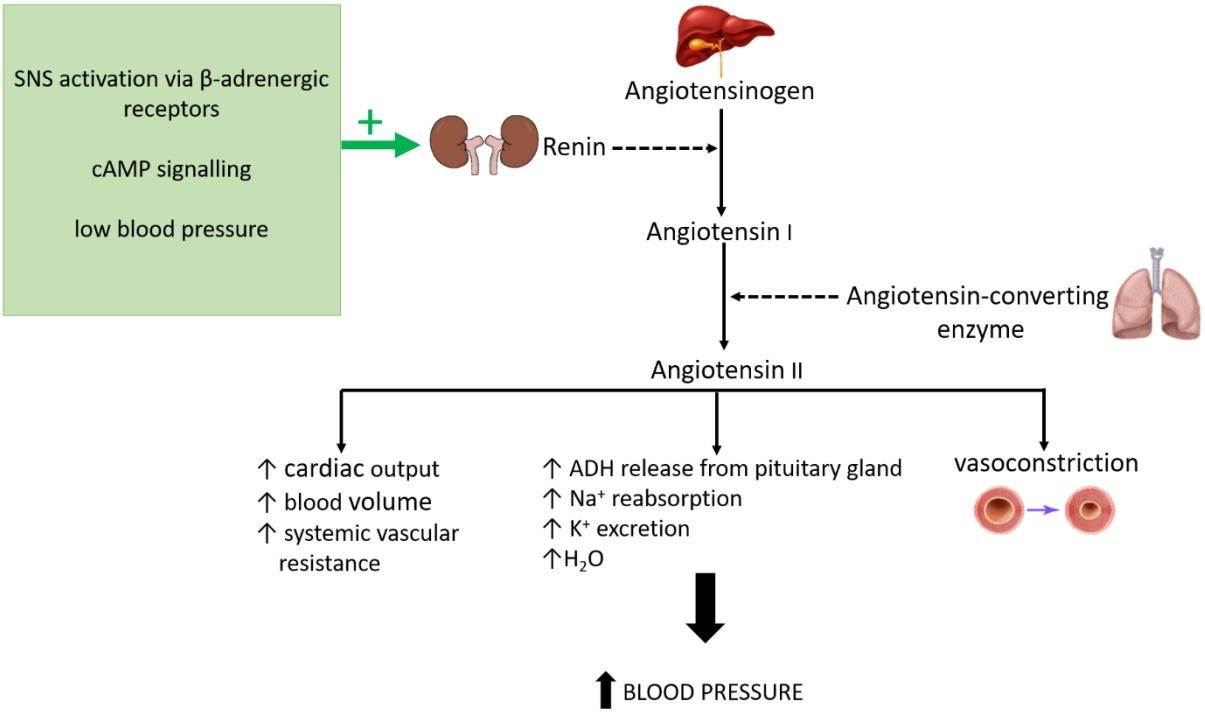

Figure 1.1. Renin-angiotensin-aldosterone system. Angiotensinogen is released from the liver into the blood plasma where it is then cleaved by renin (released by the kidney) to form angiotensin I. Angiotensin I is further cleaved by angiotensin-converting enzyme (released by the lungs) to form angiotensin II. Angiotensin II triggers the release of aldosterone (sodium reabsorption and water retention) and induces vasoconstriction in blood vessels resulting in increased blood pressure (based on Fountain and Lappin, 2019).

Table 1. 2: AT_1 and AT_2-receptor stimulated effects.

Effects of AT_1-receptor stimulation	**Effects of AT_2-receptor stimulation**
• Vasoconstriction	• Inhibition of cell growth
• Sodium retention	• Cell differentiation
• Water retention (vasopressin release)	• Tissue repair
• Renin suppression (negative feedback)	• Apoptosis
• Myocyte and smooth-muscle hypertrophy	• Vasodilation
• Stimulation of vascular and myocardial fibrosis	• Kidney and urinary-tract development
• Activation of sympathetic nervous system	• Protection against ischaemia
• Increase endothelin secretion	

1.4 Hypertension treatment

The rising global prevalence of hypertension has a huge economic impact on public healthcare. Most approaches towards blood pressure control have relied on pharmacological intervention of the RAAS (Fig. 1.2) through the implementation of either ACE inhibitors (inhibiting Ang II formation), AT_1-receptor blockers (ARBs; prevention of Ang II receptor binding) or renin-inhibitors (prevention of renin enzyme activity in Ang II synthesis) as the primary treatment options (Steckelings et al., 2009). However, these treatment options remain palliative and the use of RAAS blockers during pregnancy is reported to have adverse effects on *in utero* fetuses especially during the weeks 14-27 of pregnancy (Lewis et al., 1993; Lonn et al., 1994). Effects of which include, intrauterine growth restriction, reduced amniotic fluid reduction, irregular renal development, oliguria, renal injury, and death (Cragan et al., 2015; Daïkha-Dahmane et al., 2006; Tabacova et al., 2003). Thus, more effective, and safer treatments for hypertension are necessary. In addition, non-pharmacological treatments for management of hypertension are highly recommended. This includes lifestyle changes such as increased exercise, diet and alcohol consumption (Stoll et al., 2018). A diet of reduced sodium intake, increased potassium, or adopting the DASH (Dietary Approaches to Stop Hypertension) diet or a Mediterranean diet are proven to be effective in hypertension prevention (Bazzano et al., 2013).

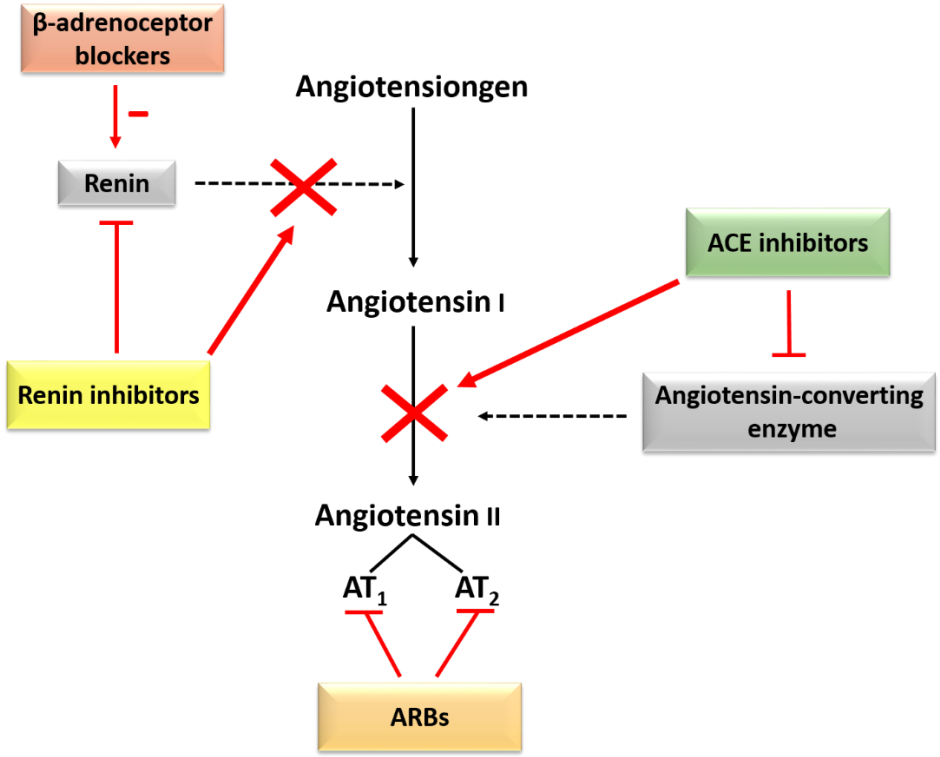

Figure 1.2. Mechanism of action of common therapeutics targeting RAAS. B-adrenoreceptors will inhibit the synthesis and release of renin triggered by sympathetic nervous system (SNS) activation while renin inhibitors will inhibit renin activity thus stopping the conversion of angiotensinogen to angiotensin I. Angiotensin-converting enzyme (ACE) inhibitors will prevent the conversion of angiotensin I to angiotensin II. Lastly angiotensin receptor blockers (ARBs) will inhibit Ang II from binding to its AT_1 and AT_2 receptors thus preventing vasoconstriction, aldosterone release and increased blood volume.

1.5 Renin regulation

Renin, which is encoded for by the *REN* gene, is an aspartyl protease. Its active site contains two aspartate residues which use an acid-base hydrolysis mechanism to cleave peptide substrates. Renin will cleave Ang between a leucine and valine at positions 10 and 11, respectively to form the decapeptide Ang I. The molecular mechanisms through which renin biosynthesis occurs are complex and under the control of several regulatory proteins that may interact in a multitude of ways given the size and complexity of the regulatory region of the *REN* gene (Fig. 1.3). The transcription of *REN* is maintained through multifaceted tissue specific and developmental stage regulation (Li and Kenneth, 2005). Of particular importance in *REN* expression, is the cAMP-response element binding protein (CREB). CREB is a potent transcription factor (TF) facilitating *REN* induction when binding to cAMP response elements (CRE) in the proximal promoter and enhancer (Germain et al., 1996; Adams et al., 2006; Zhou et al., 2006; Lopez et al., 2009) region of the gene. Early studies using mouse renin-expressing

As4.1 cells, have helped to identify this proximal promoter (−197 to −50 bp) and enhancer (−2866 to −2625 bp) region upstream of the *Ren-1c* gene that may have a pivotal role in controlling the rate of *REN* expression (Glenn et al., 2013). In addition, the discovery of a short sequence within the *Ren-1c* promoter region (−72 to −50), essential for *REN* transcriptional control, was done through *in vitro* experiments conducted on the As4.1 cell line. This sequence is highly conserved in mice, rats and humans (Germain et al., 1998).

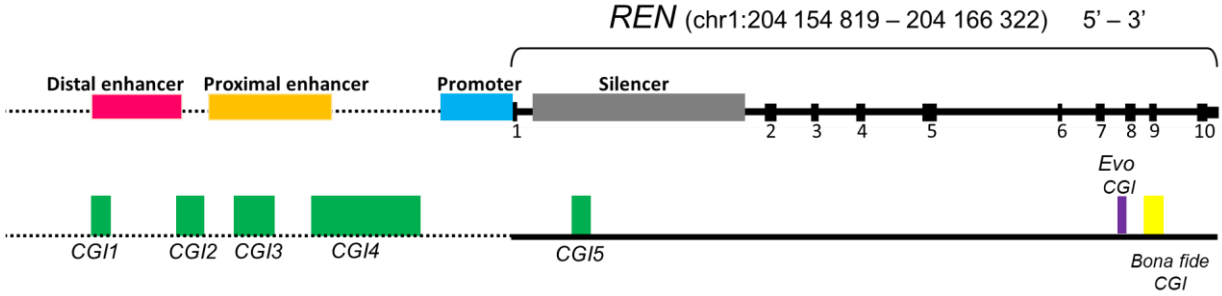

Figure 1.3. The human *REN* gene structure. A simplified structure of *REN* showing a large regulatory region consisting of both a distal (pink; chr1: 204 171 390 – 204 172 959) and proximal (orange; chr1: 204 168 923 – 204 171 222) enhancer, as well as a promoter (blue; chr1: 204 166 222 – 204 167 337) and silencer (grey; chr1: 204 162 166 – 204 166 193). General CGIs (green) were identified and annotated in *REN.* Of the five CGIs identified, two overlap the distal enhancer (211 bp and 336 bp), two overlap the proximal enhancer (405 bp and 1847 bp) and one CGI overlaps the silencer (218bp). A *Bona fide* CGI was identified in exon 9 (yellow; 216 bp) as well as an evolutionarily conserved (Evo) CGI was identified 33 bp upstream of the *Bona fide* CGI (Adapted from Govender et al., 2020).

Although transcription is initiated via the binding of RNA polymerase II to the promoter regions, there are several co-regulatory elements upstream which may enhance or supress transcriptional activity and which are critical for both rat and human *REN* expression (Borensztein et al., 1994; Petrovic et al., 1996). Furthermore, the locations of these key regulatory elements have significant homology between species (Mrowka et al., 2003; Persson et al., 2003).

Studies on *REN* regulation are limited by the lack of an accurate expression model. Before the use of the kidney-derived As.4.1 *REN*-expressing cell line, progress in the field was minimal (Sigmund et al., 1990). There is still considerable caution when using animal models as no system is without limitations such as species differences and lack of conservation between non-coding regions in mouse and human which are a significant factor in epigenetic

regulation. In addition, human studies on *REN* transcriptional regulation remain incomplete (Glenn et al., 2013) and a mammalian cell model is therefore necessary.

CREB function is directly influenced by the biologically active metabolite of vitamin D; 1,25-dihydroxyvitamin D_3 ($1,25(OH)_2D_3$) when bound to its nuclear receptor, the vitamin D receptor (VDR). Using a mouse model, Yuan et al. (2007) showed that liganded VDR binds to CREB, inhibiting binding to the CRE element to effectively down-regulate *REN* expression. They proposed a mechanism (Fig. 1.4) by which $1,25(OH)_2D_3$/VDR blocks the formation of the CRE-CREB-CBP complex that is necessary for *REN* expression (Yuan et al., 2007).

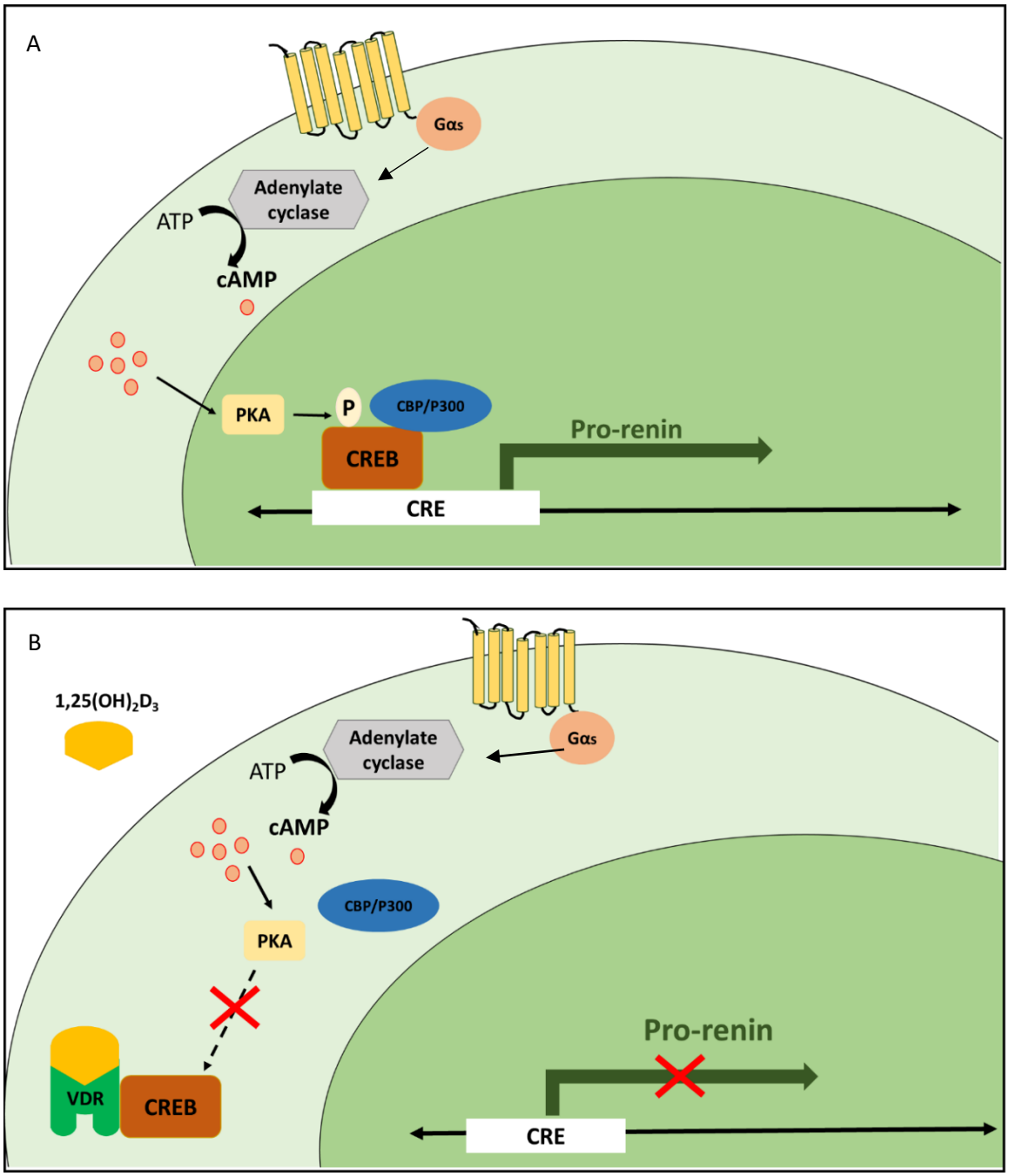

Figure 1.4. Proposed mechanism of $1,25(OH)_2D_3$/ VDR mediated inhibition of CREB induced renin expression. In the absence of Vitamin D (A), Adenylate cyclase is activated by a GαS-coupled protein triggering the conversion of adenosine triphosphate (ATP) into cAMP. The increased cAMP levels then signal protein kinase A (PKA) whose catalytic subunit will move to the nucleus to phosphorylate the cAMP response element-binding protein (CREB). CREB is then able to bind the cAMP-dependent response element (CRE) in the promoter region of the renin gene. The recruitment of the co-activators CREB-binding protein (CBP) and p300 co-activators form a CREB-CBP-CRE complex which induces the transcription of pro-renin mRNA. In the presence of Vitamin D (B), the active $1,25(OH)_2D_3$ metabolite will bind to its VDR receptor and this $1,25(OH)_2D_3$/VDR complex will then bind to CREB and prevent it from being phosphorylated by PKA. The unphosphorylated CREB is then unable to bind the CRE in the renin gene or recruit the necessary co-activator molecules thus supressing pro-renin mRNA expression.

While the interaction between VDR and CREB provides a molecular mechanism for the reported associations (Burgess et al., 1990; Resnick, 1986) between vitamin D deficiency and hypertension risk (Judd and Tangpricha, 2008; Kendrick et al., 2009; reviewed in Khieri et al., 2018), mutations in the CRE element do not fully negate $1,25(OH)_2D_3$-mediated suppression of *REN* (Yuan et al., 2007). This suggests that additional cis-acting elements are present which may be independently linked to $1,25(OH)_2D_3$-dependent regulation of *REN*. For example, a silencer in intron A has been identified as important in cell-specific repression of *REN* (Germain et al., 1999). Regulation of *REN* expression could thus be facilitated by TF binding to enhancers and/ or the silencer, and crosstalk between these regions and the promoter. Extensive research has already confirmed the importance of both the promoter (Germain et al., 2001; Morris et al., 1994) and enhancers (Adams et al., 2006; Ekker et al., 1989; Pan et al., 2003) in driving *REN* expression. However, the molecular role of $1,25(OH)_2D_3$ in *REN* transcriptional regulation and particularly what drives enhancer/silencer-mediated suppression, remains unclear. Nonetheless, it is known that the capacity of enhancers and silencers to induce or repress gene expression is dependent on proximity and chromatin accessibility.

1.6 Vitamin D

Vitamin D is an interesting regulator of the RAAS that is often overlooked. Several biological systems in both the human and mouse genome associated with disease progression are either under the direct or indirect control of vitamin D endocrine pathways (Bouillon et al., 2008). It can therefore be assumed that vitamin D deficiency/insufficiency may have severe consequences for human health. Some of the important physiological roles of vitamin D include the maintenance of healthy bones, immune system functioning, insulin homeostasis, cellular differentiation, support of lung function and cardiovascular health and regulation of genes associated with cancer development (Wilson, 2017). Vitamin D_3 is a fat-soluble pre-hormone that has a functional role in several biological systems within the human body. It is synthesised from its predecessor molecule, 7-dehydrocholesterol which occurs in the skin (Fig. 1.5), through ultraviolet beta (UVB) light activation via a process known as photolysis (MacLaughlin et al., 1982). Cholecalciferol is formed within the plasma membrane of skin cells. This formation occurs when a *cis* isomer of pre-vitamin D_3 which is thermodynamically unstable, rapidly rearranges its double bonds to produce cholecalciferol (Matsuoka et al., 1987). This newly synthesised vitamin D_3 is then binds to the vitamin D-binding protein (DBP)

and is subsequently transported in the blood to the liver where 25-hydroxylation can occur (Christakos et al., 2010). Vitamin D_3 is first hydroxylated to form 25-hydroxyvitamin D_3 ($25(OH)D_3$), which is the form in which Vitamin D can extracellularly circulate, making serum $25(OH)D_3$ levels the main biomarker of vitamin D status (Christakos et al., 2010). The serum $25(OH)D_3$ is transported to the kidneys or target cells for further hydroxylation at the C_1 position to form the hormonally active 1,25-dihydroxyvitamin D_3/calcitriol ($1,25(OH)_2D_3$) (Valdivielso, 2009). It is this form of vitamin D which is responsible for most of its biological activities. It is clear that 25-hydroxylation is an integral process in the bioactivation of vitamin D (Zhu et al., 2013). A group of cytochrome P450 enzymes, termed vitamin D_3-hydroxylases (CYP2R1, CYP24A1, CYP27B1, CYP3A4 and CYP2D25), mediate these hydroxylation steps (Cheng et al., 2003; Guo et al., 1993; Gupta et al., 2005; Jones et al., 2014; Kaufmann et al., 2011). The 1α-hydroxylation step necessary for synthesis of the biologically active $1,25(OH)_2D_3$ is catalysed by 1α-hydroxylase which is encoded by *CYP27B1* (Anderson et al., 2003).

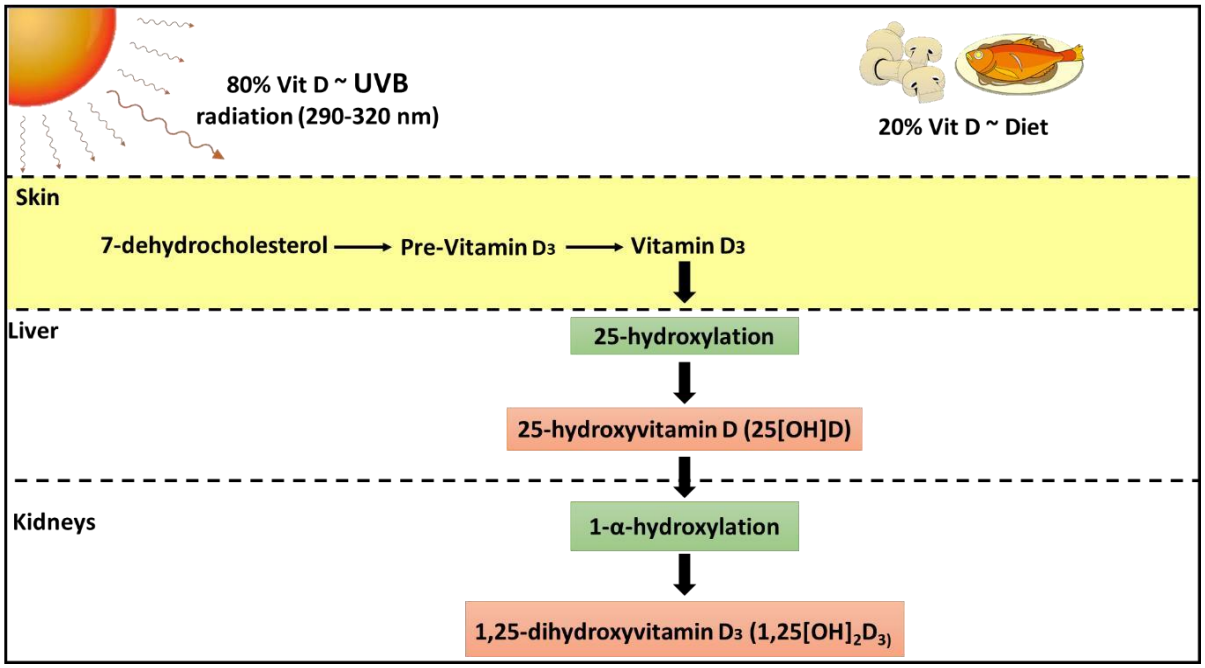

Figure 1.5. Vitamin D endogenous synthesis and metabolism. Two main sources of Vitamin D are available to humans. The largest source comes from sunlight exposure (80%) where UVB radiation produces Vitamin D_3 via a photochemical reaction. Vitamin D_3 is first hydroxylated in the liver (25hydroxylation) and then further hydroxylated in the kidney (1-α-hydroxylation) thus producing the metabolically active 1,25-dihydroxyvitamin D_3 ($1,25[OH]_2D_3$) molecule.

1.7 The vitamin D receptor

The Vitamin D receptor (VDR) which is a nuclear receptor, facilitates the biological functions of $1,25(OH)_2D_3$. In terms of structure, two major components that comprise the VDR include an N-terminal which has a DNA binding domain (DBD). This domain is capable of binding major grooves of hexameric sequences within DNA with the aid of its two zinc-finger motifs. These site-specific DNA binding regions are termed vitamin D response elements (VDREs). The VDR C-terminal has a ligand binding domain (LBD) with a hinge region that joins the two domains (Bikle, 2014). This receptor is a transcription factor that is activated by ligand-binding and act to facilitate calcium homeostasis, cell growth and differentiation, as well as regulating adaptive and innate immunity (Baeke et al., 2011). Binding of the hormonally active ligand to the LBD results in structural changes in the conformation of VDR which alters the DBD's ability to bind protein complexes that function together with the VDR to regulate transcription (Fieldman et al., 2011). The VDR when active will occur as a heterodimer with retinoid X receptor (RXR) forming the VDR/RXR complex (Pike et al., 2012). This complex has the capability to bind various genomic sequences with great specificity. VDR/RXR usually carries out its function near the promoter regions of its specific target genes or VDREs. The VDREs typically consist of DR3 motifs where repeats of hexanucleotides have a 3-nucleotide spacing between the half sites (Bikle, 2014). Recruitment of several transcription factors and co-regulatory molecules is signalled by VDR (Haussler et al., 2013). In this way, VDR is able to respond to certain cell/ environmental conditions to regulate genes associated with molecular and cellular functions including cell proliferation and differentiation, growth regulation, cell immunity, tumour suppression and cell cycle regulation (Kato, 2000). Binding of the $1,25(OH)_2D_3$- VDR complex to VDREs (Fig. 1.6) triggers the assembly co-regulatory element complexes that allow $1,25(OH)_2D_3$ to carry out both gene and cell-type specific translational activity.

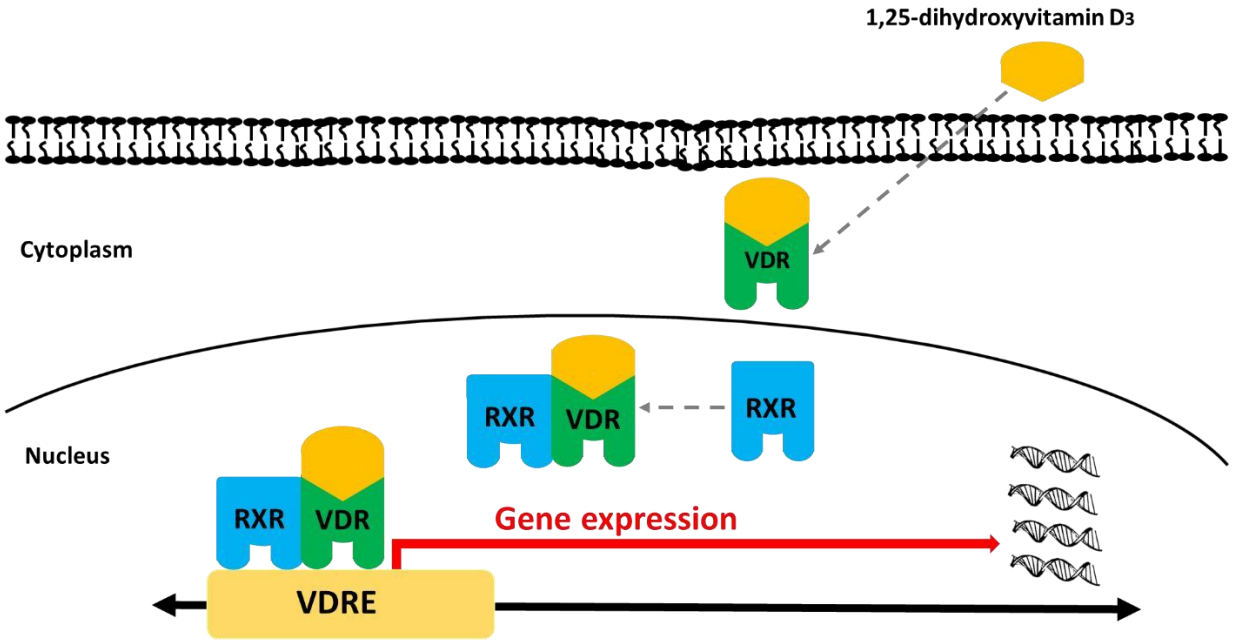

Figure 1.6. 1,25-dihydroxyvitamin D_3/VDR mediated gene expression in target cells. Within the cytoplasm of target cells, the active $1,25(OH)_2D_3$ metabolite will bind to its VDR receptor now acting as a nuclear transcription factor. This $1,25(OH)_2D_3$/ VDR complex will then enter the nucleus and heterodimerise with the retinoic acid receptor (RXR). This VDR/RXR heterodimer is then able to interact with the vitamin D responsive elements (VDREs) present in the promoter regions of various target genes to induce gene expression.

The metabolites of vitamin D have long been associated with the regulation of blood pressure (Resnick, 1994; Vaidya and Williams, 2012). Observational studies have reported increased blood pressure trends during the months of winter in regions further from the equator which suggests that low ultraviolet radiation and subsequent lower capability for cutaneous vitamin D synthesis are linked with hypertension (Rostand, 1997). Most notably, Li et al. (2002) reported that $1,25(OH)_2D_3$ negatively regulated the RAAS. With respect to mammals, VDR is predominantly expressed in tissues of the kidney, intestines, skin and thyroid gland while more moderate expression is present in almost all tissues (Bookout et al., 2006). Notably, up to 20 000 genomic VDR-binding sites have been detected in several human cell culture model systems in the presence of a ligand in comparison to cells not stimulated with $1,25(OH)_2D_3$ (Fleet et al., 2019; Meyer et al., 2012; Ding et al., 2013; Nurminen et al., 2018; Tuoresmäki et al., 2014; Heikkinen et al., 2011). The characterisation of these VDR binding sites differ between cell types, as well as with the time and concentration of vitamin D administration (Carlberg et al., 2012). The ability of the

$1,25(OH)_2D_3$-VDR complex to directly influence the expression of genes related with blood pressure regulation could be one of the causal mechanisms linking vitamin D to cardiovascular health.

1.8 Vitamin D and the epigenome

The use of the term "epigenetics" is credited to Conrad Waddington who described it as "the interaction between genes and the environment to produce phenotype" (Waddington, 1942). The prefix "Epi-'' meaning "above or on top of" refers to changes in gene expression not related to gene sequence. Epigenetics is now an extensive field of molecular biology that aims to elucidate the role of the environment in disease progression to provide a more accurate understanding of transcriptional regulation that encompasses both intrinsic and extrinsic control of the genome. The common disease genetic and epigenetic (CDGE) hypothesis has changed our understanding introduced the concept that the epigenome regulates genetic variation by modulating gene expression via the action of proteins that induce dynamic chromatin and DNA methylation changes (Bjornsson et al., 2004). The epigenome is, in turn, influenced by several environmental factors such as diet (presence of methyl donors), age, exposure to toxins, growth factors and hormones (Feinberg, 2007). The CDGE hypothesis therefore supports the idea that epigenetic variance is of equal importance as genetic variation when describing the influence of the environment on disease phenotype (Bjornsson et al., 2004). In general, epigenetics encompasses all functionally relevant and potentially heritable genomic modifications that do not alter the nucleotide sequence (Wu and Morris, 2001). It is clear that epigenetic inheritance defines cellular growth and differentiation thus emphasising the role of epigenetics in disease progression. The structure of the genome is often approached in a single dimension, but in reality, it exists as a complex three-dimensional conformation within the nucleus (Dekker and Mirny, 2016; Pombo and Dillon, 2015). Gene expression is often controlled by the distal regulatory elements that are located kb to Mb distances away from their associated gene promoter (Bulger and Groudine, 2011; West and Fraser, 2005). The spatial folding of chromatin defines the interaction between distal enhancers and promoters in localised regions of the genome (Bickmore, 2013). The disruption of enhancer-promoter crosstalk can underlie disease susceptibility and developmental malformations. Epigenetic gene regulation is established through three major mechanisms that are closely linked. These mechanisms include DNA methylation, post-translational modifications of histones and long-distance chromatin interactions. Currently, the exact

mechanisms through which DNA methylation/demethylation, as well as histone modifications, influence gene-specific regulation of hypertension remain incomplete.

1.9 DNA methylation

Aberrant DNA methylation is associated with disease and is a widely studied epigenetic mark. DNA methylation is a significant epigenetic mode of gene regulation and is essential in maintaining important cell processes such as differentiation, the cell cycle and genomic imprinting (Moore et al., 2013). DNA methylation in humans usually occurs in sequences where a cytosine is followed by a guanine known as a CpG site. Cytosine methylation within genomic DNA was one of the first epigenetic features identified (Holliday and Pugh, 1975). A region of DNA enriched with CpGs is called a CpG island (CGI) (Wang and Leung, 2004). CGIs are usually enriched in the promoter regions of genes where transcriptional regulation of genes often occurs (Saxonov et al., 2006). DNA methylation is a transient modification where the C-5 position of a cytosine is methylated. This reaction (Fig. 1.7) is catalysed by DNA methyltransferases (DNMTs), which use *S*-adenosyl-methionine (SAM) as the methyl donor (Miranda and Jones, 2007). There are three different types of DNMTs. DNMT1 acts to maintain established methylation patterns and is thus a maintenance methyltransferase while *de novo* methylation is regulated by DNMT3A and DNMT3B. In contrast, the demethylation process involves a group of dioxygenase proteins called ten-eleven translocation enzymes (TETs) which oxidise 5-methylcytosine (5-mC) to 5-hydroxymethylcytosine (5-hmC) *in vivo* and *in vitro* (Tahiliani et al., 2009; Koh et al., 2011). The TETs may then further oxidise 5-hmC to 5-formylcytosine (5-fC) and 5-carboxylcytosine (5-caC). Equal to DNA methylation, DNA demethylation has a significant impact on gene expression and subsequent disease progression. DNA hypomethylation has been linked to diseases such as systemic lupus erythematosus (Teruel and Sawalha, 2017) as well as neurological disorders as reviewed by Bayraktar and Kreutz, (2018).

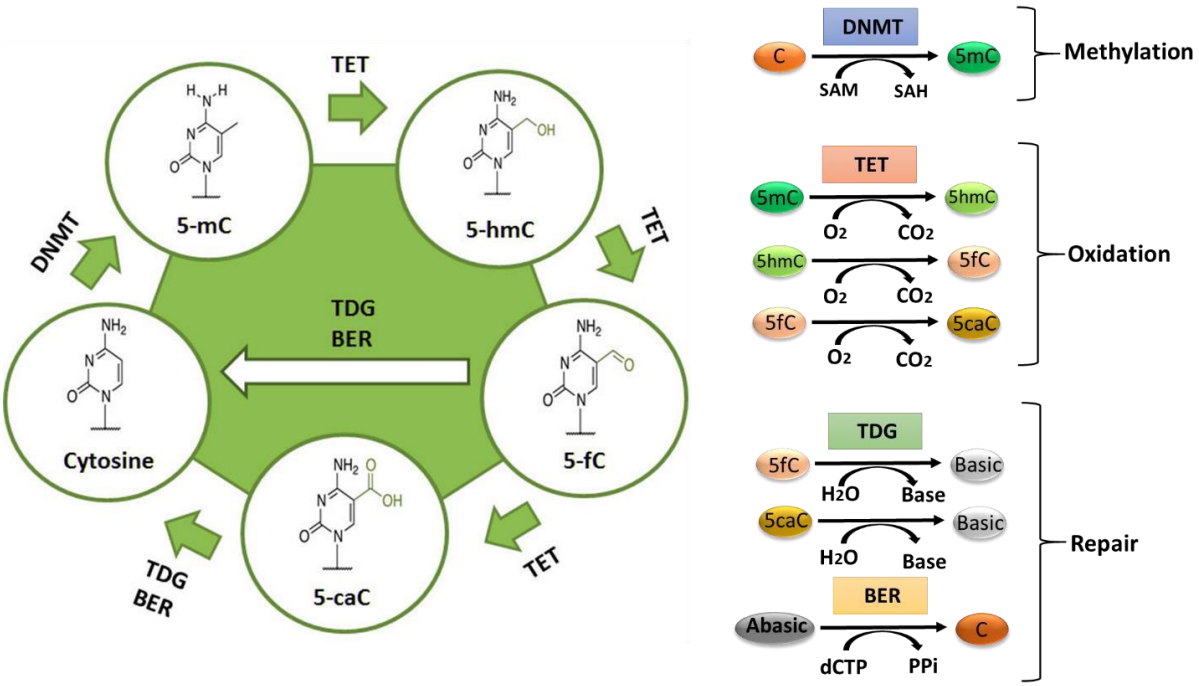

Figure 1.7. The DNA methylation and demethylation process. At the C5 position cytosine is methylated by DNMT1 during DNA replication or de novo by DNMT3A or DNMT3B forming 5methylcytosine (5-mC). In this reaction the methyl donor S-Adenosyl methionine (SAM) is converted to S-Adenosyl homocysteine (SAH). Active demethylation 5-mC can then occur through iterative oxidation by TET1/2 producing 5-hydroxymethylcytosine (5-hmC), 5-formylcytosine (5-fC), and 5carboxylcytosine (5-caC). These cytosine analogues may hinder binding and activity of maintenance methylation machinery and chromatin remodelling proteins. Both 5-fC and 5-caC are bases that form substrates for thymine DNA glycosylase (TDG) which is a DNA repair protein that is able to excise various cytosine and 5-mC derivatives thus reproducing an unmodified cytosine. Active demethylation implements both TDG and the DNA base excision repair (BER) system to form an apurinic/apyrimidinic (AP-site; abasic; adapted from Kohli and Zhang, 2013.)

CGIs are commonly enriched in the promoter regions of a gene, and this has led to the belief DNA methylation modulates gene expression solely through promoters (Portela and Esteller, 2010). In contrast, more recent discoveries suggest the presence of intragenic regions with CGI methylation which may also regulated gene expression (Jeziorska et al., 2017; Lee et al., 2017). Normally, transcriptional control of gene expression is controlled through the maintenance of hypomethylated promoter CGIs and hypermethylated gene bodies in genes that are actively transcribed. This prevents unregulated expression of genes. In contrast, silenced genes will have higher methylation in promoter CGIs with lowly methylated gene bodies (Singal and Ginder, 1999). Aberrant DNA methylation is often associated with various diseases states such as CVD and cancer (Bergman and Cedar, 2013). It is important to note that genetic variation only accounts for a small fraction of these inherited diseases and the epigenetic mechanisms driving these associations are unclear (Petronis, 2010).

With respect to vitamin D, consistent associations between vitamin D and DNA methylation changes have been reviewed by Fetahu et al. (2014). Additionally, sunlight exposure which is a major source of vitamin D has been linked to methylation changes in a North American population (Aslibekyan et al., 2014). Notably, Zhu et al. (2016) reported that vitamin D supplementation in leukocytes of African Americans induced an increase in global DNA methylation. In addition, a reduction in DNA methylation in the promoter of e-cadherin in triple negative bCa (breast carcinoma) cell line MDA-MB-231 following $1,25(OH)_2D_3$ supplementation was reported by Lopes et al. (2012). Moreover, circulating $25(OH)D_3$ level correlates with changes in DNA methylation (Tapp et al., 2013; Becket et al., 2016; Zhu et al., 2016; Meyer et al., 2017). Despite the anti-proliferative effects of vitamin D, a recent study of prostate cancer cells reported a reduction in the expression and activity of DNMT1 and DNMT3B in response to (Lai et al., 2020). Additionally, an inverse relationship between *DNMT3A* mRNA and 25(OH)D has previously been reported by Castellano-Castillo et al. (2018). Furthermore, an experimentally validated VDR binding site, overlapping the VDR binding partners PU.1, RXR and GABPA, has been observed in the *TET1* promoter region (Fornes, 2019). In addition, it has been reported that $1,25(OH)_2D_3$-induced active DNA demethylation within 1–4 h of treatment in prostate cancer cells (Doig et al., 2013). This suggests that dynamic changes to the epigenome brought about by vitamin D may be due to the activation or deactivation of the TET and DNMT molecules.

1.10 Histone post-translational modifications

The basic unit of chromatin structure begins with DNA tightly wound around four pairs of histone proteins (H3, H4, H2A, H2B and H1) forming the nucleosome. Modifications to these proteins will either disrupt and loosen the chromatin forming “euchromatin” or tighten the DNA-histone interaction resulting closely packed “heterochromatin”. These modifications will either inhibit or enable TF access to DNA binding sites resulting in either inactivation or activation of transcription. Histone methylation, acetylation, phosphorylation, ubiquitylation and sumoylation are post-translation modifications that affect chromatin accessibility (Strahl and Allis, 2000). These covalent modifications form what is considered the histone code, which defines the transcriptional state of any local genomic region at a specific time.

Identifying these histone codes can reveal gene activation or gene silencing sites, as well as the location of enhancers, promoters, silencers, and other gene regulatory regions. Histone

acetylation is when an acetyl group ($COCH_3$) is enzymatically added to the histone which weakens the DNA-histone interaction and is necessary for various cellular processes. Histone acetylation usually occurs near the promoters of active genes on H3 (H3K9ac and H3K27ac). Histone methylation takes place when enzymes called histone methyltransferases (HMTs) facilitate the transferral of a methyl group to either a lysine or arginine residue on a histone protein. Methylation of lysine or arginine residues of histones H3 and H4 is common. Arginine methylation is often associated with activating transcription while methylation at lysine residues results in both site-dependent stimulation and suppression of transcription (Greer et al., 2012). Mono-, di- or tri-methylation of lysines further specify the function at each site. Mono-methylation (H3K4me1) and tri-methylation (H3K4me3) at K4 of histone H3 are markers of activation which have functional diversity. H3K4me1 classically mark enhancers, while H3K4me3 mark gene promoters. In contrast, tri-methylation of K36 on H3 (H3K36me3) is an activation marker within gene bodies. Conversely, triple methylation of K9 and K27 of histone H3 (H3K9me3 and H3K27me3) are known as markers of repression. Conversely, the removal of methyl groups from histones is carried out by histone demethylases (HDMs). It has now become clear that DNA nucleosome structures are not static, but rather their dynamic arrangement is part of the machinery that drives cell-specific gene expression which are involved in various disease pathways. The VDR protein is capable of contacting chromatin modifiers through its interaction with coactivator and corepressor proteins such as HATs, HDACs, HMTs. Interestingly several gene families involved in chromatin modification and remodelling including Jumonji C (JmjC)-domain containing HDMs and lysine-specific demethylases (LSDs) are major VDR targets. Lastly, evidence suggests that specific VDR ligands are capable of demethylating DNA as treatment of cells with $1,25(OH)_2D_3$, coupled with either histone deacetylase or DNA methyltransferase inhibitors are shown to have complimentary effects (Fetahu et al., 2014).

1.11 Chromatin accessibility and long-distance interactions

It is well understood that the combined action of various transcription factors mediates cell type specific gene expression. Chromatin, which modulates DNA accessibility, is the context in which TF binding and gene regulation take place. Transcriptional regulation is not accomplished via the promoter-proximal region of a gene alone, but also through distal regulatory elements such as enhancers and silencers within the 3D genomic landscape (Yan et al., 2019). The proximity of gene regulatory regions is controlled by chromosome territories

and topologically associating domains (TADS); often defined by structural proteins such as CCCTC-binding factor (CTCF) and cohesin (Andersson and Sandelin, 2020). The dynamic chromatin landscape allows for the interaction of distal regulatory elements which establishes various gene transcriptional states that are sometimes associated with disease (Grubert et al., 2015). Novel techniques including chromosome conformation capture (3C) (Sati and Cavalli, 2017) and high-throughput chromosome conformation capture (Hi-C) (Lieberman-Aiden et al., 2009) have helped to identify long-range chromatin interactions with high resolution and sensitivity. Although it is not well understood, the CTCF defines the 3D genome structure through DNA loops and in 1D by defining boundaries which can isolate different chromatin regions and with differing transcriptional states (Clarkson et al., 2019). CTCF has shown to have multifunctional genomic roles in complex transcriptional processes (Filippova et al., 1996). It must be noted that CTCF, a highly conserved chromatin remodeler (Phillips and Corces, 2009), has a conserved binding site in *REN* intron 1, and has recently been shown to be crucial in the regulation of *REN* expression (Martinez et al., 2020). In conjunction with CTCF, the aptly named Yin Yang 1 (YY1) protein with both activator and repressor activity, has a binding site in the silencer region. It has been reported that YY1 interacts with members of the ATF/CREB family of TFs to repress transcription (Zhou et al., 1995). It is possible that differential methylation in the *REN* silencer region influences CTCF and YY1 binding and subsequent silencer activity. Both CTCF and YY1 binding have been described as methylation-sensitive (Hark et al., 2000; Kim et al., 2003), although some reports have suggested binding of these TFs as methylation-independent (Maurano et al., 2015). Moreover, an emerging model suggests that TFs like CTCF and YY1, have the ability to induce demethylation when bound as reviewed by Héberlé and Bardet (2019). Notably, $1,25(OH)_2D_3$ has been shown to directly modulate genome-wide CTCF binding (Carlberg et al., 2014). The above-mentioned associations suggest an interaction between $1,25(OH)_2D_3$, *REN* silencer methylation and *REN* expression. It is thus unclear whether $1,25(OH)_2D_3$ directs CTCF and YY1 binding to the *REN* silencer resulting in demethylation effects, or whether it directly induces demethylation to influence subsequent TF binding.

Considering the significant impact of $1,25(OH)_2D_3$ on the epigenome, coupled with its consistent association with the RAAS, identifying therapeutic targets for the disease should focus on epigenetic regulation of *REN* and the identification of proteins or DNA cis-regulatory elements involved in enhancer-promoter or silencer-promoter crosstalk. Despite most

Mendelian disorders falling within protein-coding regions, the larger component of these heritable diseases lies within the non-coding regions and are most commonly found in enhancers specific to disease related cell types (Gasperini et al., 2020). Although age, obesity and diet influence hypertension risk, it does not fully account for hypertension prevalence. The binding of TFs at site-specific cis-regulatory elements in DNA is able to either positively or adversely affect the transcription of specific genes, thus resulting in specific disease phenotypes. This suggests an epigenetic mechanism for control of hypertension progression.

It must also be noted that emerging studies have now made previous understandings of enhancer and promoter activity not as distinct as two separate functioning regions but have rather introduced a concept of "regulatory elements" with both enhancer and promoter function of varying degrees (Andersson and Sandelin, 2020). Furthermore, the use of reninproducing cell lines to identify proximal cis-regulatory elements in *REN* transcription *in vitro* and *in vivo* tend to have differing significance due to difficulty in recreating the complex physiological and nuclear micro-environment in a cell culture dish (Tanimoto et al., 2008; Tamura et al., 2000). Most studies focusing on *REN* transcriptional regulation neglect the effect of distal regulatory elements as the limited DNA fragment sizes introduced into plasmid vectors tend to highlight more proximal regulatory elements near the coding region of the gene. However, emerging studies have now shown that gene transcription is under the control of more distally located regulatory elements putting greater focus on identifying interactions with target promoters through chromatin looping (Dekker et al., 2015).

Many studies evaluating the effects of high-dose vitamin D supplementation in suppressing a wide range of diseases have been conducted and concluded that vitamin D does have a beneficial effect. These include maintaining bone health (Tripkovic et al., 2012), reducing CVD risk markers (Zitterman et al., 2009) as well as survival rates of cancer patients (Akutsu et al., 2020). There are numerous analogues of vitamin D that have been marketed towards treatment of chronic renal failure that is linked to secondary hyperthyroidism (Dobnig et al., 2008; Malluche et al., 2002). Implementation of $1,25(OH)_2D_3$ and its analogues have been reported to successfully subdue signs of cardiac hypertrophy, while the absence of *VDR* in heart cells resulted in hypertrophy (Chen et al., 2011; Gardner et al., 2013). It must however be noted that of the more than 40 randomised clinical trials aimed at identifying the effect of vitamin D supplementation on BP, most displayed mixed and inconsistent results (Forman

et al., 2013; Pilz et al., 2009; Pittas et al., 2010; Witham et al., 2009). This is probably due to the gap in knowledge of vitamin D's effect on hypertension resulting in inefficient large-scale clinical trial designs.

Several studies have highlighted the role of $1,25(OH)_2D_3$ at the genomic and epigenomic level (Bouillon et al., 2008; Carlberg et al., 2012; Fetahu et al., 2014; Nurminen et al., 2018; Plum and DeLuca, 2010). $1,25(OH)_2D_3$ may influence DNA methylation by recruiting DNA methyltransferases (DNMTs) to methylate, or ten-eleven translocation enzymes (TETs) to influence local genomic transcriptional states resulting in *REN* suppression. Flexible modifications to the epigenome brought about by $25(OH)D_3$ deficiency have been reported to diminish the effects of the RAAS (Wimalawansa, 2018). Thus, unravelling the molecular link between $1,25(OH)_2D_3$, DNA methylation and *REN* transcription could improve our understanding of factors involved in the development of hypertension.

1.12 Hypothesis

Thus, we hypothesise that $1,25(OH)_2D_3$ along with its nuclear receptor, VDR, represses *REN* expression through changes in DNA methylation in the CGIs characterised within the regulatory regions of *REN*. It is predicted that $1,25(OH)_2D_3$ will induce hypermethylation of CGIs overlapping the *REN* enhancer and promoter and demethylation of the CGIs overlapping the *REN* silencer. The observed methylation changes could be facilitated by $1,25(OH)_2D_3$induced recruitment of TET and/or DNMT proteins that will alter *REN* methylation, thus allowing the binding of TFs involved in transcriptional repression in the silencer region or inhibiting the binding of transcriptional activators in the enhancer and promoter regions.

1.13 Aims and Objectives

The aim of this study was thus to assess the effect 1,25$(OH)_2D_3$ on *REN* methylation and expression to understand the epigenetic mechanisms regulating *REN* transcription. To achieve this goal, the following objectives were set:

1) To establish both control and experimental (*VDR*$^-$ & *VDR*$^+$) HEK293 cells to be treated with and without 1,25$(OH)_2D_3$ via siRNA transfection.

2) To confirm successful gene knockdown of *VDR* in HEK293 cells by means of percentage knockdown via RT-qPCR and protein expression via Flow-cytometry.

3) To obtain high-quality and pure DNA extracts to quantify changes in methylation within the annotated CGI regions of *REN* in HEK293 cells following 1,25$(OH)_2D_3$ supplementation via matrix-assisted laser desorption/ionisation-time of flight mass spectrometry (MALDI-TOF MS).

4) To extract high quality, intact RNA from HEK293 cells and quantify the effect of 1,25$(OH)_2D_3$ on the expression of genes that act to regulate and maintain DNA methylation (*DNMT1, DNMT3A, DNMT3B, TET1, TET2, TET3*) as well as *VDR, REN* and *CYP24A1*.

5) To use appropriate statistical tests to analyse the effect of 1,25$(OH)_2D_3$ on *REN* methylation and the expression in HEK293 cells.

2.1 Cell culture and treatment

REN expressing, human embryonic kidney 293 cells (HEK293; Passage 21) were cultured with the use of Dulbecco's Modified Eagle Medium (DMEM; Pan Biotech) supplemented with 10% (v/v) foetal bovine serum (FBS; Pan Biotech, Aidenbach, Germany) and 1% (v/v) Penicillin Streptomycin mix (Sigma Aldrich, St. Louis, MO) to about 80 – 90% confluency. FBS which is the blood drawn from a bovine fetus is a necessary supplement used in the growth of *in vitro* cell cultures. Several components in the serum contribute to adequate cell growth including a buffering capacity, nutrient sources, proteins, electrolytes, hormones, carbohydrates, enzymes, and growth factors all with a reduced level of antibodies making it compatible for use in several cell types. Additionally, antibiotics such as penicillin and streptomycin act to inhibit bacterial growth which would contaminate cell cultures specifically gram-positive and gram-negative bacteria. A major consequence of bacterial contamination of *in vitro* cell cultures includes the altering of cellular characteristics (cell morphology, metabolism and cell proliferation) which would affect the reliability of experimental results thus necessitating the use of antibiotics in cell culture medium. When the cells reached confluency they were supplemented with either 10 nM $1,25(OH)_2D_3$ (Sigma Aldrich, St. Louis, MO) or the vehicle control (99% ethanol; Sigma Aldrich, St. Louis, MO) for 18 h. A concentration of 10 nM $1,25(OH)_2D_3$ was considered effective in inducing measurable effects based on previous studies in which the 10 nM $1,25(OH)_2D_3$ dose induced significant cellular responses, changes in target genes and VDR activity (Edfeldt et al., 2010; Felicidade et al., 2018; Liu et al., 2006; Weeres et al., 2014). HEK293 cell cultures were incubated at 37°C in 5% CO_2. HEK239 is an adherent cell line and was therefore detached via trypsinisation for experimental procedures. Cell detachment was performed by adding 2 ml of 1X trypsin (Sigma, St. Louis, MO) to cells which were then briefly incubated for 3–5 min at 37°C. Media was then added to inactivate the trypsin and the cells were aspirated to ensure complete detachment from the culture dish. The detached cells were then pelleted at 500 *× g* and the excess media and trypsin was discarded. Cells then resuspended in either fresh media or phosphate-buffered saline (PBS; 0.01 M phosphate buffer, 0.0027 M potassium chloride and 0.137 M sodium chloride, pH 7.4; Sigma, St. Louis, MO) for cell counting and viability assessment via Trypan Blue exclusion assay

(Section 2.4). An adequate number of cells used in downstream analysis was aliquoted and either used directly for experimentation or stored at –80°C for RNA and DNA extraction.

2.2 *VDR* knockdown via siRNA transfection

RNA interference (RNAi) is a conserved eukaryotic cellular mechanism which mediates posttranscriptional gene silencing (Hannon, 2002). The absence of the *VDR*, can highlight changes in cell function and reveal its complex relation to other genes in the context of hypertension progression (National Institute of Health, 2013). *VDR* was silenced using small interfering RNA (siRNA) (Ambion, VDR Silencer® Select siRNA ID: s14777 cat#: 439084, USA) according to the manufacturer's guidelines (Ambion Life technologies, Protocol Pub. No. MAN0007836 Rev. 1.0). A non-targeting negative control siRNA (Ambion Silencer™ Select Negative Control No. 1 siRNA, Invitrogen, cat# 4390843, USA) was used prior to transfection, the lyophilised siRNA was reconstituted in nuclease-free water to produce a stock solution with a final concentration of 100 µM for prolonged storage. The stock was then used to make 10 µM working stocks for immediate use to avoid freeze-thaw cycles which can degrade the siRNA overtime and reduce its efficiency. Freeze-thaw cycles can degrade siRNA due to pH fluctuations which can aid RNase activity and physical shearing by ice-crystals (Yadava et al., 2007). All transfection reagents were made fresh on the day of transfection. Cells were seeded to be 75–80% confluent at the time of transfection. Cell should not be fully confluent at the time of transfection as they do not take up foreign nucleic acids in the stationary or quiescent phase as well as when they are actively dividing. The transfection reagent was made by first diluting 54 µl of Lipofectamine (Thermofischer Scientific, Lipofectamine™ RNAiMAX™, cat# 13778075) with 900 µl of antibiotic and serum-free media (for 6 reactions). The choice of media used is important as lipofectamine is a cationic lipid-mediated mode of transfection which can easily be affected by serum proteins thus reducing the efficacy of the siRNA. Albumin within the serum interact with the lipofectamine reducing its interaction with the cell membrane and cellular receptors (Wallenstein et al., 2010). Most cells will survive for hours in serum-free medium and can be supplemented with complete medium at a later stage thus allowing for efficient transection and successful gene knockdown. In separate tubes, 24 µl (10 µM) of the *VDR* siRNA or non-targeting siRNA was diluted with 900 µl of antibiotic and serum-free media and was left to incubate at room temperature for 5 min. The HEK293 cells were then removed from the CO_2 incubator and brought into the laminar hood. Old media was discarded and 150 µl of the diluted lipofectamine was added to each transfection well

along with 150 µl of diluted *VDR*/non-targeting siRNA which was then left to further incubate at room temperature for 30 min in the wells. This incubation period allows for the formation of the siRNA-lipid complex which is needed to penetrate the cell membrane so siRNA can enter the cytoplasm. Following incubation, the cells were topped up with complete media to a final volume of 4ml. The cells were then left to incubate at 37°C at 5% CO_2 for 1–2 days. The recommended siRNA final concentration for transfection of 6 nM was adjusted to 10 nM per plate for the 6-well format as it provided greater knockdown efficiencies. $1,25(OH)_2D_3$ treatment was done 24-hours post transfection and cells were then analysed and used for downstream analysis within 48-hours post transfection. Percentage knockdown of *VDR* was validated by gene expression analysis. Percent Knockdown (%KD) of *VDR* was calculated using the ΔΔCq method (section 2.13) and samples with %KD of 80 or higher were considered effective knockdowns and were used for further analysis. VDR protein expression was quantified via flow cytometry (section 2.12).

2.3 *Mycoplasma* detection

Prior to collection of the *VDR* $^{+}$/*VDR* $^{-}$ samples for DNA methylation analysis, the LookOut® *Mycoplasma* qPCR Detection Kit (Merck Life Science [Pty] Ltd, Modderfontein, SA) was used to confirm that the HEK293 cell cultures used for experimentation were pure and free of *Mycoplasma* contamination. The detection kit is a PCR with a specific primer and probe that specifically detects a well conserved 23S rRNA operon coding region of the *Mycoplasma* genome. Cell culture supernatants were tested directly. 100 µl of HEK293 cell culture supernatant was collected in a sterile amplification tube and incubated at 95° C for 5 min. This high temperature incubation step was done to denature any proteins or contaminants that could affect the PCR reaction. Prior to use in PCR the sample was briefly centrifuged (5 seconds) to pellet any cellular debris. The PCR reactions were prepared and set according to manufacturer guidelines (see Table 2.1). The ready-to-use lyophilised reaction mixtures required a final reaction volume of 25 µl with one unit of Taq per reaction. 0,5 µl for the OneTaq® 2X Master Mix DNA polymerase (NEB, Ipswich, MA, Cat.no. M0482) was diluted with 22 µl of rehydration buffer which was then added to the reaction tube. For the positive control, 0.5 µl of the OneTaq® 2X Master Mix was diluted with 22 µl of rehydration buffer which was then added to the reaction tube. Following rehydration of the reaction mixture, 2 µl of HEK293 cell supernatant was added to the test reaction. Both the test reaction and

positive control reactions were mixed gently by flicking the tube. For the PCR reaction, samples were placed in a thermal cycler (SimpliAmp™ Thermal Cycler, Cat.no.: A24811) according to the manufacturer cycling conditions (Table 2.2). After PCR was completed, samples were cooled to 4–8°C on ice and 8 µl of each PCR sample (Test reaction and Positive control reaction) was loaded onto a 1.5% (w/v) agarose gel for electrophoresis (Section 2.8). Loading gel and dye were already present in the reaction tubes and therefore not necessary. Electrophoresis was stopped after 30 min and bands were visualised under UV light.

Table 2.1: Reaction mixture for Lookout *Mycoplasma* detection kit

Cycle Step	Sample (µl)	Positive control (µl)
DNA polymerase/ Rehydration buffer	23	25
Sample volume	2	-
DNA-free water	-	-

Table 2.2: Thermocycler incubation steps for Lookout *Mycoplasma* detection kit

Cycle Step	Temperature (°C)	Time (Seconds)	Cycles
Initial Denaturation	94	30	1
Extension	94	30	30
	55	60	
Final extension	68	60	1

2.4 Trypan blue assay

Cell viability was quantified using the trypan blue (Sigma, St. Louis, MO) exclusion assay. This assay is based on the property that healthy cells obtain intact cell membranes which will prevent a dye like Trypan blue from entering the cell. Conversely non-viable cells often have degraded membrane which allow the dye to enter (Strober, 2001). By this principle, cells that are penetrated by the trypan blue were considered non-viable, whereas cell that remained clear were considered viable. To perform the assay, the cell suspension was diluted 2X with trypan blue solution (i.e. 10 µl of cells was added to 10 µl of Trypan blue solution). The solution (10 µl) was loaded onto a slide and placed into the Countess II FL Automated Cell Counter (Invitrogen, Carlsbad, California) from where viability was estimated.

2.5 Genomic DNA (gDNA) extraction

gDNA from 1×10^6 HEK293 cells were extracted using the QIAamp DNA Blood Mini Kit (Qiagen, Hilden, Germany) according to the manufacturer's guidelines. All extraction reagents were kept at room temperature and centrifugation steps were done at 6 000 x *g* at room temperature unless stated otherwise by the manufacturer. All working surfaces and apparatus were thoroughly washed with 70% (v/v) Jik followed by a 70% (v/v) ethanol wipe to ensure a nuclease-free environment and prevent DNA degradation during the extraction procedure. Frozen cell pellets were left to thaw on ice and were resuspended in PBS to a final volume of 200 µl followed by the addition of 20 µl of Proteinase K (Qiagen, Hilden, Germany) which is a broad-spectrum serine protease and is used in the degradation of cellular membrane proteins to aid in cell lysis. It also facilitates inactivation of DNases to increase the nucleic acid isolation yield (Barrett et al., 2012). Thereafter, 3 µl of RNase A (1 mg/ml) was added to ensure RNA degradation and prevent RNA contamination in the extracted gDNA sample. RNase A is a digestive enzyme which specifically hydrolyses RNA but not DNA polymers (Raines, 1998). Thereafter, 200 µL of buffer AL (Qiagen, Hilden, Germany) was thoroughly mixed with the sample to ensure efficient cell lysis by pulse-vortexing for 15 seconds. Buffer AL is a lysis buffer containing guanidinium chloride which is a chaotropic agent which promotes lysis of cell membranes through denaturation of membrane proteins (Hatefi and Hanstein, 1974; Penefsky and Tzagoloff, 1971). The sample was then incubated for 10 min at 56°C in a heating block following cell lysis. The sample was then mixed with 200 µl of 100% (v/v) molecular-grade ethanol (Sigma-Aldrich, Saint Louis, Missouri, USA) by

pulse- vortexing for 15 seconds, followed by a 1 min centrifugation step. Ethanol is used to facilitate DNA aggregation and precipitation by removing the DNA solvation shell (Green and Sambrook, 2016). The mixture was then moved into a QIAamp Mini spin column (placed in a 2 ml collection tube) containing a silica-membrane and centrifuged for a further 1 min. Adsorption of the DNA onto the QIAamp silica membrane occurs during this quick centrifugation step. Additionally, specific pH and salt conditions are maintained in the cell lysate to ensure that there is no retention of protein or other contaminants on the QIAamp membrane, which could inhibit PCR or any downstream enzymatic reactions (Berensmeier, 2006; Melzak et al., 1996). Silica matrix purification is popular and effective as it works on the principle of ion exchange where the positively charged particles on the silica membrane have a high affinity for the negatively charged sugar-phosphate backbone of DNA (Esser et al., 2006). The DNA will bind to the silica matrix until it is eluted. The spin column was then transferred to a new collection tube and 500 µl of buffer AW1 (Qiagen, Hilden, Germany) was added to the column followed by a 1 min centrifugation. Buffer AW1 serves to further denature proteins allowing them to easily be eluted following centrifugation. Following removal of the filtrate the spin column was then placed in a clean collection tube. Thereafter, 500 µl of Buffer AW2 was added to the sample (Qiagen, Hilden, Germany) followed by centrifugation at full speed (16000 x *g*) for 4 min. AW2 is a Tris-based ethanol solution used to remove excess salts prior to nucleic acid elution. The spin column was then placed in a clean collection tube and 200 µl of elution buffer AE (10 mM Tris·Cl; 0.5 mM EDTA; pH 9.0) was added to the column and incubated at room temperature (15–25 °C) for 5 min, followed by a 1 min centrifugation step. The elution buffer is a low salt solution helps the DNA release from the silicia membrane and be eluted from the column. The purity, quantity and quality of the extracted gDNA were assessed using the Qubit fluorimeter (section 2.6). DNA integrity was assessed using agarose gel electrophoresis (section 2.9). gDNA passing quality control was stored at –30°C prior to downstream applications.

2.6 DNA quantification and purity assessment

Prior to downstream experiments, accurate and precise DNA quantification is necessary as adequate concentrations and amounts of pure DNA within a sample are needed for reliable methylation analysis. The Qubit 2.0 Fluorometer (Invitrogen, Cat. no. Q32866, Carlsbad, California) was used to quantify the concentration of DNA in both *VDR* $^{+}$ and *VDR* $^{-}$ control and treated HEK293 samples prior to methylation analysis. The fluorometer is used in conjunction

with the Qubit™ dsDNA HS Assay Kit (Invitrogen, Cat. no. Q32851, Carlsbad, California). The Qubit assay was performed at room temperature as per manufacturer's guidelines. The instrument must be calibrated upon each new assay. To calibrate the machine, two high sensitivity (HS) standards were prepared from diluting both Qubit® stock standard 1 and Qubit® stock standard 2 provided in the kit. First a Qubit® working solution was prepared by diluting the Qubit® dsDNA HS Reagent in Qubit® dsDNA HS Buffer in a 1:200 dilution in a clean plastic tube. The final reaction volume for each sample as well as the standards was 200 µl and each tube required a minimum of 190 µl working solution and 1–10 µl of sample or standard. The required number of thin, clear-walled 0.5 mL tubes for two standards and all samples was set up. For the Qubit® standard assays, 10 µl of Standard 1 and 2 was added to 190 µl working solution. For the sample assays 2 µl of DNA sample was added to 198 µl of working solution and all tubes were incubated for 3 min at room temperature prior to measurement. Following incubation both Standard 1 and Standard 2 assays were read on the Qubit 2.0 first. Following successful calibration each sample assay was measured. The principle of Qubit fluorometry is based on the use of fluorescent dyes. Fluorochromes present in the working solution will bind the DNA and emit fluorescent signal which is detected by the Qubit detector. The amount of DNA present is calculated based on the difference between bound and unbound fluoro-molecules (Mardis and McCombie, 2017). Another method of DNA quantification is Spectrophotometry which does not require any additional reagents. However, spectrophotometry is limited by the fact that various molecules other than DNA also absorb light at 260 nm including proteins, free nucleotides and RNA thus reducing the reliability of the results making Qubit fluorometry a more reliable method quantification and purity assessment of DNA.

2.7 RNA extraction

Total RNAs were extracted from 1×10^6 HEK293 cells using the Direct-zol™ RNA Mini-prep kit, (Zymo Research, Irvine,CA) as per manufacturer guidelines. All centrifugation steps were done at 16 000 x *g for* 30 seconds at 4°C and all steps were done on ice unless stated otherwise by the manufacturer. All working surfaces and apparatus were thoroughly washed with 70% (v/v) Jik followed by a 70% (v/v) ethanol wipe to ensure an RNase-free environment. Cell pellets were resuspended in 300 µl TRI Reagent® (Sigma, St Louis, MO) and aspirated to inhibit nuclease activity following cell lysis. An equal amount of molecular grade ethanol (99%; Sigma, St Louis, MO) was then added to the pellet and aspirated until the solution was clear

pink and homogenous. The cell lysate transferred to a Zymo-SpinTM IIICG column in a collection tube followed by centrifugation. Following centrifugation, 90 µl of a DNase I treatment (15 µl of DNase I & 75 µl of DNA digestion buffer) was added to the column. The column was then incubated at room temperature for 15 min. This step was recommended to ensure DNA degradation and prevent DNA contamination in the extracted RNA sample. Thereafter, 400 µl of Direct-zol RNA Prewash was added to the column followed by centrifugation. This step was done twice. Following the Prewash steps, 700 µl of Direct-zol RNA wash buffer was then added to the column followed by a 2 min centrifugation step. The excess reagents eluted into the collection tube was discarded after each centrifugation step prior to elution. The RNA was eluted and dissolved in 20 µl of RNase-free dH_2O. The extracted RNA quantity and quality were assessed using nanodrop spectrophotometry (Thermo Scientific™, NanoDrop™ One microvolume UV-Vis Spectrophotometer). RNA integrity was assessed using agarose gel electrophoresis (section 2.8). The RNA was then stored at –80°C for later use in RT-qPCR studies.

2.8 Quantitative reverse transcriptase PCR (RT-qPCR)

To assess the role of *DNMT1, DNMT3A, DNMT3B, TET1, TET2* and *TET3*, *CYP24A1* and *VDR* on $1,25(OH)_2D_3$-mediated expression of *REN*, cDNA synthesis and qPCR were performed using the LunaScript® RT SuperMix Kit (NEB, Ipswich, MA, Cat.no. E3010) and the Luna® Universal qPCR Master Mix (NEB, Ipswich, MA, Cat.no. M3003) according to manufacturer's instructions. Normalisation of gene expression was done against the *GAPDH* and *UBC* reference genes. All cDNA synthesis master mixes were prepared on ice (Table 2.3). After preparation of the cDNA reaction mixtures, the PCR reaction tubes were placed in the SimpliAmp thermal cycler (Thermo Fisher Scientific, Waltham, MA) for cDNA synthesis (Table 2.4). After cDNA synthesis the reaction mixtures were incubated at 4°C prior to use in qPCR. The cDNA template was added to the qPCR reaction mixture (Table 2.5). The CFX-96 Thermal Cycler (Bio-Rad, Hercules, CA) was used to amplify the target genes according to the appropriate cycle settings (Table 2.6). PRIMER3 software (v4.1.0; http://primer3.ut.ee/) was used to design the primers for *REN*, *DNMT3A, DNMT3B, TET1, TET2 and TET3*, while the primers for *DMNT1*, *VDR, GAPDH* and *UBC* were obtained from RTPrimerDB (Table 2.7). All PCR products underwent gel electrophoresis to confirm specific amplification of target gene products. (Section 2.8).

Table 2.3: Reaction components of the cDNA synthesis reaction

Component	Volume (µl)	Final Concentration/ Amount
LunaScript RT SuperMix (5X)	4	1X
RNA sample	variable	500 ng
Nuclease-free Water	to 20	

Table 2.4: Thermocycler incubation steps for the cDNA reaction

Cycle Step	**Temperature (°C)**	**Time (min)**	**Cycles**
Primer Annealing	25	2	1
cDNA Synthesis	55	10	1
Heat Inactivation	95	1	1

Table 2.5: Reaction components of the qPCR reaction

Component	Volume (µl)	Final Concentration/Amount
Luna Universal qPCR Master Mix	5	1X
10 µM forward primer	0.25	0.25 µM
10 µM reverse primer	0.25	0.25 µM
cDNA products	variable	< 100 ng
Nuclease-free water	Up to 10	

Table 2. 6: Thermocycler incubation steps for the qPCR reaction

Cycle Step	Temperature	Time	Cycles
Initial Denaturation	95 °C	60 seconds	1
Denaturation	95 °C	15 seconds	40-45
Extension	60 °C	30 seconds	
Melt Curve	60–95 °C		1

Table 2.7: Primer sequences used to amplify the target and reference genes

Gene	Primer Sequences[a]	Product Size (bp)	RTprimerDB number	Reference
DNMT1	FP: GTGGGGGACTGTGTCTCTGT RP: TGAAAGCTGCATGTCCTCAC	204	3628	Bestor et al., 1988
DNMT3A	FP: CTGTGGGAGCCTCAATGTT RP: GCAGTTGTTGTTTCCGCAC	175	N/A[b]	
DNMT3B	FP: CTCGTGTGGGGAAAGATCAA RP: CCAAATTAAAGTGCTGGCTGA	187	N/A[b]	
TET1	FP:AGATAAGGGCAGTGGAAAAGAA RP: TGGGGTTCGGTTTCACTTTT	151	N/A[b]	
TET2	FP: GTCCTATTGCTAAGTGGGTGG RP: CGTGCCGTATTTCCTCAGC	194	N/A[b]	
TET3	FP: GACACACCTGCCAAGAGAG RP: TATCACTCACCGCTCCTCC	152	N/A[b]	
VDR	FP: CTGACCCTGGAGACTTTGAC RP: TTCCTCTGCACTTCCTCATC	277	2787	Vienonen et al., 2003
REN	FP: GAAAGCCTGAAGGAACGA RP:GTACTGGGTGTCCATGTAGTT	129	7779	
CYP24A1	FP: ATGAGCACGTTTGGGAGGAT RP:TGCCAGACCTTGAG	71	1817	Zhao et al., 1998
GAPDH	FP: GTCAGTGGTGGACCTGACCT RP: AGGGGAGATTCAGTGTGGTG	395	2093	Wichmann et al., 2002
UBC	FP: ATTTGGGTCGCGGTTCTTG RP: TGCCTTGACATTCTCGATGGT	133	1528	Max et al., 2001

[a] The Forward (FP) and reverse (RP) primer sequences are given in the 5' - 3' direction.
[b] Not applicable – These primers were designed using Primer3 (Untergasser et al., 2012)

2.9 Agarose gel electrophoresis

For both DNA, RNA and PCR product quality assessment, agarose gel electrophoresis was used. 500 ng of either RNA/DNA added and aspirated to either 2X RNA Gel Loading Dye (95% formamide, 0.025% SDS, 0.025% bromophenol blue, 0.025% xylene cyanol FF 0.025% ethidium bromide 0.5 mM EDTA; Thermofischer, Cat. no.: R0461, Vilnius, Lithauania) or DNA Gel Loading Dye (6X) (10 mM Tris-HCl (pH 7.6) 0.03% bromophenol blue, 0.03% xylene cyanol FF, 60% glycerol 60 mM EDTA; Thermofischer, Cat. no.: R0611, Vilnius, Lithauania) in a 1:6 respectively. Samples of DNA or RNA were allowed to electrophorese on a 1% (w/v) agarose gel for 30 min while PCR products were electrophoresed on a 3% (w/v) agarose gel for 1–2 hours. In agarose gel electrophoresis, molecules are separated based on size and charge. An electric field influences the migration of the molecules. DNA, RNA and all negatively charged molecules migrate towards the positive pole. Large molecules migrate slower than small molecules through the gel (Sambrook and Russell, 2001). The gel was electrophoresed in TBE buffer consisting of 0.89 M Boric acid (Merck, Modderfontein, South Africa), 0.89 M Tris (Sigma Aldrich, St Louis, Missouri) and 0.5 M Ethylenediamintetra-acetic acid (EDTA) disodium salt (Sigma Aldrich, St Louis, Missouri) at a pH of 8. TBE buffer was used to prevent hydrolysis of the DNA as due to its slightly alkaline pH which works to chelate magnesium ions needed for hydrolysis (Stellwagen et al., 2000). To ensure visualisation of the nucleic acid, 10 mg/ml Ethidium Bromide (9 µL per 150 ml gel, Sigma Aldrich, St Louis, Missouri) was added to the gel before it was poured for setting. The UV-fluorescent dye, Ethidium bromide, intercalates into the DNA which can then be visualised under a UV light. Intact DNA presents as a single bright and distinct band while a smeared band is indicative of degraded DNA under UV light (Mayjonade et al., 2016).

2.10 Intracellular VDR protein quantification via flow cytometry

Flow cytometry is a commonly used method for the detection and quantification of both the physical chemical features of either a population of cells or any biological particle. A suspension of cells within in a fluid is injected into the flow cytometer ensuring that the cells are separated from each other and detected individually. It is commonly used to analyse the expression of target molecules on either the cell surface or within cells. Cell surface or intracellular molecule expression is quantified when the flow-cytometer detects and calculates fluorescence intensity which is emitted by fluorescently labelled antibodies (McKinnon, 2018). During experimentation, antibodies remained on ice and were protected

from light to not affect fluorescence detection during quantification. All steps in the preparation of reagents as well as any incubation steps were conducted at room temperature. Buffers and solutions were prepared fresh on the day of cell harvesting. For this protocol, 1.5 x 10^6 cells were first washed with 100 µl of PBS to remove excess cell media. The cells were then centrifuged at 500 x *g* for 5 min, to remove PBS. Cell pellets were then resuspended in 100 µl of 10% (v/v) heat-inactivated human serum in PBS and incubated for 1 min to block Fc receptors. The human serum was obtained from the University of Johannesburg and prepared by incubating the 10% (v/v) HS at 56 °C for 45 min. The cell samples were then centrifuged at 500 x *g* for 5 min and the human serum was then discarded leaving the cell pellets in the tube. Following blocking, the cells were then fixed with 100 µl of fixation solution containing 1.5% (w/v) paraformaldehyde (Sigma Aldrich, St Louis, MO) in PBS. Fixation is necessary to maintain cells in stasis at a particular point to ensure minimal deterioration and fixed protein localisation by the time they are examined (Lanier and Warner, 1981). The fixation solution was prepared in a light protected bottle which was placed on a heated stirrer until the paraformaldehyde was fully dissolved. The solution was cooled before being added to the cells. The paraformaldehyde and cell solution were shielded from light and left to incubate for 30 min. Following incubation, the cell suspension underwent a 5 min centrifugation step at 500 x *g.* 150 µl of permeabilisation solution composed of 0.2% (v/v) Triton X-100 (Sigma Aldrich, CAS# 9002-93-1, Modderfontein, SA) in PBS was then added to the cell suspension which was then left to incubate for 15 min. Triton X-100 is a suitable permeabilisation agent which is effective in dissolving cell membranes to improve the penetration of antibodies (Frisch, 2004). The cells were then centrifuged at 800 x *g* for 8 min to discard the excess permeabilisation solution. Cell staining was then achieved by adding 50 µl of Rabbit IgG antihuman VDR primary antibody (Novus Bio, USA, Cat. no. NBP2-66778) diluted 1:100 in PBS as per manufacturer protocols. The cells were then incubated in the VDR staining solution for 30 min. After primary antibody staining, 100 µl of wash buffer (0.1% Triton X-100 in PBS) was added to the cells which was followed by centrifugation at 800 x *g* for 8 min. The wash step was repeated to ensure complete removal of all unbound primary antibody. The cells were then suspended and aspirated in 50 µl of goat anti-Rabbit IgG secondary antibody, conjugated to Allophycocyanin (APC; R&D Systems, Canada, Cat. no. F0111), diluted 1:100 in PBS as per manufacturer protocols. This was followed by a second 30 min incubation period at room temperature sheltered from light. Instead of secondary antibody solution, 100 µl of 1% (w/v)

bovine serum albumin suspended in PBS (BSA, Sigma Aldrich, St Louis, MO) was added to the auto-fluorescent controls. Following secondary antibody staining, cells were resuspended and kept in 150 µl 1% (w/v) BSA in PBS. Samples remained on ice prior to fluorescence detection and measured no later than 2 hours from preparation on the BD Accuri ™ C6 Flow Cytometer (BD Biosciences, San Jose, CA). The flow cytometer is fitted with a blue (488 nm) and red (633 nm) laser. APC-conjugated VDR was detected at a wavelength of 633 nm (excitation: 620–650 nm, emission: 660–670 nm). Prior to measurement, the flow cytometer was calibrated using prepared 6- and 8-peak calibration beads (BD Accuri™ Spherotech 6-Peak (FL4)/ 8-Peak (FL1-3) validation Beads, Franklin Lakes, NJ, USA). Distilled water was run through the cytometer for 5–10 minutes prior to sample measurement to ensure the column was clean.

2.11 *In silico* annotation of *REN* regulatory regions

Bioinformatics which is a sub-discipline of biology, focuses on the procurement, identification and analysis of biological data specifically amino acid and nucleotide sequences. A variety of computer programs, applications and software are used to determine gene and protein functions from the vast publicly available databases and quite often is used to highlight key regulatory characteristics from large volumes of sequence data. In order to uncover the potential epigenetic mechanisms underlying *REN* regulation, a validated bioinformatic workflow (Meyer et al., 2017) was used to annotate regions within *REN* where changes in DNA methylation may have significant functional consequences.

2.11.1 Mapping of *REN* promoter, enhancer and silencer regions

The *REN* gene was analysed using Ensembl (www.ensembl.org/index.html), and data for its transcript was annotated. The *REN-201* transcript which spanned 11 518 kb, originates from the negative strand and contains 10 exons and 9 introns (chr1: 204 154 819 – 204 166 337). An experimentally validated promoter region was identified using the Genomatix (v3.10) Gene2Promoter (GRCh38; December 2017) tool (Fuchs et al., 2002). This 1116kb promoter region (chr1:204 166 222 – 204 167 337) was located upstream of *REN* traversing the 5' UTR and exon 1. An experimentally validated novel proximal enhancer (chr1: 204 168 923 – 204 171 222) spanning 2 299 bp was described by Ushiki et al. (2018). A second distal enhancer (chr1: 204 171 390 – 204 172 959) spanning 1 569 bp spanning was found using GeneHancer (www.genecards.org/Guide/GeneCard) data which was manually annotated to predict

enhancer regions in UCSC. Lastly, an experimentally validated silencer spanning 4028 bp (chr1: 204 162 166 – 204 166 193) was identified in intron 1 of *REN* (Lang et al., 1996).

2.11.2 Ranking and selection of *REN* CGIs to undergo methylation analysis

With respect to the mapping of general CGIs in *REN*, the GeneInfinity CGI detector tool (geneinfinity.org/sms/sms_cpgislands.html) was used classify CGIs in *REN* according to specific parameters. A general CGI was considered to have a GC percentage greater than 55%, an $Observed\ CpG/Expected\ CpG$ ratio greater than 0.65, and a minimum gap length of 100 bp. There were 5 CGIs in REN that met these guidelines. Two CGIs overlapped the distal enhancer (CGI1: 211 bp and CGI2: 336 bp) while two overlapped the proximal enhancer (CGI3:405bp and CGI4: 1847bp), and one in intron 1 of *REN*, overlapping the silencer (CGI5: 218 bp). For the identification of the EvoCGI and *bona fide* CGI, the March 2006 NCBI36/hg18 UCSC assembly (chr1: 202 390 571 – 202 402 088) was visualised with the publicly available EvoCGI and *bona fide* CGI coordinates which were mapped onto GRCh38 build using BLAT. This resulted in the identification of one *bona fide* CGI found spanning 216 bp located in exon 9 as well as one evolutionary CGI spanning 98 bp. Following annotation and mapping of key regulatory regions and CGIs within *REN*, a custom ranking system (Govender et al., 2021) was used to score genetic and epigenetic overlapping features of *REN* to select regions with the highest functional importance which were likely to be affected by changes in methylation. The scoring system found high scoring regions between the promoter and enhancer region overlapping CGI2. In order to reduce bias and represent the gene body, the highest scoring region within the silencer overlapping CGI5 was also selected for methylation analysis. In addition, the *Bona fide* CGI was also selected for further analysis.

2.11.3 Identification and annotation of putative TFBS within selected *REN* CGIs

Following ranking and selection of the *REN* CGIs, putative TFBS within the selected CGIs were identified using the The MatInspector tool (v.11.0; Quandt *et al*., 1995) available in the Genomatix Software Suite. In total, 478 out of the 3531 of the TFBS identified for all 7 CGIs. TFBS for the 3 selected CGIs were tabulated. Only TFBS core sequences with a matrix similarity of 0.9 or higher were selected and searched using the BLAT tool using the hg38 UCSC assembly to confirm their presence in *REN*.

2.11.3 Identification putative VDR binding sites within *TET1*, *TET2* and *TET3*

To confirm potential recruitment of TETs to induce active demethylation of *REN* in response to vitamin D, JASPAR (http://jaspar.genereg.net) data was used to identify putative VDR binding sites within the TETs. JASPAR, which is an open access database, contains several TF binding profiles which are encoded as position frequency matrices (PFM). This PFM TF-model represents the DNA binding specificity of a given TF based on the summary of each nucleotide at each position based on experimental data. The JASPAR 2018 track (Khan et al., 2018) was used as it contained sequences for human VDR (MA0693.3) in the collection, while the 2020 and 2022 tracks currently only have sequences for mouse VDR (MA0693.3) available as a track in the UCSC genome browser. A PFM score of 450 and above was used to select the highlighted putative VDR binding sites which is the equivalent of a P-value of $10^{-4.5}$

2.12 Quantitative DNA methylation analysis by MALDI-TOF MS

High-resolution quantitative DNA methylation analysis was outsourced to Inqaba Biotech (Biotechnical Industries (Pty) Ltd, Hatfield 0028, South Africa) who performed site-specific methylation analysis using MALDI-TOF MS, based on the EpiTYPER® approach (Fig. 2.1) developed by Agena Bioscience (Ehrich et al., 2007, 2005). The three highest scoring CGIs, CGI2 (Chr1: 204 171 238 – 204 171 573), CGI5 (Chr1: 204 171 238 – 204 171 573) and the *bona bide* CGI (Chr1: 204 155 754 – 204 155 968) were selected for further analysis as they yielded maximum information for single CpG dinucleotides. Primers (Table 2.8) were designed using the EpiDesigner software (Agena bioscience, http://www.epidesigner.com/start3.html). The software provides a detailed breakdown of these distinct CpG sites that were covered by the assay. The selected amplicons were located in the enhancer (CGI2) and silencer (CGI5) regions as well as intron 9 (*Bona fide* CGI) of *REN*. First the extracted HEK293 cell genomic DNA (10 nM $1,25(OH)_2D_3$ -treated and Control *VDR* $^+$ and *VDR* $^-$ samples) underwent bisulfite treatment. During bisulfite-conversion nonmethylated cytosine residues are converted into uracil while methylated cytosine residues are not unmodified (Frommer et al., 1992; Li and Tollefsbol, 2011). This step results in the generation of a DNA template with methylation-dependent sequence changes. The first step of the EpiTYPER assay begins with the use of T7-promoter-tagged reverse primers which amplify the target regions in a PCR reaction which will maintain the bisulfite -induced sequence modifications following *in-vitro* transcription. Thereafter, shrimp alkaline phosphatase (SAP) was used to dephosphorylate the deoxynucleotides in the PCR reaction to

inactivate them dephosphorylation using. Following SAP treatment, an *in vitro* transcription step results in specific cleavage at uracil residues by RNase A. MALDI-TOF MS is then used to analyse the cleavage products. The accumulated sequence changes which are generated through bisulfite treatment produce fragments with differing size and mass. This difference allows the data analysis software to generate quantitative information for each analysed target fragment. The differing mass-to-charge ratio between methylated vs unmethylated samples produces signal intensities which are correlated with the degree of DNA methylation which is then calculated as a percentage by the software.

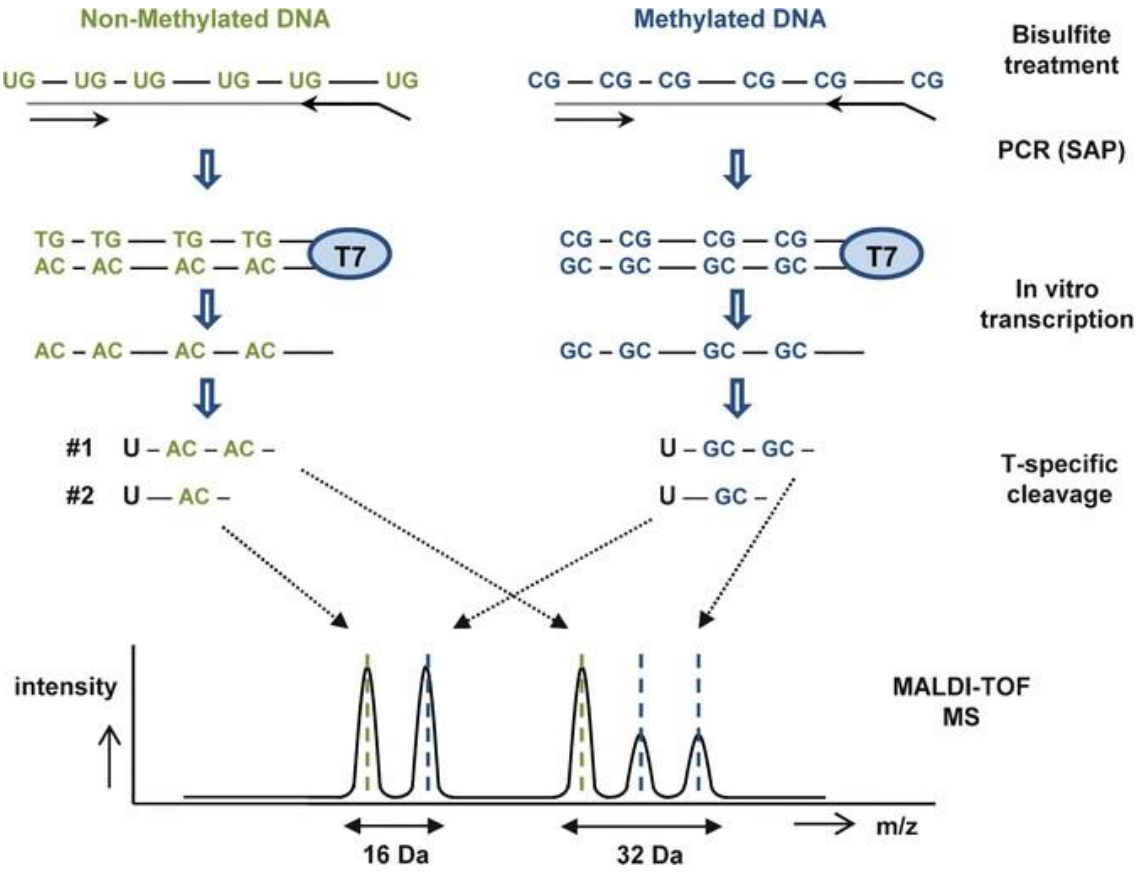

Figure 2.1. Overview of Epityper and MALDI-TOF MS process. Genomic DNA samples undergo bisulfite treatment to produce methylation-dependent sequence changes which are maintained by the T7-promoter-tagged reverse primer following *in vitro* transcription. The RNA fragments are then cleaved at uracil-specific residues resulting in differing mass-to-charge ratios (m/z) between methylated and non-methylated samples. MALDI-TOF MA analysis produces signal pattern pairs representing non-methylated (green) and methylated DNA (blue).

Table 2.8: Primer sequences for CGIs designed in Epidesigner for Epityper sequencing.

CGI	Primer Sequences	Product Size (bp)
CGI2	Forward: GAGGAATTAAGTTAGTAATAGGTGGTTA Reverse: ATAAAAACCCACAAACCTACAAACC	402
CGI5	Forward: GAATAAATTAGGTTTGGAATTATGGGT Reverse: CAAAATTTCTCCATATTAATCAAACT	324
Bona fide CGI	Forward: GTTTTAATATGATTTGTGTATTGTAATTTG Reverse: CAACCCTCTCCAACAAAAAAAC	294

2.13 Data processing and Statistical analysis

Data for RT-qPCR (Cq values), flow-cytometry (Fluorescence intensity) and methylation (%) were checked for outliers which were removed prior to statistical testing. For the siRNA transfection, %KD was calculated using the comparative ΔΔCq method (Livak and Schmittgen, 2001) for calculating relative gene expression by normalising to the reference gene (*GAPDH*) and the non-targeting control. In RNAi experiments, normalisation the nontargeting siRNA control is necessary to adjust for any off-target effects resulting from the transfection procedure. Percent knockdown was calculated by subtracting the normalized ΔΔCq expression from 1, which is set as the level of expression for the untransfected sample and multiplying by 100. Samples with a %KD of 80 or higher were used for gene expression and methylation analysis. Statistical analysis was conducted with IBM® SPSS® Statistics software (v. 26; SPSS Inc. Chicago, IL). Three biological replicates, each with 2 technical replicates, was done for the flow-cytometry, RT-qPCR and methylation experiments. For the gene expression analysis, Ct values were normalised to the geometric mean of the reference genes (*GAPDH* and *UBC*) and were expressed as values relative to the control average according to the MIQE guidelines (Vandesompele et al., 2002). For Flow-cytometry, auto-fluorescence

measurements for VDR protein level were subtracted from the Control and Treated sample fluorescence intensity values during data processing. The gene expression, VDR protein expression and Methylation percentage data were tested for normal distribution using the Kolmogorov–Smirnov tests to confirm normality. The Levene's test for equality of variance was used to evaluate the variance of data which then informed the use of the t-test result. An independent T-test (two-tailed) was used to assess the observed $1,25(OH)_2D_3$ induced changes in gene expression and protein level. Tests were analysed with a confidence interval of 95% and a P-value of < 0.05 was considered significant.

3.1 Quality control

3.1.1 HEK293 cell cultures were pure and free from *Mycoplasma* contamination

Mycoplasmas are a common bacterial contaminant and concern for cell culture growth as they are resistant to most common antibiotics used and can have a variety of effects on infected cells sometimes affecting cell viability and reducing the reliability of experimental results (Drexler and Uphoff, 2002; Rottem and Barile, 1993). To confirm that the cell cultures used in this study were pure and free from *Mycoplasma* contamination, the cultures were tested for *Mycoplasma* contamination by amplifying the *Mycoplasma* specific 23S rRNA operon coding gene using PCR. Both siRNA-lipofectamine transfected (*VDR* $^{-}$) or untransfected (*VDR* $^{+}$) HEK293 cells were cultured and treated with or without 10 nM 1,25$(OH)_2D_3$ and cell culture samples were used in a *Mycoplasma* PCR detection kit to confirm if any *Mycoplasma* was present. The results obtained showed no 259 bp band present in the test reaction lane confirming that no *Mycoplasma* was present in the cell media samples (Fig. 3.1).

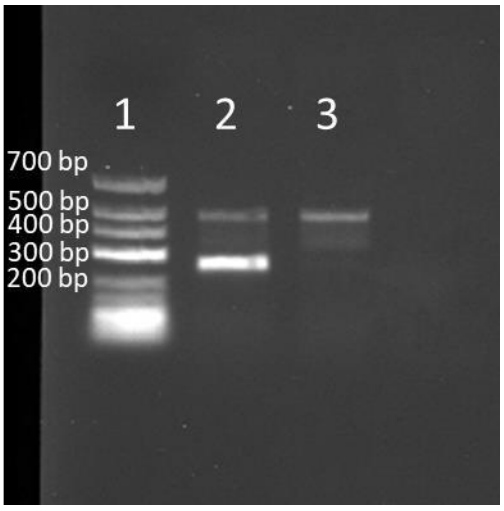

Figure 3.1. Representative agarose gel showing amplicon products from a *Mycoplasma* PCR detection test. The above 1% (w/v) agarose gel shows the *Mycoplasma* detection kit PCR reaction products. Lane 1 was loaded with a molecular weight marker. Lane 2 was loaded with the PCR product from the positive control sample and shows a distinct 259 bp band indicative of *Mycoplasma* as well as a faint 481 bp band due to the internal control DNA within the reaction mixture. Lane 3 contains the PCR product from the test sample reaction with supernatant from the media of the HEK293 cell culture used in the experiments. Lane 3 only contains the 481 bp band of the internal control DNA but has no bands matching the 259 bp *Mycoplasma* positive control band indicating that samples were free from *Mycoplasma* contamination.

3.1.2 Lipofectamine transfection and 1,25(OH)$_2$D$_3$ supplementation induced no significant change in cell viability in HEK293 cells

To confirm whether the siRNA lipofectamine based transfection, as well as 1,25(OH)$_2$D$_3$, influenced cell viability, the trypan blue exclusion assay was performed. It was observed that 10 nM 1,25(OH)$_2$D$_3$ supplementation did not significantly alter cell viability in either *VDR* $^+$ and *VDR* $^-$ HEK293 cells (Fig. 3.2). The lipofectamine siRNA transfection slightly reduced cell viability when compared to untransfected cell culture models (average untransfected viability = % vs transfected viability = %). The reduction in cell viability in the transfected cell culture models was not significant and the HEK293 cultures maintained a viability of > 85%, which was deemed sufficient for downstream analysis.

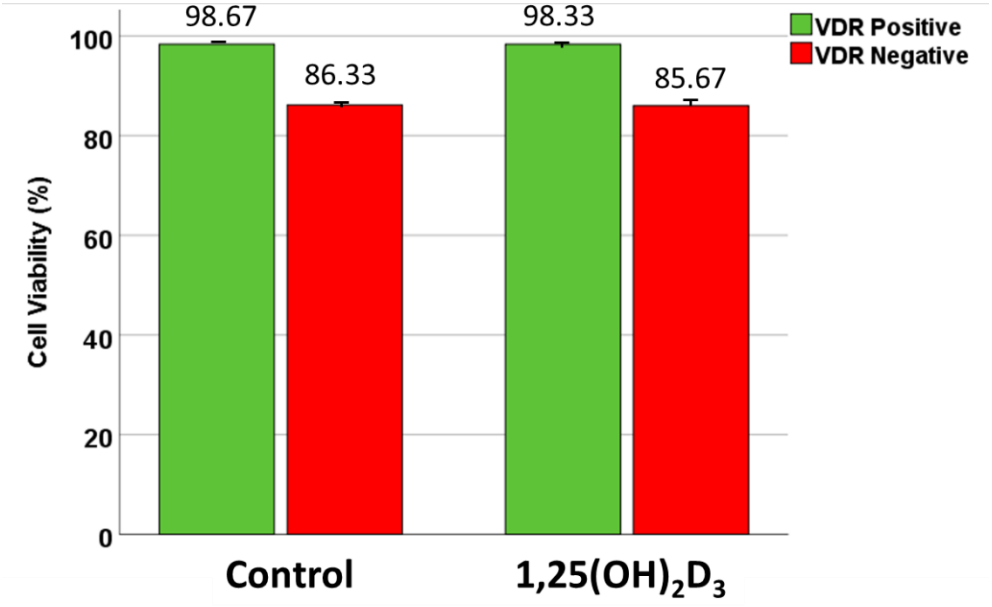

Figure 3.2. HEK293 cell viability was not significantly affected by 1,25(OH)2D3 supplementation cells. The bar graph shows the percentage HEK293 cell viability as calculated by means of Trypan blue exclusion assay in response to 10 nM 1,25(OH)$_2$D$_3$ supplementation in the *VDR* $^+$ samples (green) and the *VDR* $^-$ samples (red). The percentage cell viability is presented as the average ratio between the live cell count and the total cell count for each biological replicate.

3.1.3 Nucleic acid extractions

To assess the quality of the extracted nucleic acids, a sample of RNA/DNA from cells treated with or without 1,25(OH)$_2$D$_3$ was run on a 1.5% (w/v) agarose gel prior to RT-qPCR or bisulfite sequencing, respectively. The presence of two distinct and clear bands indicative of the 28S and 18S subunits of ribosomal RNA confirmed that the RNA extracts were intact (Fig. 3.3A).

The presence of intact DNA was confirmed by the thick bright band at the top of the agarose gel indicative of a high molecular weight (Fig. 3.3B). For DNA, 260/280 ratios of 1.8–2.0 and 260/230 ratios ranging between 2.0–2.2 ensured that the extracts were of high purity with little to no protein or RNA contamination. Additionally, RNA extracts also maintained high purity and were free from phenol and DNA contamination with 260/280 and 260/230 ratios of 1.7–2.0 and 2.0–2.2, respectively.

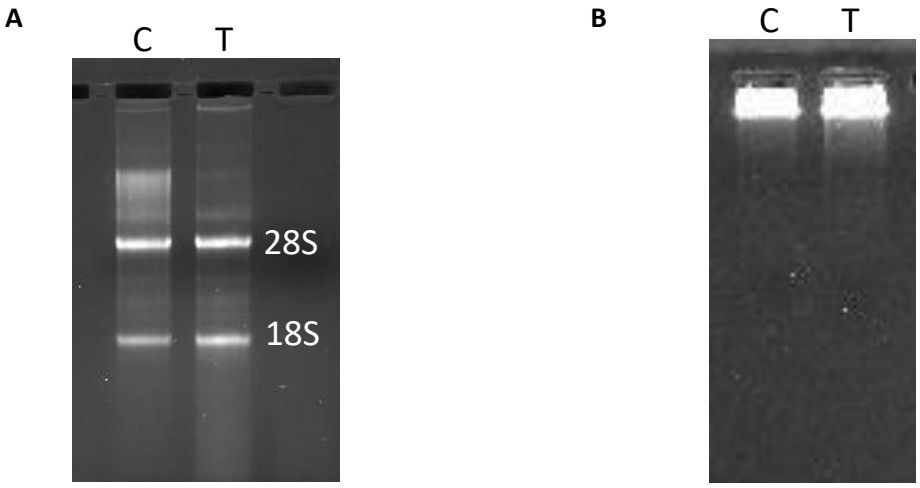

Figure 3.3. A representative 1.5% agarose gel showing intact high-integrity RNA and DNA extracts from HEK293 cells. The representative gels show RNA (A) and DNA (B) extracted from control (C) and treated (T; 10 nm $1,25(OH)_2D_3$) HEK293 cells using the RNA miniprep extraction kit and the QIAamp DNA Blood Mini kit, respectively. The two bands represent the 28S and 18S subunits of ribosomal RNA (A).The gels loaded with the nucleic acid extracts were visualised by under UV exposure and fluorescence of the intercalating agent ethidium bromide.

3.1.4 All RT-qPCR gene products were intact and specific to the target

Gene expression analysis was done via RT-qPCR to assess the effect of $1,25(OH)_2D_3$ on the expression of several target genes that may influence the regulation of *REN* through epigenetic mechanisms. The melt curve (Fig. 3.4) of each gene was analysed to verify that only one product, indicated by a single peak, was amplified using the Bio-Rad CFX Maestro software (v2.2) (Bio-Rad Laboratories, CA, USA). The melt-curve analysis showed that all PCR products generated a single peak above the threshold line (based on the no template control) with *REN* producing a slight shoulder peak below the threshold line. Additionally, to ensure the correct target amplicon was amplified during RT-qPCR for *REN, VDR, CYP24A1, NFKB1, DNMT1, DNMT3A, DNMT3B, TET1, TET2, TET3* as well as the reference genes *GAPDH and UBC*, all RT-qPCR products were run on 3% (w/v) agarose gels along with an appropriate molecular

weight marker (MWM; Fig. 3.5). The product sizes predicted by *in silico* PCR (https://genome.ucsc.edu/cgi-bin/hgPcr) matched the observed qPCR target amplicon sizes. This included a 277 bp product for *VDR*, a 71 bp product for *CYP24A1*, a 129 bp product for *REN,* a 151 bp product for *TET1*, a 194 bp product for *TET2*, a 152 bp product for *TET3*, a 204 bp product for *DNMT1*, a 175 bp product for *DNMT3A*, a 187 bp product for *DNMT3B*, a 395 bp product for *GAPDH* and a 133 bp product for *UBC.*

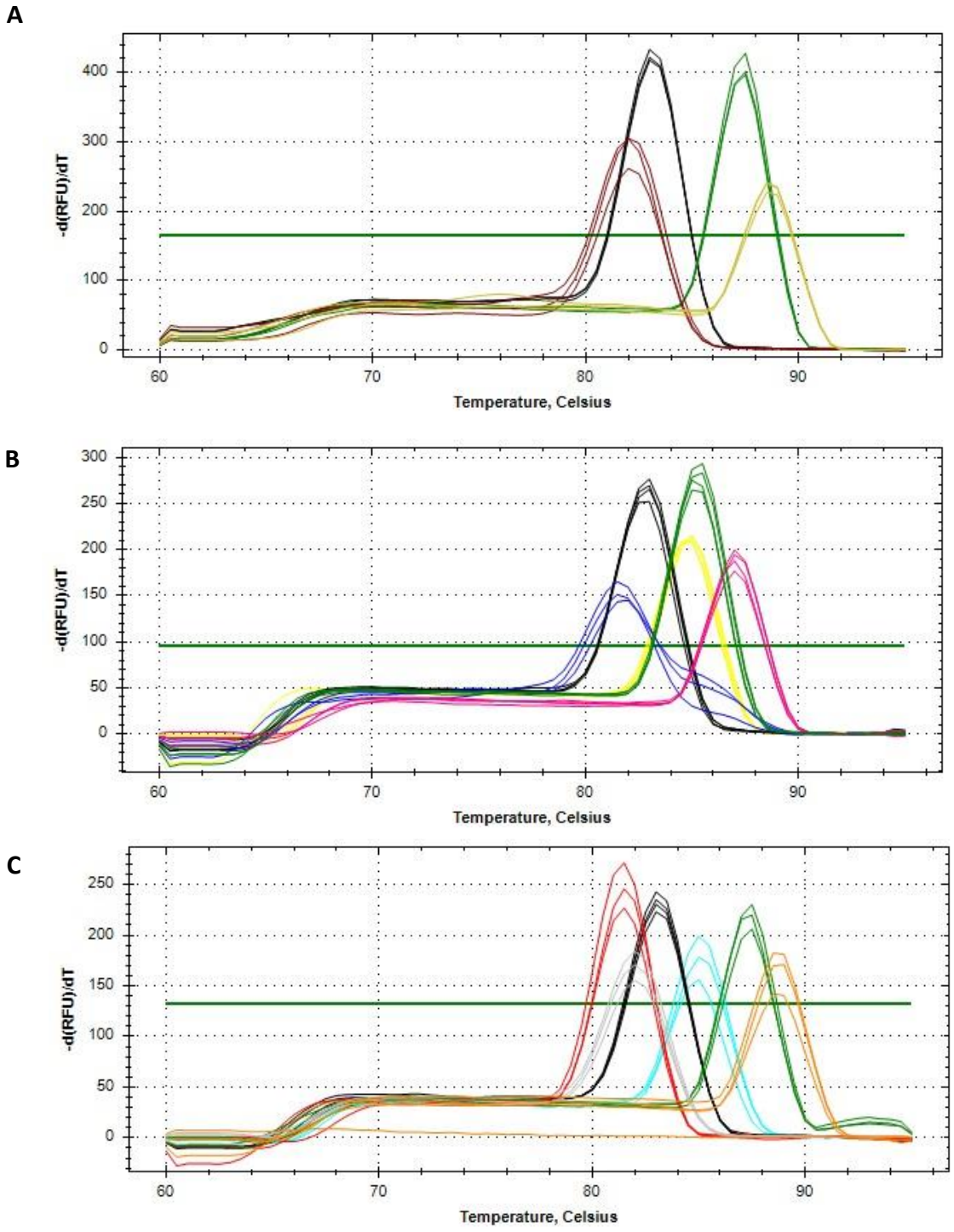

Figure 3.4. Representative melt curves of genes amplified by means of RT-qPCR. The melt curves show the change in relative fluorescence units over time (-d(RFU)/dT) against temperature (°C) and shows single melt peaks for the reference genes UBC (black) and *GAPDH* (dark green), as well as target genes *CYP24A1* (A; orange),*TET1* (A; Cyan) *DNMT1* (A; red), *DNMT3A* (A; grey), *REN* (B; Blue), *DNMT3B* (B; yellow), *TET2* (B; pink), *VDR* (C; beige) and *TET3* (C; maroon).

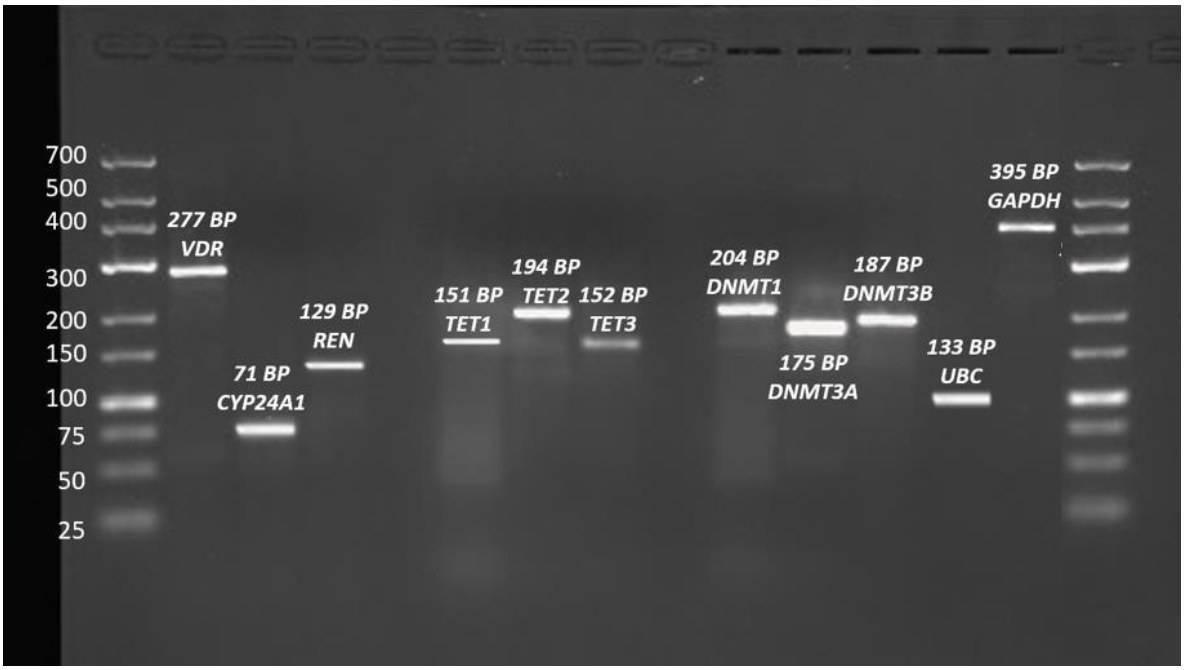

Figure 3.5. A representative agarose gel showing amplified genes of interest after RT-qPCR. The representative 3% agarose gel shows the RT-qPCR products of each primer pair (Lanes from left to right: VDR*, CYP24A1, REN, TET1, TET2, TET3, DNMT1, DNMT3A, DNMT3B, UBC* and *GAPDH*). A single band is observed for each gene at the expected base pair (bp) size using the GeneRuler™ Ultra Low Range DNA Ladder (Thermo Scientific™)

3.2 Both *VDR* mRNA and protein level increased in response to $1,25(OH)_2D_3$ supplementation in *VDR* $^+$ cells

The effects of $1,25(OH)_2D_3$ are mediated by VDR. Thus, expression of *VDR* may indicate an active cellular response to $1,25(OH)_2D_3$ treatment. To confirm whether $1,25(OH)_2D_3$ in conjunction with the VDR transcription factor influences *REN* regulation, HEK293 cells were cultured in the presence or absence of 10 nM $1,25(OH)_2D_3$ and both *VDR* mRNA and protein levels were quantified via RT-qPCR and flow-cytometry respectively. Both *VDR* expression ($P < 0.050$; Fig. 3.6 A) and protein level ($P < 0.050$; Fig. 3.6.D) was significantly increased in response to $1,25(OH)_2D_3$ supplementation.

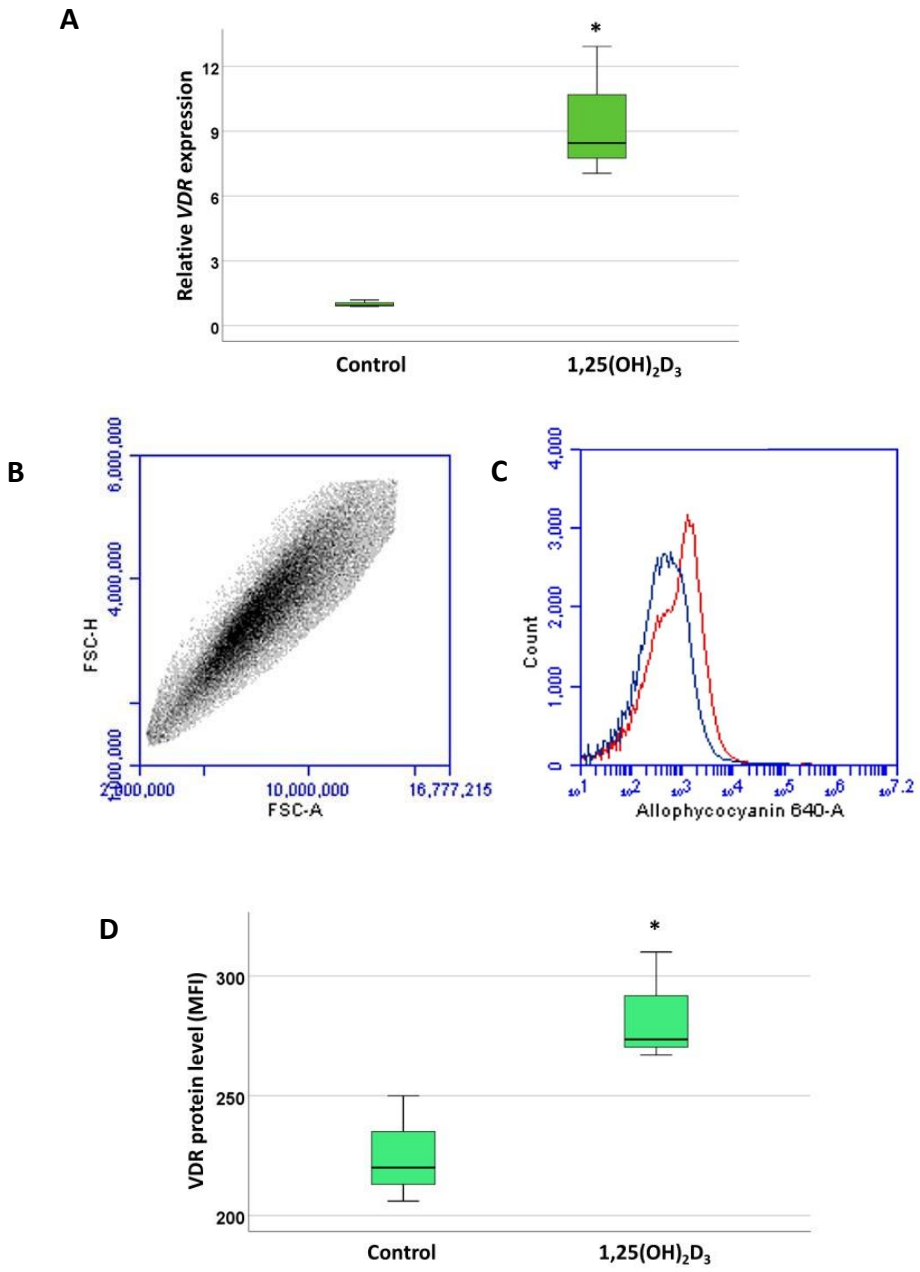

Figure 3.6. $1,25(OH)_2D_3$ significantly increased both VDR mRNA and protein level in HEK293 cells. The boxplots show the change in *VDR* expression (A) and protein level (D) in response to 10 nM $1,25(OH)_2D_3$, as quantified by RT-qPCR and flow cytometry, respectively. Pairwise comparisons indicate a significant increase in *VDR* (*P < 0.050) in response to 10 nM $1,25(OH)_2D_3$ (A). The representative density plot shows the forward-scatter (FSC-H) against the side-scatter (SSC-A) for HEK293 following gating to remove cell debris and cell doublets where each dot represents a cell (B). The fluorescence intensity (FI) histogram overlay displays the relative quantification of VDR protein in control (blue) and 10 nM $1,25(OH)_2D_3$ treated (red) cells showing an increase in the intensity of nuclear membrane expression of VDR per cell (C). Pairwise significant differences show an increase in VDR protein expression (* P < 0.050). Error bars show 95% confidence interval (n = 3).

3.3 *CYP24A1* mRNA level increased in response to $1,25(OH)_2D_3$ supplementation in *VDR* $^+$ cells

To confirm whether $1,25(OH)_2D_3$ in conjunction with the VDR transcription factor was functional in the HEK293 cells, the expression of *CYP24A1* was quantified as a marker of VDR activity. *CYP24A1* is a primary $1,25(OH)_2D_3$ target gene with known VDREs (Chen and DeLuca, 1995; Ohyama et al., 1996; Zierold et al., 1994). As expected, *CYP24A1* expression increased significantly in response to $1,25(OH)_2D_3$ ($P < 0.050$; Fig. 3.7). This confirms that VDR is not only expressed but is functional in HEK293 cells.

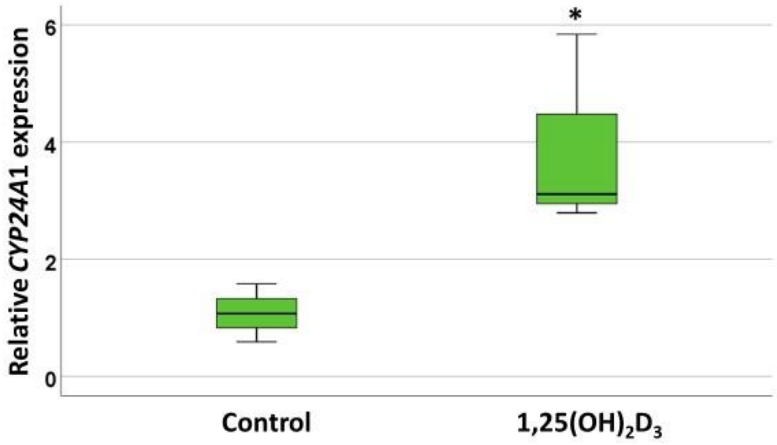

Figure 3.7. $1,25(OH)_2D_3$ induced CYP24A1 expression in *VDR* $^+$ HEK293 cells. The boxplot shows *CYP24A1* expression in response to 10 nM $1,25(OH)_2D_3$ in HEK293 cells, as quantified by RT-qPCR. Pairwise comparisons indicate a significant increase in *CYP24A1* (*$P < 0.050$) in response to 10 nM $1,25(OH)_2D_3$. Error bars show 95% confidence interval (n = 3).

3.4 *REN* mRNA level decreased in response to $1,25(OH)_2D_3$ supplementation in *VDR* $^+$ cells

To confirm whether $1,25(OH)_2D_3$ may be associated with blood pressure and the RAAS, *VDR* $^+$ HEK293 cells were cultured in the presence or absence of 10 nM $1,25(OH)_2D_3$ and expression of *REN* – the rate-limiting factor in the RAAS pathway- was quantified via RT-qPCR. *REN* expression, decreased significantly in response to $1,25(OH)_2D_3$ ($P < 0.010$; Fig. 3.8).

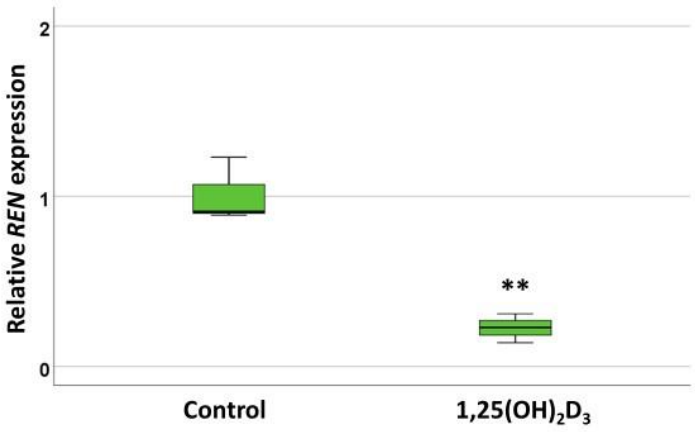

Figure 3.8. $1,25(OH)_2D_3$ significantly decreased REN expression in *VDR* $^+$ HEK293 cells. The boxplot shows *REN* expression in response to 10 nM $1,25(OH)_2D_3$ in HEK293 cells, as quantified by RT-qPCR. Pairwise comparisons indicate a significant increase in *CYP24A1* (*P < 0.010) in response to 10 nM $1,25(OH)_2D_3$. Error bars show 95% confidence interval (n = 3).

3.5 10nM $1,25(OH)_2D_3$ supplementation induced significant demethylation at the *REN* silencer and increased methylation at the *REN* enhancer in *VDR* $^+$ HEK293 cells

DNA methylation, which is a widely studied epigenetic mark can affect the binding of TFs to DNA to regulate gene expression (Esteller, 2008; Héberlé and Bardet, 2019). To confirm whether the observed *REN* suppression is linked to changes in *REN* methylation, methylation of high-ranking selected CGIs -CGI2 (Chr1: 204 171 238 – 204 171 573), CGI5 (Chr1: 204 171 238 – 204 171 573) and a *bona fide* CGI (Chr1: 204 155 754 – 204 155 968) within the regulatory regions of *REN* were quantified using the Epityper approach via MALDI-TOF mass array. On average, the selected CGIs were hypermethylated. On a regional level, CGI5 was significantly less methylated than both CGI2 and the *bona fide* CGI for both control and treated conditions (** P < 0.005). Additionally, there was a significant difference in regional methylation of CGI5 between control and treated conditions (* P < 0.05), while no significant difference in regional methylation was observed for CGI2 or the *bona fide* CGI in response to 10 nM $1,25(OH)_2D_3$ treatment in *VDR* $^+$ HEK293 cells. On a site-specific level, CpG sites 1 and 5 of CGI5 became hypomethylated in the presence of $1,25(OH)_2D$ with CpG site 1 methylation significantly decreasing in response to 10 nM $1,25(OH)_2D_3$ (P < 0.050) in *VDR* $^+$ HEK293 cells. In contrast, methylation of CpG sites 13 and 15-17 of CGI2 overlapping the *REN* enhancer increased in response to 10 nM $1,25(OH)_2D_3$ in the *VDR* $^+$ HEK293 cells (Fig. 3.9). 10 nM

$1,25(OH)_2D_3$ supplementation does not appear to have an effect on the *bona fide* CGI that overlapping intron 9 of *REN*.

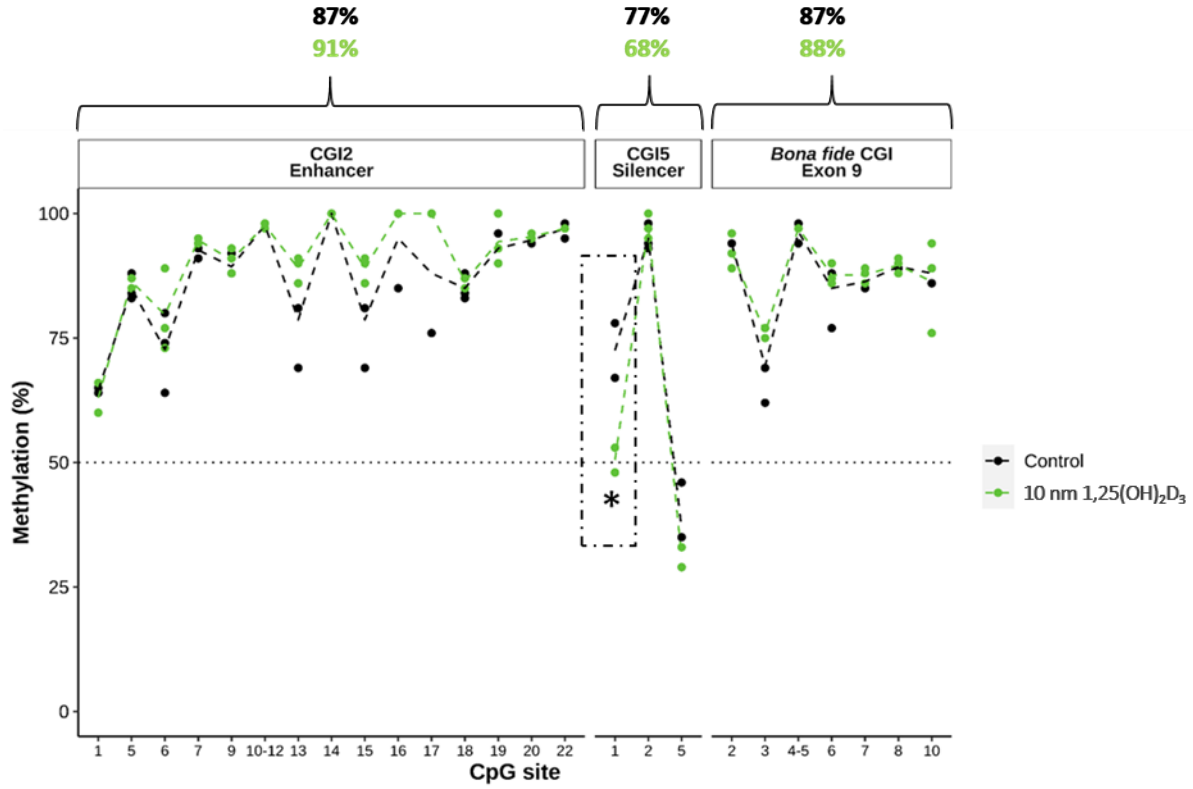

Figure 3.9. $1,25(OH)_2D_3$ induced changes in methylation at both the REN silencer and enhancer regions in *VDR*$^+$ HEK293 cells. *In vitro* changes in regional methylation of selected *REN* CGIs were quantified via MALDI-TOF mass spectrometry in both control and treated cells (treated for 18 h with 10 nM $1,25(OH)_2D_3$). Pairwise comparisons indicate a significant decrease in *REN* methylation at CpG site 1 of CGI5 (Chr 1: 204 165 151 – 204 165 368) located near the silencer in *VDR*$^+$ HEK293 cells (*$P < 0.050$) in response to 10 nM $1,25(OH)_2D_3$. Methylation at CpG sites 13, 15, 16 and 17 of CGI2 (Chr1: 204 171 238 – 204 171 573) located near the enhancer showed increased in response to 10 nM $1,25(OH)_2D_3$. Average % methylation for each region was calculated for both control and treated samples.

3.6 TFBS were mapped and annotated within the high-ranking selected CGI regions of *REN* used for methylation analysis

Gene transcriptional regulation is often mediated by TFs which are able to bind specific regions of DNA at a given time to either induce or repress a gene's transcription. To identify and confirm the role of methylation-dependent TF binding in the transcription of *REN* in response to $1,25(OH)_2D_3$, the MatInspector tool (Matbase v11.0) (Quandt et al., 1995) from the Genomatix software suite (v3.10) was used to identify putative TFBS in *REN*. The core binding sequences of TFs with a matrix similarity score of 0.9 and above were identified. TFs known to be specifically associated with *REN* transcription and exclusively expressed in the kidneys were then selected and tabulated (Tables 3.1–3.3). Each core binding sequence provided by genomatix was then searched in the UCSC browser with the BLAT tool to confirm their presence in *REN* and were then annotated on the CGI sequences (Fig. 3.10–12).

Table 3.1: TFBS families important for expression of *REN* as identified using MatInspector from Genomatix in CGI

CGI 2 – Chr1: 204 171 238 – 204 171 573					
Matrix Family	**Matrix**	**Detailed Family Information**	**Matrix score**	**Sequence**	**Coordinates (Chr 1)**
NF1F	V$NF1.04	Nuclear factor 1	0.922	ATGGCGTGAACCCGGGAAGCG	204171292-204171312
MAZF	V$MAZ.01	Myc associated zinc fingers	0.903	AATGGCGTGAACC	204171301-204171313
ZTRE	V$ZTRE.04	Zinc transcriptional regulatory element	0.998	GGCAGGAGAATGGCGTG	204171305-204171321
KLFS	V$BKLF.02	Krueppel like transcription factors	0.939	TGAGGCAGGAGAATGGCGT	204171306-204171324
NDPK	V$NM23.01	Nucleoside diphosphate kinase	0.918	AGGCAGGAGAATGGCGT	204171306-204171322
CREB	V$XBP1.01	cAMP-responsive element binding proteins	0.920	TGGCTAACAAGGTGAAACCCC	204171397-204171417
EBOX	V$MNT.01	E-box binding factors	0.990	GCTAACAAGGTGAAACC	204171399-204171415
HMTB	V$MTBF.01	Human muscle-specific Mt binding site	0.902	TCGAGACCA	204171421-204171429
RBPF	V$RBPJK.02	RBPJ - kappa	0.954	GGAGATCGAGACC	204171422-204171434
AP4R	V$AP4.03	AP4 and related proteins	0.972	ATCATGAGGTCAGGAGA	204171430-204171446
HOXF	V$NANOG.01	Paralog hox genes 1-8 from the four hox clusters A, B, C, D	0.957	GCTCACGCCTGTAATCCCA	204171473-204171491
YBXF	V$YB1.01	Y-box binding transcription factors, multifunctional proteins involved in transcriptional and translational regulation, mRNA splicing, DNA replication and repair	0.933	ACGCCTGTAATCC	204171475-204171487
NF1F	V$NF1.04	Nuclear factor 1	0.929	GAAAGTAGGCTTGCGGCTGG	204171499-204171519
ZFXY	V$ZFX.01	Zfx and Zfy - transcription factors implicated in mammalian sex determination	0.996	GTAGAAAGTAG	204171512-204171522
EBOX	V$USF.04	E-box binding factors	0.906	GACGCCATTTGGTAAGT	204171521-204171537
ZFHX	V$SIP1.01	Two-handed zinc finger homeodomain transcription factors	0.985	ACGCCATTTGGTA	204171524-204171536
ZFHX	V$DELTAEF1.02	Two-handed zinc finger homeodomain transcription factors	1.000	AGCTTAGGGACGC	204171533-204171545

Table 3.2: TFBS families important for expression of *REN* as identified using MatInspector from Genomatix in CGI5

CGI 5 (Chr1: 204 171 238 – 204 171 573)					
Matrix Family	**Matrix**	**Detailed Family Information**	**Matrix score**	**Sequence**	**Coordinates (Chr 1)**
KLFS	V$GKLF.02	Krueppel like transcription factors	0.961	ATGGAGAAACCCTGTCTCT	204165154-204165172
TAIP	V$CSRNP1.01	TGF-beta induced apoptosis proteins	1.000	AAGACCA	204165184-204165190
EBOX	V$USF1.01	E-box binding factors	0.956	AGCAGTGGCTCACGCCT	204165247-204165263
E2FF	V$E2F1.01	E2F-myc activator/cell cycle regulator	0.992	TTTGGCCGGGAGCAGTG	204165257-204165273
XBBF	V$RFX4.02	X-box binding factors	0.919	TTCTTACAAATATCAAAAG	204165279-204165297
AHRR	V$AHRARNT.03	AHR-arnt heterodimers and AHR-related factors	0.971	AGTACTACAGGATAGATTCTTACAA	204165289-204165313
KLFS	V$GKLF.03	Krueppel like transcription factors	0.988	TACTGTTAGTACTACAGGA	204165302-204165320
YY1F	V$YY1.02	Activator/repressor binding to transcription initiation site	0.944	TGGGCACGTTGTAAGAGCCCAGC	204165321-204165343
ZF11	V$ZBTB3.01	C2H2 zinc finger transcription factors 11	0.995	GGAGATAAGGC	204165353-204165363

Table 3. 3: TFBS families important for expression of *REN* as identified using MatInspector from Genomatix in *bona fide* CGI

***Bona Fide* CGI (Chr1: 204 155 754 – 204 155 968)**					
Matrix Family	**Matrix**	**Detailed Family Information**	**Matrix score**	**Sequence**	**Coordinates (Chr 1)**
KLFS	V$GKLF.01	Krueppel like transcription factors	0.918	GGACAGAGACCCTCAAAGA	204155759-204155777
SPZ1	V$SPZ1.01	Testis-specific bHLH-Zip transcription factors	0.951	CAGGGAGAAAG	204155781-204155791
HAND	V$TAL1_E2A.02	Twist subfamily of class B bHLH transcription factors	0.991	TCGAGTCGGCCCCCTCGGTGG	204155792-204155812
SP1F	V$SP1.03	GC-Box factors SP1/GC	0.933	GCGGACTATGTATTTCA	204155821-204155837
KLFS	V$KLF2.01	Krueppel like transcription factors	0.991	CCCCGACATCTCTTTCCAC	204155868-204155886
CLOX	V$CPHX.01	CLOX and CLOX homology (CDP) factors	0.957	CGTGAAGTGTAACGAGGGCCCTA	204155891-204155913
CREB	V$CREB1.02	cAMP-responsive element binding proteins	0.948	ATGTCGTGAAGTGTAACGAGG	204155897-204155917
NEUR	V$NEUROD1.02	NeuroD, Beta2, HLH domain	0.972	CCCCCACCCCAGTAT	204155916-204155930
EREF	V$ESR2.01	Estrogen response elements	0.904	TTTGCCCCCCACCCCAGTA	204155917-204155935
MAZF	V$MAZ.01	Myc associated zinc fingers	0.920	CCACCAGCGCAGG	204155980-204155992

CGI2 Chr1: 204 171 238 – 204 171 573 (without flanking region) 336 bp

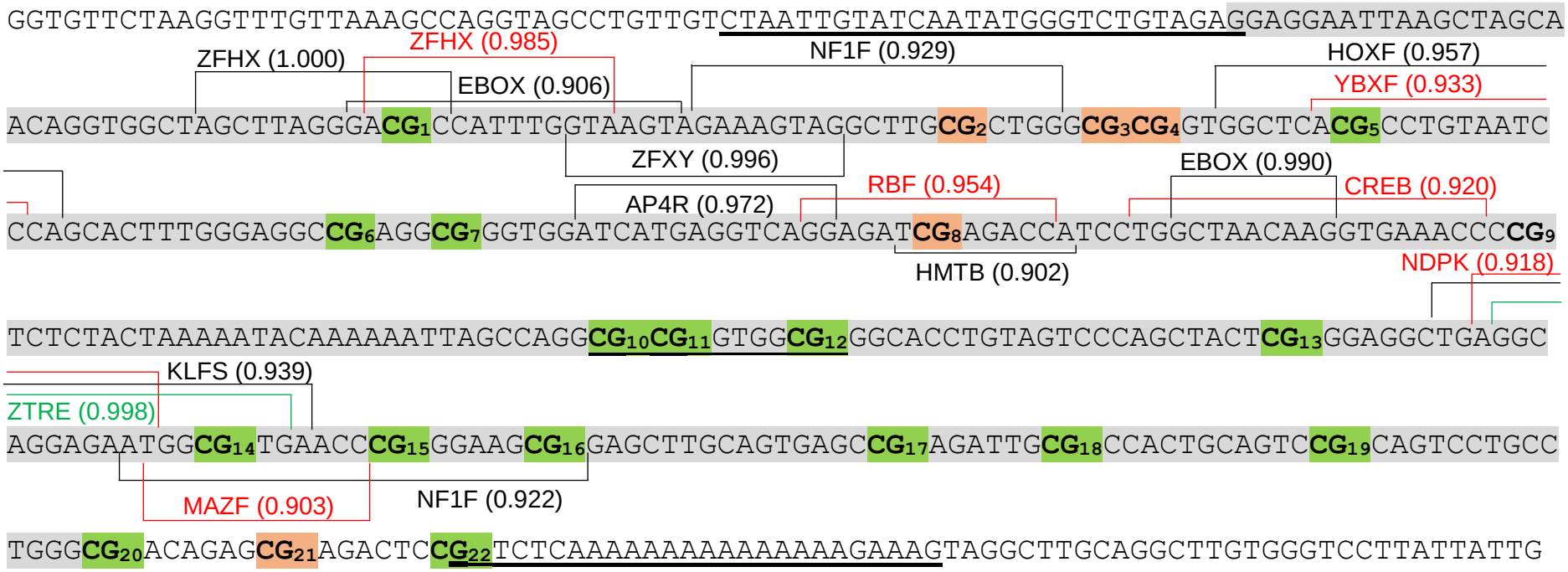

Figure 3.10. The PCR-amplified region of the *REN* gene spanning CGI 2 containing 20 CpG sites and several putative transcription factor binding sites. The diagram shows the PCR-amplified region (primer binding sites underlined) of *REN* in CGI 2 (chr1: 204 171 238 – 204 171 573; shaded in grey) and flanking region (unshaded), used in the Epityper approach to quantification of regional methylation via MALDI-TOF mass array in response to 10 nM $1,25(OH)_2D_3$ supplementation in *VDR* $^+$ and *VDR* $^-$ HEK293 cells. The diagram shows the CpG dinucleotides covered with the Epityper assay (Shaded light green) and the CpGs that were not covered (Shaded pink). Core binding motifs for putative transcription factor binding sites with a matrix similarity > 90% are shown (mapped by Genomatix MatInspector Professional v11.0).

CGI5 Chr1: 204 165 151 – 204 165 368 (without flanking region) 218 bp

Figure 3.11. The PCR-amplified region of the *REN* gene spanning CGI 5 containing 5 CpG sites and several putative transcription factor binding sites. The diagram shows the PCR-amplified region (primer binding sites underlined) of *REN* in CGI 5 (204 165 151 – 204 165 368; shaded in grey) and flanking region (unshaded), used in the Epityper approach to quantification of regional methylation via MALDI-TOF mass array in response to 10 nM $1,25(OH)_2D_3$ supplementation in HEK293 cells. The diagram shows the CpG dinucleotides covered with the Epityper assay (Shaded light green) and the CpGs that were not covered (Shaded pink). Core binding motifs for putative transcription factor binding sites with a matrix similarity > 90% are shown (mapped by Genomatix MatInspector Professional v11.0).

***bona fide* CGI Chr1: chr1: 204 155 754 – 204 155 968 (without flanking region) 215 bp**

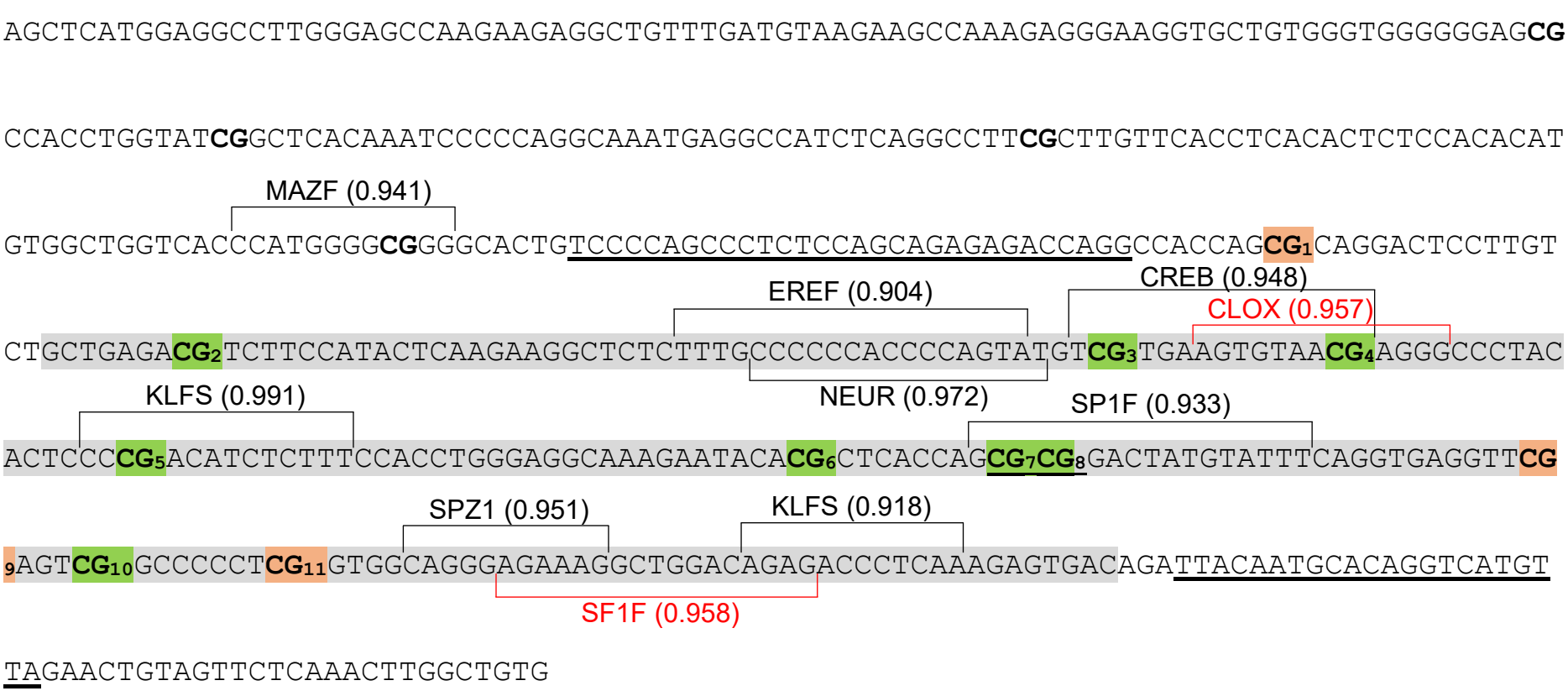

Figure 3.12. The PCR-amplified region of the *REN* gene spanning the *bona fide* CGI containing 11 CpG sites and several putative transcription factor binding sites. The diagram shows the PCR-amplified region (primer binding sites underlined) of *bona fide* CGI (chr1: 204 155 754 – 204 155 968; shaded in grey) and flanking region (unshaded), used in the Epityper approach to quantification of regional methylation via MALDI-TOF mass array in response to 10 nM $1,25(OH)_2D_3$ supplementation in HEK293 cells. The diagram shows the CpG dinucleotides covered with the Epityper assay (Shaded light green) and the CpGs that were not covered (Shaded pink). Core binding motifs for putative transcription factor binding sites with a matrix similarity > 90% are shown (mapped by Genomatix MatInspector Professional v11).

3.7 *DNMT1*, *DNMT3A* and *DNMT3B* gene expression did not change in response to $1,25(OH)_2D_3$ supplementation in *VDR* $^+$ HEK293 cells

To assess whether the changes in DNA methylation in HEK293 cells, in response to 10 nM $1,25(OH)_2D_3$ supplementation, correspond to a change in the expression of genes encoding DNA methylating enzymes, *DNMT1*, *DNTM3A* and *DNMT3B* gene expression levels were quantified by RT-qPCR. In *VDR* $^+$ HEK293 cells, 10 nM $1,25(OH)_2D_3$ had no significant on *DNMT1*, *DNTM3A* and *DNMT3B* expression (Fig. 3.13).

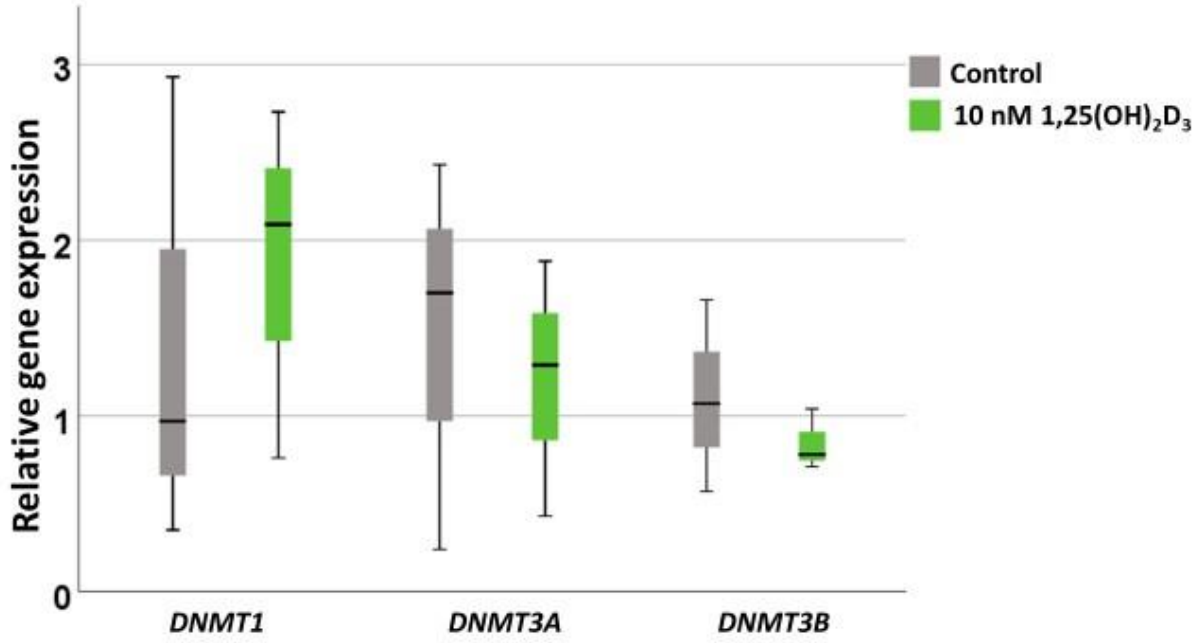

Figure 3.14. $1,25(OH)_2D_3$ had no significant effect on *DNMT1*, *DNMT3A* and *DNMT3B* expression in *VDR* $^+$ HEK293 cells. The boxplot shows *DNMT1, DNMT3A* and *DNMT3B* expression in response to 10 nM $1,25(OH)_2D_3$ in HEK293 cells, as quantified by RT-qPCR. Pairwise comparisons indicate no significant increase in any *of the DNMTs* in response to 10 nM $1,25(OH)_2D_3$. Error bars show 95% confidence interval (n = 3).

3.8 *TET1* and *TET2* mRNA level increased in response to 1,25(OH)$_2$D$_3$ supplementation while *TET3* expression was not changed *in VDR* $^+$ cells

To assess whether the observed 10 nM 1,25(OH)$_2$D$_3$ induced demethylation at the *REN* silencer in *VDR* $^+$ HEK293 cells was mediated by the DNA demethylating enzymes, *TET1, TET2* and *TET3* gene expression levels were quantified by RT-qPCR. It was found that 10 nM 1,25(OH)$_2$D$_3$ significantly induced both *TET1* ($P < 0.050$) and *TET2* expression ($P < 0.050$), but induced no significant change in *TET3* in *VDR* $^+$ HEK293 cells (Fig. 3.14).

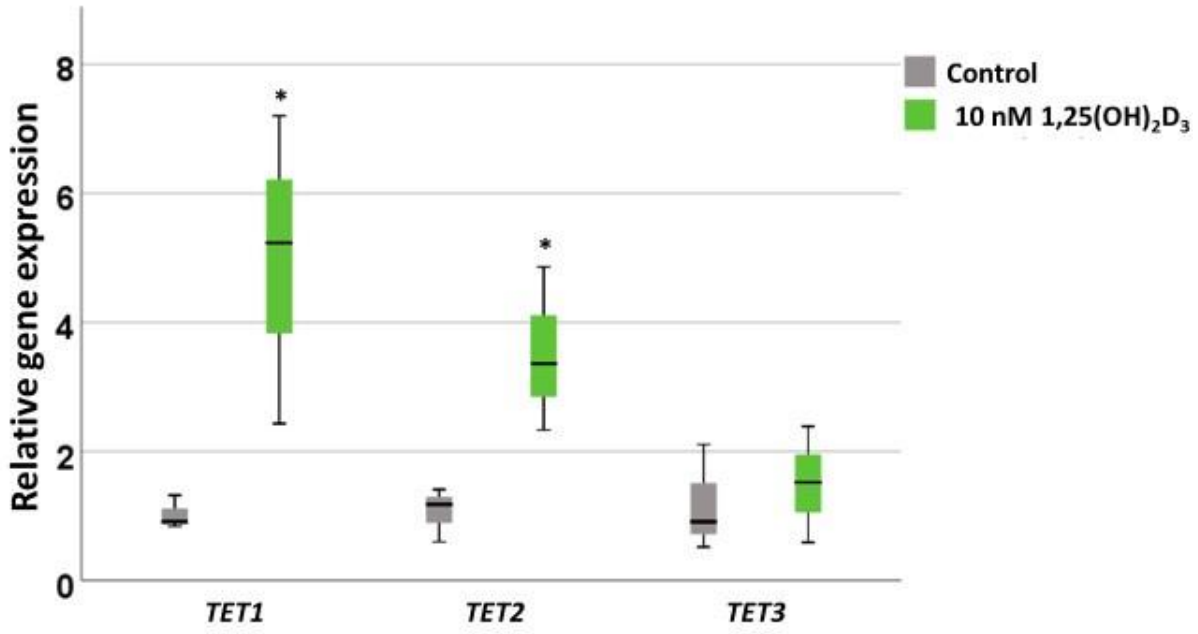

Figure 3.15. 1,25(OH)$_2$D$_3$ induced *TET1* and *TET2* expression but had no significant effect on *TET3* expression in *VDR* $^+$ HEK293 cells. The boxplot shows *TET1, TET2* and *TET3* expression in response to 10 nM 1,25(OH)$_2$D$_3$ in HEK293 cells, as quantified by RT-qPCR. Pairwise comparisons indicate a significant increase in *TET1* (* $P < 0.050$) and TET2 (* $P < 0.050$) but no significant difference in TET3 in response to 10 nM 1,25(OH)$_2$D$_3$. Error bars show 95% confidence interval (n = 3).

3.9 *TET1, TET2* and *TET3* contain putative VDR binding sites

To further confirm that the observed demethylation at the *REN* silencer in response to 10 nM $1,25(OH)_2D_3$ was mediated via VDR recruitment of TETs, putative VDR binding sites were identified in all 3 TETs using the JASPAR 2018 track -containing putative binding sites for human VDR- which was added to the UCSC genome browser (https://genome.ucsc.edu/) on the Human (GRCh38/hg38) assembly. All 3 TETs contained putative VDR binding sites scattered across both the gene body and upstream and downstream flanking regions (Fig. 3.15). VDR binding sites were highlighted to show their position within the gene.

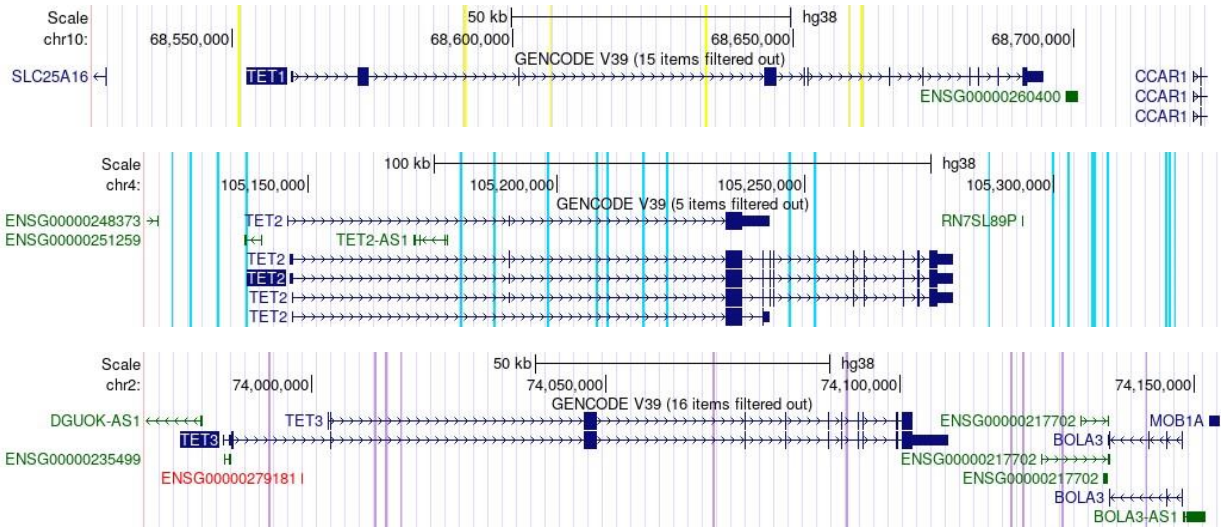

Figure 3.16. Putative VDR binding sites located in TETs. The UCSC genome browser was used to annotate VDR binding sites within *TET1* (yellow), *TET2* (blue) and *TET3* (purple). Only binding sites with a PFM of 450 and above were highlighted. *TET1* contained 6 VDR binding sites overall with one in the 5' UTR and 5 in intronic regions. *TET2* contained 21 VDR binding sites with 4 in the 5' UTR, 9 in intronic regions and 8 in the 3' UTR. TET3 contained 10 VDR binding sites with 6 in intronic regions and 4 in the 3' UTR.

3.10 siRNA-mediated *VDR* gene knockdown established a *VDR* $^{-}$ HEK293 cell culture

To confirm the role of 1,25$(OH)_2D_3$ and VDR in regulating *REN* expression, the *VDR* gene was silenced in HEK293 cells via lipofectmine- based siRNA transfection in order to conduct and compare experimental results in both *VDR* $^{+}$ and *VDR* $^{-}$ cell culture models. To confirm successful gene knockdown, *VDR* mRNA level and protein level was quantified via RT-qPCR and flow-cytometry respectively. Up to 80% gene knockdown was achieved (Fig. 3.16 A) in both the control and treated samples. VDR protein expression significantly decreased (Fig. 3.16 B) following siRNA transfection in both the control and treated samples.

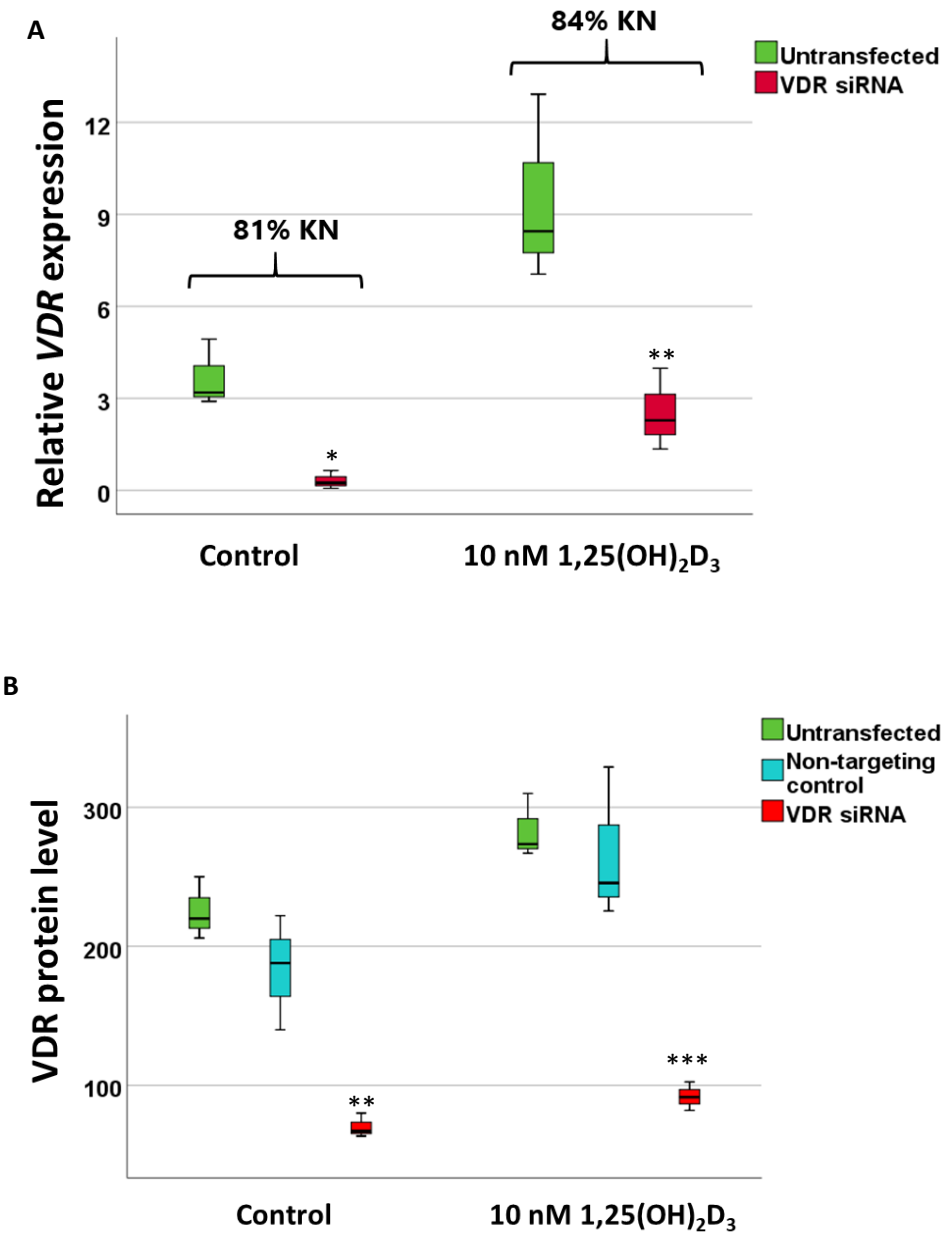

Figure 3.17. Boxplots showing VDR mRNA and protein level in response to 10 nM $1,25(OH)_2D_3$ in *VDR* $^+$ and VDR $^-$ HEK293 cells. siRNA targeted against *VDR* was transfected into HEK293 cells and cDNA was synthesised from RNA isolated 48 hours post-transfection. *VDR* and reference gene (*GAPDH*) cDNA was amplified by qPCR. Relative gene expression values were used to calculate % KD following normalisation to a non-targeting siRNA control. *VDR* mRNA level in the *VDR*-targeting siRNA treated samples significantly decreased when compared to the untransfected samples in both the $1,25(OH)_2D_3$ treated (** $P < 0.010$) and vehicle control (* $P < 0.050$) groups in HEK293 cells (A). VDR protein level was quantified and compared between the untransfected-control, non-targeting control and *VDR*-targeting siRNA samples via flow-cytometry (B). VDR protein level in *VDR*-targeting siRNA treated samples significantly decreased when compared to the samples in both the $1,25(OH)_2D_3$ treated (*** $P < 0.001$) and vehicle control (** $P < 0.010$) groups in HEK293 cells. Pairwise significant differences are shown. Error bars show 95% confidence interval (n = 3).

3.11 *REN*, *TET1* and *TET2* mRNA level did not change in response to 1,25(OH)$_2$D$_3$ supplementation in *VDR* $^-$ HEK293 cells

In order to confirm that the observed changes in *REN*, *TET1* and *TET2* expression in the *VDR* $^+$ HEK293 cells in response to 1,25(OH)$_2$D$_3$ were a direct result of 1,25(OH)$_2$D$_3$ supplementation and subsequent VDR activity, gene expression analysis via RT-qPCR was repeated in the *VDR* $^-$ HEK293 cells. No significant changes in either *REN*, *TET1* or *TET2* gene expression was observed in the *VDR* $^-$ samples in response to 10 nM 1,25(OH)$_2$D$_3$ (Fig. 3.17)

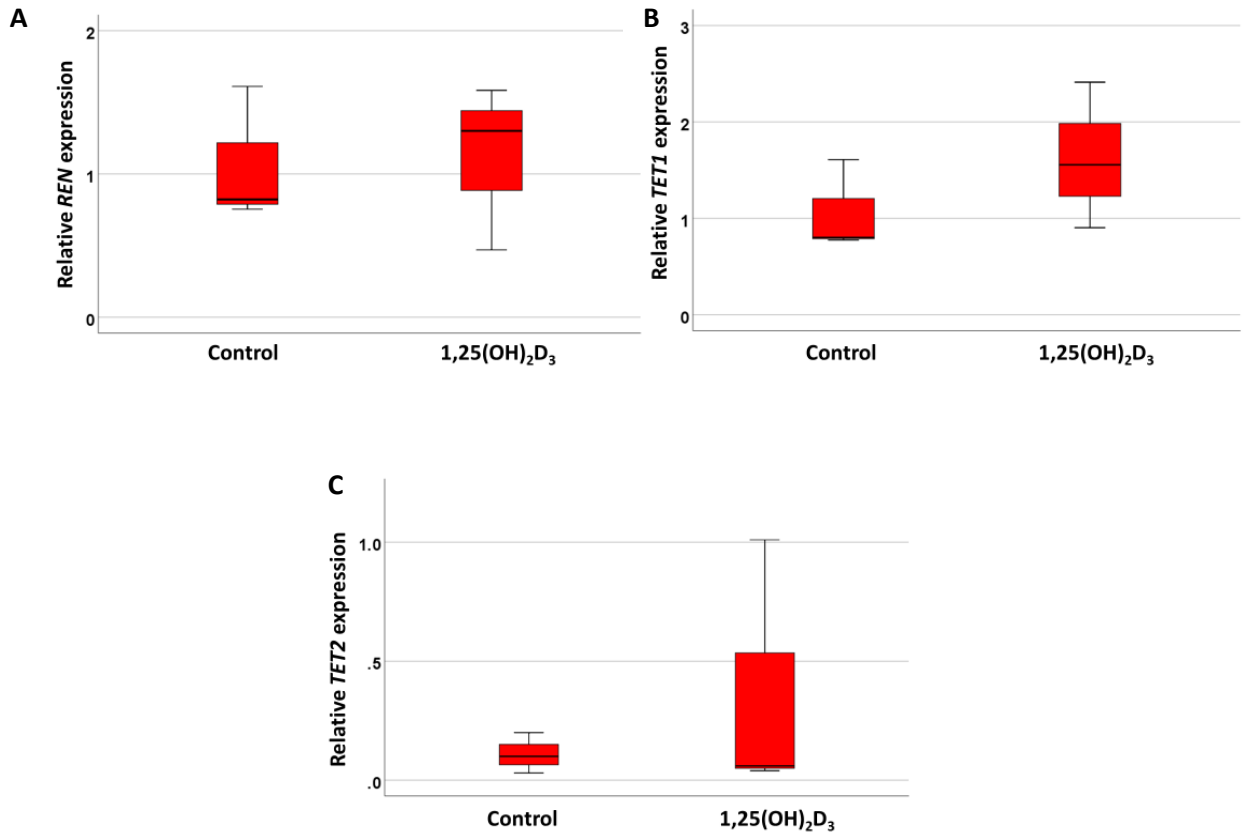

Figure 3.18. 1,25(OH)$_2$D$_3$ supplementation did not significantly effect *REN, TET1* and *TET3* expression in *VDR* $^-$ HEK293 cells. The boxplot shows *REN, TET1* and *TET2* expression in response to 10 nM 1,25(OH)$_2$D$_3$ in *VDR* $^-$ HEK293 cells, as quantified by RT-qPCR. Pairwise comparisons indicate no significant increase in either *REN*, *TET1* or *TET2* in response to 10 nM 1,25(OH)$_2$D$_3$. Error bars show 95% confidence interval (n = 3).

3.12 10nM 1,25(OH)$_2$D$_3$ supplementation induced no significant change in *REN* methylation in *VDR* $^-$ HEK293 cells

To confirm that the observed changes in *REN* methylation were a direct result of VDR activity, methylation of CGI2, CGI5 and a *bona fide* CGI within *REN* was again quantified in *VDR* $^-$ HEK293 cells. No significant changes in methylation at any of the 3 CGI regions were observed in response to 10 nM 1,25(OH)$_2$D$_3$ (Fig. 3.18). On average, each CGI region was relatively hypermethylated. There was no significant difference in regional methylation between the three CGIs in both the control and 10 nM 1,25(OH)$_2$D$_3$ conditions. On a CpG site level, methylation of CpG site 2 of the *bona fide* CGI increased in response to 10 nM 1,25(OH)$_2$D$_3$.

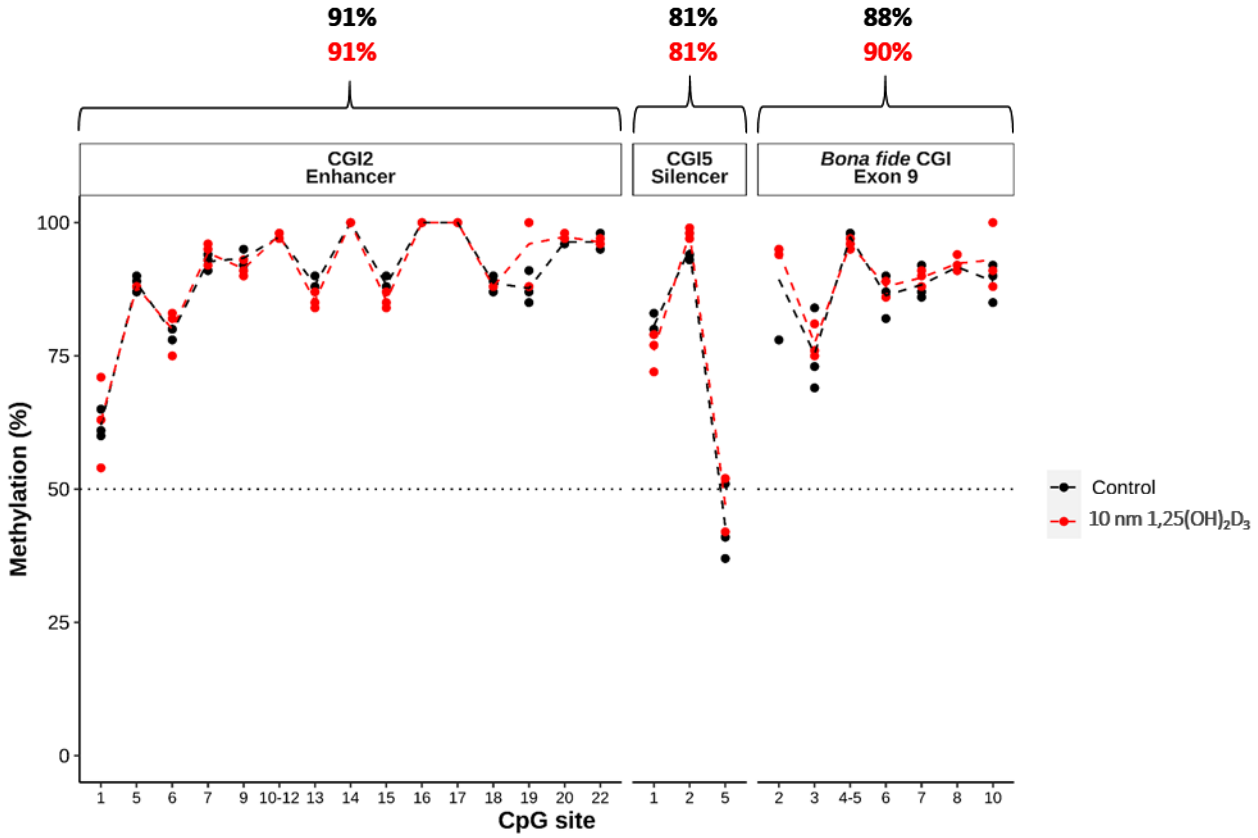

Figure 3.19. 1,25(OH)$_2$D$_3$ induced no significant changes in methylation in *REN* in *VDR* $^-$ HEK293 cells. *In vitro* changes in regional methylation of high-ranking selected *REN* CGIs were quantified via MALDITOF mass spectrometry in both control and treated cells (treated for 18 h with 10 nM 1,25(OH)$_2$D$_3$). Pairwise comparisons indicate no significant changes in *REN* methylation at CGI2 (Chr1: 204 171 238 – 204 171 573), CGI5 (Chr 1: 204 165 151 – 204 165 368) and a *bona fide* CGI (Chr1: chr1: 204 155 754 – 204 155 968) in *VDR* $^-$ HEK293 cells in response to 10 nM 1,25(OH)$_2$D$_3$.

Renin is integral to the regulation of blood pressure as it catalyses the rate-limiting step in the RAAS. Modulating *REN* expression is multifaceted as it appears to be controlled in part by the interplay of the primary promoter, enhancers, and a silencer element, with inducible transcription factors in the 3D genome. This study aimed to assess the effect of $1,25(OH)_2D_3$, a key regulator of RAAS, on the methylation of a *REN* enhancer, silencer element, and *bona fide* CGI in HEK293 cells. Results obtained show that $1,25(OH)_2D_3$ significantly downregulated *REN* expression while increasing *VDR, CYP24A1, TET 1,* and *TET2* expression. These changes in gene expression were linked to increased methylation in the enhancer region and decreased methylation in the silencer region of *REN* in response to $1,25(OH)_2D_3$ in *VDR*$^+$ cells.

4.1 Quality control

4.1.1 The HEK293 cells were free from *Mycoplasma* contamination

Mycoplasma are a common concern for cell culture as they are simple organisms not capable of performing most metabolic functions on their own due to their small genome (Razin et al., 1998). Existing as parasites, they rely on their hosts to survive with little to no observable changes to cell cultures. Their small size allows them to go undetected within cell cultures and are tricky to remove (Razin et al., 1998). Considering that *Mycoplasma* is easily spread through cell culture labs, a PCR-based *Mycoplasma* detection kit was used to ensure all HEK293 cell samples were free from contamination. Although *Mycoplasma* contamination can be prevented through good laboratory practice including regular disinfection of all cell culture equipment, workbenches and storage, they are robust and hard to detect (Lincoln and Gabridge, 1998). Additionally, they can have negative effects on eukaryotic cells that alter cell function thus reducing the reliability of experimental results. Several methods exist to detect *Mycoplasma* such as DNA staining, agar growth, and enzyme-linked immunosorbent assay (ELISA). PCR detection was used as it was specific, relatively quick, and inexpensive to perform. Considering that the best approach to *Mycoplasma* detection is routine and regular repeated testing, a quick and costly method like PCR was ideal. *Mycoplasma* detection was especially necessary for cell culture samples used in the methylation analysis. This is because any form of PCR-based methylation detection will have a bias towards smaller fragments of DNA (Warnecke et al., 1997). Thus, confirming that the samples were free from *Mycoplasma*

contamination (Fig. 3.1) was necessary for the reliability of the methylation results. The contaminant *Mycoplasma* DNA will also result in non-specific amplification leading to misleading results.

4.1.2 HEK293 cell viability was not affected by 1,25(OH)$_2$D$_3$ supplementation

Cell viability assays calculate the ratio of healthy and live cells in comparison to dead cells within a population. Routinely measuring cell viability prior to experimentation is necessary as it measures the general health of cells as well as determining cell survival in response to treatment. This allows for optimisation of cell culture protocols or experimental conditions to improve cell survival and reliability of results. Supplementation with 10 nM 1,25(OH)$_2$D$_3$ supplementation did not significantly change HEK293 cell viability. This indicates that a dose of 10 nM 1,25(OH)$_2$D$_3$ exerts no toxic effect on the cells. The required effective dose of 1,25(OH)$_2$D$_3$ necessary for VDR activation lies in the concentration range of 1–10 nM (Norman, 2006) and has therefore been used for studying vitamin D effects without compromising cell culture viability**.** Similarly, studies have reported no cell death effects in response to vitamin D treatment (Djukic et al., 2014; Tobler et al., 1988). In contrast, Baek *et al.* (2011) reported that vitamin D$_3$ significantly reduced the viability of gastric cancer and cholangiocarcinoma cells. In addition, Zhang et al. (2021) reported both the vitamin D binding protein and 1,25(OH)$_2$D$_3$ synergistically inhibited the viability of rheumatoid arthritis synovial fibroblasts. However, it must be noted that the toxic effects observed are likely both dose and time dependant. The overall cell viability of *VDR* $^-$ HEK293 cells was lower than *VDR* $^+$ cells, however there was not significant change in viability between control and treated *VDR* $^-$ cells. This decrease is most likely due to the Lipofectamine transfection which can often affect the protein homeostasis of the cell (Jacobsen et al., 2009). Additionally, the serum free media used in the initial stages of transfection can reduce cell viability due to the lack of nutrients (Rashid and Coombs, 2019). Cell toxicity effects post-transfection will vary between cell lines however, HEK293 is a commonly used robust transfection cell line that has shown to undergo siRNA transfection with high efficacy.

4.1.3 Extracted nucleic acids for downstream analysis were intact and pure

Extracted DNA and RNA from the cells were non-degraded, pure, and intact (Fig. 3.3) Considering that degraded RNA can strongly affect PCR (Imbeaud et al., 2005), high-quality nucleic acid extracts with acceptable 260/280 and 260/230 ratios are essential for gene

expression analysis via RT- qPCR (Vermeulen et al., 2011). RNA quality closely affects the repeatability, reliability and accuracy of any downstream analyses which is why isolating high-quality RNA is a necessary pre-requisite for RT-qPCR. Common contaminants in RNA extractions include: gDNA which results in overestimation of the RNA concentration as it can be amplified along with the cDNA, RNases which can degrade RNA before analysis, DNases which can degrade cDNA and proteases which can denature enzymes used in downstream analysis and hinder PCR analysis. Moreover, degraded DNA might have an impact on downstream methods used for quantifying the methylation status leading to a false reading due to the sensitivity of PCR- based methylation quantification methods such as Epityper (Rhein et al., 2015). Importantly, there is a clear correlation between the variance of methylation to DNA degradation levels (Rhein et al., 2015). It is therefore necessary to ensure that all nucleic acids used in either RT-qPCR or methylation analysis are of high integrity, quality and are and pure to achieve repeatable and reliable results. The use of agarose gel electrophoresis and either spectrophotometry and fluorometry in the quality assessment and quantification of all nucleic extract used for downstream analysis was imperative to ensure the reliability of both the gene expression analysis (RNA) and methylation analysis (DNA).

4.1.4 Primers specifically amplified the gene of interest after cDNA synthesis

The target genes were amplified by RT-qPCR which was confirmed by both the amplification curves and agarose gel electrophoresis. The presence of a single distinct band of expected size on the agarose gel is a common indicator of specific amplification of target genes and a successful PCR. This is necessary as a frequent difficulty in PCR is the formation of primer dimers as well as non-specific amplification which results in incorrect fragments in addition to your desired product thus reducing the reliability of Cq values for a specific target (Mikeska and Dobrovic, 2009). Amplification specificity is an important consideration when using intercalating dyes instead of probe-based assays as intercalating dyes will bind any double-stranded DNA product and it is not necessarily sequence specific (Arya et al., 2005). For *REN*, a smaller shoulder peak was observed with a lower melting temperature to the target product (Fig. 3.4B). The double peaks observed are most likely a reflection of an intermediate state during amplification where the DNA is both in ssDNA or dsDNA configuration which would cause a dip in the dissociation curves and a subsequent second peak in the melt curve. It must therefore be noted that although a single peak is often indicative of a single target amplicon,

a double peak being produced in a melt-curve is not always confirmation of non-specific amplification (Bruzzone et al., 2013; Dwight et al., 2011). The agarose gel electrophoresis (Fig. 3.5) further confirms the presence of a single product being generated as there is only one band at the expected 129 bp size for the REN.

4.1.5 Successful *VDR* knockdown was achieved establishing a *VDR* $^{-}$ HEK293 cell culture

To confirm that the observed gene expression and methylation changes observed were a direct result of VDR activity, a *VDR*$^{-}$ HEK293 cell culture was established in order to conduct both the gene expression and methylation analysis in the presence and absence of VDR activity. Up to 80% *VDR* gene knockdown was achieved (Fig. 3.16A) and both *VDR* gene expression and protein level were significantly reduced. Gene knockdown studies help to determine the function of a specific gene as well as how it is related to other genes. A successful gene knockdown will temporarily reduce the expression of a target gene to essentially halt its functional activity in an organism without altering the DNA (O'Keefe, 2021). Although quantifying gene expression alone is an accepted measure of the knockdown efficiency, it is also recommended to confirm reduced activity of the gene at a protein level. Often times RT- qPCR cannot detect the knockdown alone as the degradation of the 3' mRNA fragment following siRNA mediated cleavage is prevented thus providing an mRNA fragment that will form a template for cDNA synthesis resulting in false positives (Holmes et al., 2010). As an added measure, VDR protein quantification via specific antibody was used to further assess the degree of *VDR* knockdown.

4.2 10 nM, 1,25(OH)$_2$D$_3$ supplementation significantly increased both *VDR* and *CYP24A1* while decreasing *REN* expression in *VDR* $^{+}$ but not *VDR* $^{-}$ HEK293 cells

10 nM, 1,25(OH)$_2$D$_3$ supplementation induced *VDR* expression (Fig. 3.6A) which was combined with an increase in *CYP24A1* expression (Fig. 3.7). This is not surprising as *VDR* has long been reported to regulate transcription of *CYP24A1* (Fraser, 1980; Issa et al., 1998; Kumar, 1984; Li et al., 2016). Furthermore, *CYP24A1* is expressed as a physiological response to facilitate the catabolism of 1,25(OH)$_2$D$_3$ (Clements et al., 1992). Thus, reducing 1,25(OH)$_2$D$_3$-related signals and in turn 1,25(OH)D$_3$ stores. This feedback mechanism is necessary as increased levels of 1,25(OH)$_2$D$_3$ are reported to contribute to hypercalcemia (Jones et al., 1987; Makin et al., 1989). The induction of *CYP24A1* in response to 1,25(OH)$_2$D$_3$

is an essential homeostatic mechanism and in turn, *CYP24A1* can therefore be considered as a marker of *VDR* activity. *VDR* mRNA and protein level (Fig. 3.1) increased in response to 10 nM $1,25(OH)_2D_3$ which is in agreement with several reports (Blufstein et al., 2021; Chen et al., 2017; Edfeldt et al., 2010; Liu et al., 2006) and was expected considering most of the cellular responses to $1,25(OH)_2D_3$ treatment are mediated by VDR activity. This observed *VDR* induction serves to confirm that *VDR* is expressed and functional in HEK293 cells. The increase in *VDR* and *CYP24A1* was coupled to a significant decrease in *REN* expression in response to $1,25(OH)_2D_3$. Consequently, VDR and its ligand, $1,25(OH)_2D_3$, may play a potential role in the regulation and subsequent decrease in *REN* observed. This decrease in *REN* expression in response to 10 nM, $1,25(OH)_2D_3$ (Fig. 3.8) is in agreement with studies that report $1,25(OH)_2D_3$ as a negative endocrine regulator of *REN* (Li et al., 2002; Resnick, 1986; Yuan et al., 2007). However, it has been shown that *VDR* induces *CYP24A1* expression independent of $1,25(OH)_2D_3$ in primary keratinocytes (Ellison et al., 2007). Nonetheless, the inverse correlation between *REN* and *VDR* expression observed here supports the longstanding model where $1,25(OH)_2D_3$-bound VDR downregulates *REN* expression by preventing CREB binding to CRE elements in *REN* (Yuan et al., 2007). Furthermore, observational studies in humans reported that lower serum 25(OH)D is associated with increased RAAS activity and blood pressure (Judd et al., 2008; Scragg et al., 2007). Despite the widely reported association between Vitamin D deficiency and hypertension (Kunutsor et al., 2013; Tomaschitz et al., 2010; Vimaleswaran et al., 2014), there is still discrepancy on the beneficial effects of vitamin D on blood pressure as several, but not all interventional studies conclude no blood pressure benefit from vitamin D supplementation (Beveridge et al., 2015; Kunutsor et al., 2013; Wu et al., 2010). The disputing reports may be due to the differences in both baseline RAAS activity and serum 25(OH)D levels of the participants as well as different doses and metabolites of vitamin D being repleted in the individuals. This may explain the inconsistent association between vitamin D and hypertension and why vitamin D supplementation appears to reduce blood pressure more effectively in individuals specifically with a low baseline vitamin D status reviewed by Kheiri et al. (2018). Taken together the observed changes in *VDR*, *CYP24A1* and *REN* suggests an inverse association between $1,25(0H)_2D_3$ and *REN* expression which may partially explain the prevalence of hypertension in Vitamin D deficient individuals.

4.3 10 nM, 1,25(OH)$_2$D$_3$ supplementation decreased CGI5 methylation in *REN* silencer region in *VDR* $^+$ HEK293 cells

In response to 1,25(OH)$_2$D$_3$ supplementation, methylation of CpG site 1 of CGI5 which overlaps the *REN* silencer region decreased significantly (Fig. 3.9). Regulation of gene expression often focuses on gene activation and an increase in gene expression, however gene repression and silencing is also a critical mechanism of gene regulation which is often overlooked. Our results show that 1,25(OH)$_2$D$_3$ induced demethylation at the *REN* silencer which was coupled to subsequent *REN* repression. This observation may highlight the role of a potential *REN* silencer. Our findings which demonstrate an active demethylation response are in agreement with cases of demethylation occurring within 1–4 hours (Doig et al., 2013). Understanding the role of the *REN* silencer is important as several validated enhancers have been identified from chromatin marks yet the identification of functional enhancers by either experimental or computational methods are limited (Doni Jayavelu et al., 2020). Interestingly, CTCF, a highly conserved chromatin remodeler (Phillips and Corces, 2009), has a conserved binding site in *REN* intron 1 which has recently been shown to be crucial in the regulation of *REN* expression (Donlon and Morris, 2019; Martinez et al., 2020). It is possible that CTCF binding sites within and around the renin gene are within functional enhancers/silencer domains which serve to maintain appropriate renin transcription activity. In conjunction with CTCF, the aptly named Yin Yang 1 (YY1) protein with both activator and repressor activity, has a binding site in the silencer region overlapping CpG site 1 of CGI5 (see Fig. 3.11). It has been reported that YY1 interacts with members of the ATF/CREB family of TFs to repress transcription (Zhou et al., 1995). Differential methylation in the silencer region may influence CTCF and YY1 binding and subsequent silencer activity. Both CTCF and YY1 binding have been described as methylation- sensitive (Hark et al., 2000; Kim et al., 2003), although some reports have suggested binding of these TFs as methylation-independent (Maurano et al., 2015). Moreover, an emerging model suggests that TFs like CTCF and YY1 can induce demethylation when bound as reviewed by Héberlé and Bardet (2019). Notably, 1,25(OH)$_2$D$_3$ has been shown to directly modulate genome-wide CTCF binding (Carlberg, 2014). It is thus unclear whether 1,25(OH)$_2$D$_3$ directs CTCF and YY1 binding to the *REN* silencer resulting in demethylation effects, or whether it directly induces demethylation to influence subsequent TF binding. Taken together, the results obtained therefore suggest that the silencer element plays an important role in regulating *REN* expression through differential methylation

4.4 10 nM, 1,25(OH)$_2$D$_3$ supplementation increased methylation of CGI2 in the *REN* enhancer region in *VDR* $^+$ HEK293 cells

Gene enhancers are significant regulatory elements which function together with TFs and protein complexes to maintain adequate gene expression. To understand the mechanisms driving *REN* regulation, methylation of CGI2 which traverses the *REN* distal enhancer was assessed in response to 1,25(OH)$_2$D$_3$ in *VDR* $^+$ cells. Our results showed that 1,25(OH)$_2$D$_3$ had no significant effect on methylation at CGI2 (Fig. 3.9), partially spanning the enhancers which remained in a hypermethylated state in both control and treated samples. This is not surprising as DNA hypermethylation is often indicative of intergenic regions in order to maintain a chromatin state that represses transcription (Herman and Baylin, 2003). *REN* enhancer methylation was not significantly changed by 1,25(OH)$_2$D$_3$ suggesting that the region is not responsible for driving the observed expression changes in HEK293 cells. Enhancer-mediated gene regulation is cell context-dependent and enhancer elements may function differently in diverse cell types, developmental stages or in response to environmental stimuli (Levine et al., 2014). Thus, it is possible that this enhancer, originally described by Ushiki et al. (2018) and validated in As4.1 mice cells, may not be equally important in driving *REN* expression in human kidney cells (Ushiki et al., 2018). Despite human and mouse genomes sharing roughly 95% of their protein coding genes, non-coding genes and regulatory regions are significantly less conserved (Waterston et al., 2002; Yue et al., 2014). This disparity is relevant considering that human variants leading to disease progression are often located in regions modulating gene expression, rather than protein structure (von Scheidt et al., 2017). Indeed, relatively poor sequence conservation between humans and mice is evident at the regulatory regions of *REN*, including the two regions identified here as functionally important. In agreement, Odom et al. (2007) demonstrated that tissue-specific TF binding sites differ greatly between human and mouse, supporting the use of human cell culture models to study *REN* regulation (Odom et al., 2007). While hypertensive mice models have been providing much insight into RAAS regulation, it has been suggested that findings from *in vivo* mouse studies be validated in representative human cells (Lerman et al., 2019). In addition, regulation of DNA methylation profiles is complex, and the dynamic environment of the cell may influence the methylation state of the enhancer at specific time points. Moreover, Zhou et al. (2006) reported that although deletion of the

enhancer decreased *REN* mRNA levels, it did not affect tissue-specific expression of human *REN*, suggesting that other regulatory elements may be necessary for tissue-specific regulation of *REN* expression (Zhou et al., 2006).

4.5 10 nM, 1,25(OH)$_2$D$_3$ supplementation had no effect on methylation of the *bona fide* CGI overlapping exon 9 of *REN* in *VDR* $^+$ HEK293 cells

To confirm whether Vitamin D regulates *REN* via epigenetic mechanisms, methylation of a *bona fide* CGI identified in exon 9 of *REN* was measured in response to 10 nM 1,25(OH)$_2$D$_3$. Vitamin D supplementation did not appear to have an effect on the methylation of the *bona fide* CGI (Fig 3.9). This suggests that the *bona fide* CGI is not integral or not strongly associated with transcription of *REN*. The apparent lack of association between the *bona fide* CGI methylation and 1,25(OH)$_2$D$_3$ is possibly due the location of the CGI which overlaps exon 9 with respect the *REN* the TSS. Both CGI2 and CGI5 are located in closer proximity to the TSS unlike the *bona fide* CGI which is located further downstream and distal to the TSS thus affecting its ability to effectively regulate *REN* expression. This is supported by a study conducted by Brenet et al. (2011), which reported that methylation of more downstream elements is poorly associated with the degree of gene expression. In terms of the observed *REN* repression, it is not surprising that the *bona fide* CGI remained hypermethylated prior to and following 1,25(OH)$_2$D$_3$ treatment as previous reports based on the Refseq database suggest that methylation of 3'- end elements is not as strongly related to gene silencing when compared to 5'-end elements (Brenet et al., 2011). It must however be noted that the relationship between gene transcriptional rate and gene body methylation is largely incomplete and can vary between cell-types and tissues.

4.6 No significant changes in *DNMT1*, *DNMT3A* and *DNMT3B* were observed in response to 10 nM 1,25(OH)$_2$D$_3$ in both *VDR* $^+$ HEK293 cells

Expression of DNMTs in both *VDR* $^+$ and *VDR* $^-$ HEK293 cells was assessed in response to 1,25(OH)$_2$D$_3$ to identify possible mechanisms of vitamin D-induced methylation changes in *REN*. Interestingly no significant changes in either *DNMT1*, *DNMT3A* or *DNMT3B* was observed (Fig. 3.13) despite a non-significant increase in methylation of CpGs within CGI2 of *REN* in treated samples when compared to the control in *VDR* $^+$ samples. There is no agreement on whether the effect of Vitamin D on DNMT expression is inhibitory or

stimulatory. Research has shown a link between $1,25(OH)_2D_3$ and changes in DNA methylation, but the exact mechanism is unclear, and it is often assumed to be a passive process. Previous reports have shown that treatment with $1,25(OH)_2D_3$ increased chromatin accessibility at several loci (Seuter et al., 2013). Additionally, Zhu et al. reported small changes in methylation of leukocyte DNA linked to vitamin D deficiency (Zhu et al., 2013). Some studies have reported downregulation in both mRNA level and activity of *DNMT1* and *DNMT3B* in response to $1,25(OH)_2D_3$ in prostate cancer cells (Lai et al., 2020). The results of this study therefore suggest that changes in *VDR* expression, does not affect the expression of DNMTs in HEK293 cells in response to vitamin D treatment and that regulation of DNMT by VDR may be cell-type and tissue specific.

4.7 10 nM, $1,25(OH)_2D_3$ supplementation increased both *TET1* and *TET2* expression while having no significant effect on *TET3 in VDR* $^+$ but not *VDR* $^-$ *HEK293 cells*

Following $1,25(OH)_2D_3$ supplementation, both *TET1* and *TET2* expression increased (Fig. 3.14) with *TET1* showing a non-significant trend while *TET2* increased significantly ($P < 0.050$). Previously it has been demonstrated that loss-of-function mutations in *TET2*, which are frequently observed in hematopoietic diseases (Scourzic et al., 2015), result in enhancer DNA hypermethylation and alter the accessibility of TFBS. Other reports suggest pioneer TFs possibly recruit TET to facilitate modifications to the epigenome which can stimulate the of other TFs (Hon et al., 2014; Lu et al., 2014; Rasmussen et al., 2019; Yamazaki et al., 2015). The observed induction of *TET1* in response to $1,25(OH)_2D_3$ suggests that TET1 activity may be linked to demethylation events at the *REN* silencer. This is in agreement with previous findings that reported *TET1* mediated demethylation of genomic loci in HEK293 cells (Guo et al., 2011; Zhang et al., 2010). Additionally, *TET1* overexpression was reported to induce slight DNA hypomethylation of gene body regions as well as CGIs in HEK293 cells (Grosser et al., 2015). This inverse correlation suggests the activity of intronic silencers. Thus, it is possible that $1,25(OH)_2D_3$ not only influences *REN* regulation through CREB-mediated effects but also induced demethylation effects mediated by either *TET1* or *TET2* activity, resulting in activation of the *REN* silencer. The observed changes in both *TET1* and *TET2* expression in response to vitamin D suggest that TET activity influences the local chromatin environment to facilitate TF binding to regulate *REN* expression. This is in agreement with recent evidence indicating an association between TFs such as transcriptional repressors and DNA demethylation to

increase genomic accessibility and subsequent TF binding (Mahé et al., 2017). It is not surprising that *TET1* induction was coupled to *TET2* induction as they seem to have similar functions as proposed in a viable TET1 and TET2 single-knockout mice study (Dawlaty et al., 2011; Li et al., 2011). Additionally, studies have found overlapping loci for the TETs suggesting they function synergistically. The lack of significant change in expression of *TET3* in response to 1,25$(OH)_2D_3$ could be due cell- specific variation in expression levels of the TETs in somatic cells.

4.8 Putative VDR binding sites were found in *TET1*, *TET2* and *TET3*

To confirm whether the observed *REN* silencer demethylation was due to vitamin D-induced recruitment of the demethylating agents, putative VDR binding sites were identified within *TET1*, *TET2*, and *TET3* using the JASPAR 2018 TFBS track in the UCSC browser Human (GRCh38/hg38) assembly. All 3 TETs contained VDR binding sites (Fig. 3.15) which is expected as associations of Vitamin D and *TET* activity is often reported. This suggests that binding of VDR and subsequent recruitment of TETs may result in the active demethylation observed at the *REN* silencer in response to 10 nM 1,25$(OH)_2D_3$. It must, however, be noted that putative binding sequences are based on prediction models and may not be a true reflection of VDR DNA binding activity. Nonetheless PFM TF-binding models are based on experimental data including chromatin immunoprecipitation sequencing (ChIP-seq), DNA affinity purification sequencing (DAP-seq), selective microfluidics-based ligand enrichment sequencing (SMiLEseq) and high-throughput systematic evolution of ligands by exponential enrichment (HTSELEX) experiments (Khan et al., 2018), making it a reliable indicator of potential VDR and TET interactions. Overall, the existence of VDR binding sites within both *TET1* and *TET2* suggest an association between vitamin D and DNA demethylating enzymes which may be driving *REN* suppression.

4.9 No significant changes in *REN*, *TET1* and *TET2* were observed in response to 10 nM 1,25$(OH)_2D_3$ in the *VDR*$^-$ HEK293 cells

To confirm a direct link between Vitamin D-bound VDR activity and the observed changes in gene expression, gene expression analysis was conducted in *VDR*$^-$ HEK293 cells.

Unsurprisingly, expression of *REN*, *TET1* and *TET2* was not significantly changed in response to 10 nM 1,25$(OH)_2D_3$ in *VDR*$^-$ samples (Fig. 3.17). This therefore suggests that it is highly likely

that VDR activity is responsible for the observed *REN* suppression and *TET1* and *TET2* induction in the *VDR* $^{+}$ samples.

4.10 10 nM, 1,25(OH)$_2$D$_3$ supplementation induced no significant change in *REN* methylation in *VDR* $^{-}$ HEK293 cells

To confirm a direct link between vitamin D-bound VDR activity and the observed changes in *REN* methylation, *REN* methylation analysis was conducted in *VDR* $^{-}$ HEK293 cells. The reduced activity of VDR resulted in little to no significant change in *REN* CGI methylation (Fig. 3.18). This suggest that significant changes in *REN* methylation which are linked to *REN* suppression are mediated by VDR activity. Interestingly, CpG site 8 of the *bona fide* CGI and CpG site 18 of the CGI2 overlapping the enhancer increased in methylation in response to 10 nM 1,25(OH)$_2$D$_3$ in the *VDR* $^{-}$ samples. DNA methylation changes are transient modifications that are often sensitive to environmental stressors. It is possible that the slight change in CpG methylation observed in the *bona fide* CGI and CGI2 are a result of siRNA transfection effects which can alter cellular processes (Daga et al., 2018). Nonetheless, overall the combined results of this study suggests that vitamin D directly induce *REN* silencer demethylation via TET activity to facilitate *REN* suppression and prevent overexpression of *REN* in the absence of cellular signals for increasing blood pressure.

Chapter 5: Conclusion

5.1 Research rationale

Hypertension progression and susceptibility is impacted by a multitude of factors. Like many disorders, it has both genetic and epigenetic elements which interact together. It is a growing public health and economic concern with South Africa having the largest measured hypertension prevalence in Southern Africa (Bradshaw et al., 2005). Despite the immense research and data obtained around RAAS regulation and hypertension, the aetiology of the disease is still not well understood with most studies focusing on Ang II and its receptors excluding the role of renin. Hypertension is however still a modifiable risk factor for cardiovascular morbidity and mortality (Gourgari et al., 2017). Understanding epigenetic mechanisms regulating blood pressure is why the RAAS pathway has immense potential for use in cardiovascular therapeutics. Current treatment for hypertension has many negative side-effects and are often inaccessible to lower-income groups despite the disease being common in poorer populations. Thus, a therapeutic approach such as vitamin D supplementation may provide a more effective solution to high blood pressure. Although vitamin D has long been linked to blood pressure, the exact molecular mechanism defining its association to hypertension progression remains unclear. Epigenetic regulation of gene expression and its role in disease is largely unexplored. In the context of hypertension, there are gaps in understanding the regulation of RAAS. Our aim was to assess the effect $1,25(OH)_2D_3$ on *REN* methylation and expression to understand the epigenetic mechanisms regulating *REN* transcription.

5.2 Summary of findings

The major findings of the study were that scored and selected CGIs overlapping the *REN* silencer and enhancer region have functional importance in the vitamin D-induced epigenetic regulation of *REN* (Govender et al., 2021). Following *in sillico* identification and annotation of the high-scoring CGIs, *in vitro* validation showed that renin-expressing HEK293 cells treated with 10 nM $1,25(OH)_2D_3$ led to a decrease in *REN* expression which was coupled to significant silencer demethylation while maintaining enhancer hypermethylation. The induction of *TET1* and *TET2* expression in response to 10 nM $1,25(OH)_2D_3$ suggests that VDR recruitment of TETs may facilitate the observed silencer demethylation. Conducting both a gene expression and

methylation analysis in both a *VDR* $^{+}$ and *VDR* $^{-}$ cell culture confirmed a direct relationship between vitamin D and *REN* which validated the bioinformatic workflow and highlighted vitamin D as a potential therapeutic agent in reducing hypertension susceptibility and progression. Here we observed that an appropriate dose and treatment time with $1,25(OH)_2D_3$ can effectively regulate renin expression in HEK293 cells which are mediated via *VDR* activity.

5.3 Implications of research

This research aimed to expand our understanding of the relationship between vitamin D, DNA methylation and *REN* transcriptional control. We found that vitamin D induced changes in methylation of the *REN* were coupled to a reduction in *REN* expression. This suggests that vitamin D regulates *REN* transcriptional activity on an epigenetic level and may in part describe the consistent association of vitamin D deficiency and hypertension progression. Based on our findings, it is clear that an optimal vitamin D status can help to maintain a healthy epigenome which is essential in blood pressure control.

5.4 Challenges and limitations

The observed *REN* gene expression and methylation changes were done *in vitro* and will need to be validated *in vivo*. Furthermore, predictive tools used to identify gene regulatory regions such as the promoter, enhancer and silencer are based on models such as mice which often vary in sequence similarity to humans. Although the reported changes have confirmed a link between *REN* suppression and vitamin D possibly through induced silencer demethylation, it should be noted that in the absence of sequence level data, exact molecular mechanisms for the observed association cannot be given. Moreover, silencer activity needs to be validated to confirm whether the observed associations are in fact functionally relevant.

5.5 Future direction

Future work to build on this project would include confirming the changes in *REN*, *TET1* and *TET1* mRNA levels at the protein level with either flow-cytometry or western-blot to confirm functional and active response to $1,25(OH)_2D_3$. Additionally, chromatin immunoprecipitation sequencing (CHIP-seq) can be used to confirm binding of TFs to the putative DNA-binding sites in *REN* to confirm their role in the repression of the gene in response to $1,25(OH)_2D_3$. Repeating the gene expression analysis using a control or alternate cell line would further confirm the observed vitamin-D induced changes. Quantifying methylation of all 7 *REN* CGIs

annotated would give a clearer picture of the methylation state of *REN* at a basal level as compared to its state following vitamin D supplementation. Future studies should investigate DNA methylation-based changes of the entire gene using sequencing.

References

Akutsu, Taisuke, Hikaru Kitamura, Shoko Himeiwa, Shinto Kitada, Tatsuya Akasu, and Mitsuyoshi Urashima. 2020. "Vitamin D And Cancer Survival: Does Vitamin D Supplementation Improve The Survival Of Patients With Cancer?". Current Oncology Reports 22 (6). doi:10.1007/s11912-020-00929-4.

Andersson, R., Sandelin, A., 2020. Determinants of enhancer and promoter activities of regulatory elements. Nature Reviews Genetics 21, 71–87. https://doi.org/10.1038/s41576019-0173-8

Armas, L.A.G., Hollis, B.W., Heaney, R.P., 2004. Vitamin D2 is much less effective than vitamin D3 in humans. J Clin Endocrinol Metab 89, 5387–5391. https://doi.org/10.1210/jc.2004-0360

Arya, M., Shergill, I.S., Williamson, M., Gommersall, L., Arya, N., Patel, H.R., 2005. Basic principles of real-time quantitative PCR. Expert Review of Molecular Diagnostics 5, 209–219. https://doi.org/10.1586/14737159.5.2.209

Aslibekyan, S., Dashti, H., Toshiko, T., Sha, J., Ferrucci, L., Zhi, D., Bandinelli, S., Borecki, I., Absher, D., Arnett, D., Ordovas, J., 2014. PRKCZ methylation is associated with sunlight exposure in a North American but not a Mediterranean population. Chronobiology International 31. https://doi.org/10.3109/07420528.2014.944266

Barrett, A.J., Woessner, J.F. and Rawlings, N.D. eds., 2012. Handbook of Proteolytic Enzymes, Second edition, Volume 1 (Vol. 1). Elsevier.

Bazzano, L.A., Green, T., Harrison, T.N., Reynolds, K., 2013. Dietary Approaches to Prevent Hypertension. Curr Hypertens Rep 15, 694–702. https://doi.org/10.1007/s11906-013-0390-z

Berensmeier, S., 2006. Magnetic particles for the separation and purification of nucleic acids. Appl Microbiol Biotechnol 73, 495–504. https://doi.org/10.1007/s00253-006-0675-0

Bergman, Y., Cedar, H., 2013. DNA methylation dynamics in health and disease. Nat Struct Mol Biol 20, 274–281. https://doi.org/10.1038/nsmb.2518

Berkin, K.E., Ball, S.G., 2001. Essential hypertension: the heart and hypertension. Heart 86, 467–475. https://doi.org/10.1136/heart.86.4.467

Berry, K.M., Parker, W., Mchiza, Z.J., Sewpaul, R., Labadarios, D., Rosen, S., Stokes, A., 2017. Quantifying unmet need for hypertension care in South Africa through a care cascade: evidence from the SANHANES, 2011-2012. BMJ Global Health 2, e000348. https://doi.org/10.1136/bmjgh-2017-000348

Beveridge, L.A., Struthers, A.D., Khan, F., Jorde, R., Scragg, R., Macdonald, H.M., Alvarez, J.A., Boxer, R.S., Dalbeni, A., Gepner, A.D., Isbel, N.M., Larsen, T., Nagpal, J., Petchey, W.G., Stricker, H., Strobel, F., Tangpricha, V., Toxqui, L., Vaquero, M.P., Wamberg, L., Zittermann, A., Witham, M.D., 2015. Effect of Vitamin D Supplementation on Blood Pressure. JAMA Intern Med 175, 745–754. https://doi.org/10.1001/jamainternmed.2015.0237

Bickmore, W.A., 2013. The Spatial Organization of the Human Genome. Annual Review of Genomics and Human Genetics 14, 67–84. https://doi.org/10.1146/annurev-genom-091212153515

Biino, G., Parati, G., Concas, M.P., Adamo, M., Angius, A., Vaccargiu, S., Pirastu, M., 2013. Environmental and Genetic Contribution to Hypertension Prevalence: Data from an Epidemiological Survey on Sardinian Genetic Isolates. PLOS ONE 8, e59612. https://doi.org/10.1371/journal.pone.0059612

Bikle, D.D., 2014. Vitamin D Metabolism, Mechanism of Action, and Clinical Applications. Chemistry & Biology 21, 319–329. https://doi.org/10.1016/j.chembiol.2013.12.016

Bjornsson, H.T., Fallin, M.D., Feinberg, A.P., 2004. An integrated epigenetic and genetic approach to common human disease. Trends in Genetics 20, 350–358. https://doi.org/10.1016/j.tig.2004.06.009

Blufstein, A., Behm, C., Kubin, B., Gahn, J., Moritz, A., Rausch-Fan, X., Andrukhov, O., 2021. Transcriptional activity of vitamin D receptor in human periodontal ligament cells is diminished under inflammatory conditions. Journal of Periodontology 92, 137–148. https://doi.org/10.1002/JPER.19-0541

Bookout, A.L., Jeong, Y., Downes, M., Yu, R.T., Evans, R.M., Mangelsdorf, D.J., 2006. Anatomical Profiling of Nuclear Receptor Expression Reveals a Hierarchical Transcriptional Network. Cell 126, 789–799. https://doi.org/10.1016/j.cell.2006.06.049

Borensztein, P., Germain, S., Fuchs, S., Philippe, J., Corvol, P., Pinet, F., 1994. cis-regulatory elements and trans-acting factors directing basal and cAMP-stimulated human renin gene expression in chorionic cells. Circ. Res. 74, 764–773. https://doi.org/10.1161/01.res.74.5.764

Bouillon, R., Carmeliet, G., Verlinden, L., van Etten, E., Verstuyf, A., Luderer, H.F., Lieben, L., Mathieu, C., Demay, M., 2008. Vitamin D and Human Health: Lessons from Vitamin D Receptor Null Mice. Endocr Rev 29, 726–776. https://doi.org/10.1210/er.2008-0004

Bradshaw, D., Nannan, N., Groenewald, P., Joubert, J., Laubscher, R., Nojilana, B., Norman, R., Pieterse, D., & Schneider, M. (2005). Provincial mortality in South Africa, 2000--priority-setting for now and a benchmark for the future. *South African medical journal = Suid-Afrikaanse tydskrif vir geneeskunde*, *95*(7), 496–503.

Brenet, F., Moh, M., Funk, P., Feierstein, E., Viale, A.J., Socci, N.D., Scandura, J.M., 2011. DNA Methylation of the First Exon Is Tightly Linked to Transcriptional Silencing. PLOS ONE 6, e14524. https://doi.org/10.1371/journal.pone.0014524

Bruzzone, C.M., Tawadros, P.S., Boardman, L.A., Steer, C.J., 2013. Enhanced primer selection and synthetic amplicon templates optimize high-resolution melting analysis of singlenucleotide polymorphisms in a large population. Genet Test Mol Biomarkers 17, 675–680. https://doi.org/10.1089/gtmb.2013.0113

Bulger, M., Groudine, M., 2011. Functional and mechanistic diversity of distal transcription enhancers. Cell 144, 327–339. https://doi.org/10.1016/j.cell.2011.01.024

Burgess, E.D., Hawkins, R.G., Watanabe, M., 1990. Interaction of 1,25-Dihydroxyvitamin D and Plasma Renin Activity in High Renin Essential Hypertension. Am J Hypertens 3, 903–905. https://doi.org/10.1093/ajh/3.12.903

Carlberg, C., 2014. Genome-wide (over)view on the actions of vitamin D. Frontiers in Physiology 5, 167. https://doi.org/10.3389/fphys.2014.00167

Carlberg, C., Seuter, S., Heikkinen, S., 2012. The First Genome-wide View of Vitamin D Receptor Locations and Their Mechanistic Implications. Anticancer Res 32, 271–282.

Castellano-Castillo, D., Morcillo, S., Clemente-Postigo, M., Crujeiras, A.B., Fernandez-García, J.C., Torres, E., Tinahones, F.J., Macias-Gonzalez, M., 2018. Adipose tissue inflammation and VDR expression and methylation in colorectal cancer. Clinical Epigenetics 10, 60. https://doi.org/10.1186/s13148-018-0493-0

Chen, K.-S., DeLuca, H.F., 1995. Cloning of the human 1α,25-dihydroxyvitamin D-3 24hydroxylase gene promoter and identification of two vitamin D-responsive elements. Biochimica et Biophysica Acta (BBA) - Gene Structure and Expression 1263, 1–9. https://doi.org/10.1016/0167-4781(95)00060-T

Chen, S., Bu, D., Ma, Y., Zhu, J., Chen, G., Sun, L., Zuo, S., Li, T., Pan, Y., Wang, X., Liu, Y., Wang, P., 2017. H19 Overexpression Induces Resistance to 1,25$(OH)_2D_3$ by Targeting VDR Through miR-675-5p in Colon Cancer Cells. Neoplasia 19, 226–236. https://doi.org/10.1016/j.neo.2016.10.007

Clarkson, C.T., Deeks, E.A., Samarista, R., Mamayusupova, H., Zhurkin, V.B., Teif, V.B., 2019. CTCF-dependent chromatin boundaries formed by asymmetric nucleosome arrays with decreased linker length. Nucleic Acids Res 47, 11181–11196. https://doi.org/10.1093/nar/gkz908

Clements, M.R., Davies, M., Hayes, M.E., Hlckey, C.D., Lumb, G.A., Mawer, E.B., Adams, P.H., 1992. The role of 1,25-dihydroxyvitamin D in the mechanism of acquired vitamin D deficiency. Clinical Endocrinology 37, 17–27. https://doi.org/10.1111/j.1365-2265.1992.tb02278.x

Cragan, J.D., Young, B.A., Correa, A., 2015. Renin-Angiotensin System Blocker Fetopathy. J Pediatr 167, 792–794. https://doi.org/10.1016/j.jpeds.2015.07.024

Daga, N., Eicher, S., Kannan, A., Casanova, A., Low, S.H., Kreibich, S., Andritschke, D., Emmenlauer, M., Jenkins, J.L., Hardt, W.-D., Greber, U.F., Dehio, C., von Mering, C., 2018. Growth-restricting effects of siRNA transfections: a largely deterministic combination of offtarget binding and hybridization-independent competition. Nucleic Acids Res 46, 9309–9320. https://doi.org/10.1093/nar/gky798

Daïkha-Dahmane, F., Levy-Beff, E., Jugie, M., Lenclen, R., 2006. Foetal kidney maldevelopment in maternal use of angiotensin II type I receptor antagonists. Pediatr Nephrol 21, 729–732. https://doi.org/10.1007/s00467-006-0070-1

Dawlaty, M.M., Ganz, K., Powell, B.E., Hu, Y.-C., Markoulaki, S., Cheng, A.W., Gao, Q., Kim, J., Choi, S.-W., Page, D.C., Jaenisch, R., 2011. Tet1 is dispensable for maintaining pluripotency

and its loss is compatible with embryonic and postnatal development. Cell Stem Cell 9, 166–175. https://doi.org/10.1016/j.stem.2011.07.010

Dekker, J., Mirny, L., 2016. The 3D Genome as Moderator of Chromosomal Communication. Cell 164, 1110–1121. https://doi.org/10.1016/j.cell.2016.02.007

Ding, Yu, Subramaniam, Sherman, Wilson, Rao, Leblanc, Coulter, He, Scott, 2013. A vitamin D receptor/SMAD genomic circuit gates hepatic fibrotic response. Cell 153, 601–613.

Dobnig, H., Pilz, S., Scharnagl, H., Renner, W., Seelhorst, U., Wellnitz, B., Kinkeldei, J., Boehm, B.O., Weihrauch, G., Maerz, W., 2008. Independent Association of Low Serum 25Hydroxyvitamin D and 1,25-Dihydroxyvitamin D Levels With All-Cause and Cardiovascular Mortality. Archives of Internal Medicine 168, 1340–1349. https://doi.org/10.1001/archinte.168.12.1340

Doig, C.L., Singh, P.K., Dhiman, V.K., Thorne, J.L., Battaglia, S., Sobolewski, M., Maguire, O., O'Neill, L.P., Turner, B.M., McCabe, C.J., Smiraglia, D.J., Campbell, M.J., 2013. Recruitment of NCOR1 to VDR target genes is enhanced in prostate cancer cells and associates with altered DNA methylation patterns. Carcinogenesis 34, 248–256. https://doi.org/10.1093/carcin/bgs331

Doni Jayavelu, N., Jajodia, A., Mishra, A., Hawkins, R.D., 2020. Candidate silencer elements for the human and mouse genomes. Nature Communications 11, 1061. https://doi.org/10.1038/s41467-020-14853-5

Donlon, T.A., Morris, B.J., 2019. In silico analysis of human renin gene–gene interactions and neighborhood topologically associated domains suggests breakdown of insulators contribute to ageing-associated diseases. Biogerontology 20, 857–869. https://doi.org/10.1007/s10522019-09834-1

Drexler, H.G., Uphoff, C.C., 2002. Mycoplasma contamination of cell cultures: Incidence, sources, effects, detection, elimination, prevention. Cytotechnology 39, 75–90. https://doi.org/10.1023/A:1022913015916

Dwight, Z., Palais, R., Wittwer, C.T., 2011. uMELT: prediction of high-resolution melting curves and dynamic melting profiles of PCR products in a rich web application. Bioinformatics 27, 1019–1020. https://doi.org/10.1093/bioinformatics/btr065

Edfeldt, K., Liu, P.T., Chun, R., Fabri, M., Schenk, M., Wheelwright, M., Keegan, C., Krutzik, S.R., Adams, J.S., Hewison, M., Modlin, R.L., 2010. T-cell cytokines differentially control human monocyte antimicrobial responses by regulating vitamin D metabolism. Proc Natl Acad Sci U S A 107, 22593–22598. https://doi.org/10.1073/pnas.1011624108

Ehrich, M., Nelson, M.R., Stanssens, P., Zabeau, M., Liloglou, T., Xinarianos, G., Cantor, C.R., Field, J.K., Boom, D. van den, 2005. Quantitative high-throughput analysis of DNA methylation patterns by base-specific cleavage and mass spectrometry. PNAS 102, 15785–15790. https://doi.org/10.1073/pnas.0507816102

Ehrich, M., Zoll, S., Sur, S., van den Boom, D., 2007. A new method for accurate assessment of DNA quality after bisulfite treatment. Nucleic Acids Res 35, e29. https://doi.org/10.1093/nar/gkl1134

Ellison, T.I., Eckert, R.L., MacDonald, P.N., 2007. Evidence for 1,25-Dihydroxyvitamin D3independent Transactivation by the Vitamin D Receptor: UNCOUPLING THE RECEPTOR AND LIGAND IN KERATINOCYTES*. Journal of Biological Chemistry 282, 10953–10962. https://doi.org/10.1074/jbc.M609717200

Esser, K.-H., Marx, W.H., Lisowsky, T., 2006. maxXbond: first regeneration system for DNA binding silica matrices. Nat Methods 3, i–ii. https://doi.org/10.1038/nmeth845

Esteller, M., 2008. Epigenetics in Cancer. N Engl J Med 358, 1148–1159. https://doi.org/10.1056/NEJMra072067

Feinberg, A.P., 2007. Phenotypic plasticity and the epigenetics of human disease. Nature 447, 433–440. https://doi.org/10.1038/nature05919

Felicidade, I., Sartori, D., Coort, S.L.M., Semprebon, S.C., Niwa, A.M., D'Epiro, G.F.R., Biazi, B.I., Marques, L.A., Evelo, C.T., Mantovani, M.S., Ribeiro, L.R., 2018. Role of 1α,25Dihydroxyvitamin D3 in Adipogenesis of SGBS Cells: New Insights into Human Preadipocyte Proliferation. CPB 48, 397–408. https://doi.org/10.1159/000491770

Ferrario, C.M., 2016. Role of Angiotensin II in Cardiovascular Disease — Therapeutic Implications of More Than a Century of Research: Journal of the Renin-AngiotensinAldosterone System. https://doi.org/10.3317/jraas.2006.003

Fetahu, I.S., Höbaus, J., Kállay, E., 2014. Vitamin D and the epigenome. Front. Physiol. 5. https://doi.org/10.3389/fphys.2014.00164

Forman, J.P., Scott, J.B., Ng, K., Drake, B.F., Suarez, E.G., Hayden, D.L., Bennett, G.G., Chandler, P.D., Hollis, B.W., Emmons, K.M., Giovannucci, E.L., Fuchs, C.S., Chan, A.T., 2013. Effect of Vitamin D Supplementation on Blood Pressure in Blacks. Hypertension 61, 779–785. https://doi.org/10.1161/HYPERTENSIONAHA.111.00659

Fountain, J.H., Lappin, S.L., 2019. Physiology, Renin Angiotensin System, in: StatPearls. StatPearls Publishing, Treasure Island (FL).

Fraser, D.R., 1980. Regulation of the metabolism of vitamin D. Physiological Reviews 60, 551–613. https://doi.org/10.1152/physrev.1980.60.2.551

Frommer, M., McDonald, L.E., Millar, D.S., Collis, C.M., Watt, F., Grigg, G.W., Molloy, P.L., Paul, C.L., 1992. A genomic sequencing protocol that yields a positive display of 5-methylcytosine residues in individual DNA strands. Proc Natl Acad Sci U S A 89, 1827–1831.

Fuchs, S., Germain, S., Philippe, J., Corvol, P., Pinet, F., 2002. Expression of Renin in Large Arteries Outside the Kidney Revealed by Human Renin Promoter/LacZ Transgenic Mouse. The American Journal of Pathology 161, 717–725. https://doi.org/10.1016/S00029440(10)64227-7

Gasperini, M., Tome, J.M., Shendure, J., 2020. Towards a comprehensive catalogue of validated and target-linked human enhancers. Nature Reviews Genetics 1–19. https://doi.org/10.1038/s41576-019-0209-0

Germain, S., Bonnet, F., Philippe, J., Fuchs, S., Corvol, P., Pinet, F., 1998. A Novel Distal Enhancer Confers Chorionic Expression on the Human Renin Gene. J. Biol. Chem. 273, 25292–25300. https://doi.org/10.1074/jbc.273.39.25292

Glenn, S.T., Jones, C.A., Gross, K.W., Pan, L., 2013. Control of Renin Gene Expression. Pflugers Arch 465, 13–21. https://doi.org/10.1007/s00424-012-1110-2

Gómez-Olivé, F.X., Ali, S.A., Made, F., Kyobutungi, C., Nonterah, E., Micklesfield, L., Alberts, M., Boua, R., Hazelhurst, S., Debpuur, C., Mashinya, F., Dikotope, S., Sorgho, H., Cook, I., Muthuri, S., Soo, C., Mukomana, F., Agongo, G., Wandabwa, C., Afolabi, S., Oduro, A., Tinto, H., Wagner, R.G., Haregu, T., Wade, A., Kahn, K., Norris, S.A., Crowther, N.J., Tollman, S., Sankoh, O., Ramsay, M., AWI-Gen and the H3Africa Consortium, 2017. Regional and Sex Differences in the Prevalence and Awareness of Hypertension: An H3Africa AWI-Gen Study Across 6 Sites in Sub-Saharan Africa. Glob Heart 12, 81–90. https://doi.org/10.1016/j.gheart.2017.01.007

Gourgari, E., Dabelea, D., Rother, K., 2017. Modifiable Risk Factors for Cardiovascular Disease in Children with Type 1 Diabetes: Can Early Intervention Prevent Future Cardiovascular Events? Curr Diab Rep 17. https://doi.org/10.1007/s11892-017-0968-y

Govender, D., Damjanovic, L., Gaza, C.A., Meyer, V., 2021. Vitamin D decreases silencer methylation to downregulate renin gene expression. Gene 786, 145623. https://doi.org/10.1016/j.gene.2021.145623

Green, M.R., Sambrook, J., 2016. Precipitation of DNA with Ethanol. Cold Spring Harb Protoc 2016, pdb.prot093377. https://doi.org/10.1101/pdb.prot093377

Grosser, C., Wagner, N., Grothaus, K., Horsthemke, B., 2015. Altering TET dioxygenase levels within physiological range affects DNA methylation dynamics of HEK293 cells. Epigenetics 10, 819–833. https://doi.org/10.1080/15592294.2015.1073879

Grubert, F., Zaugg, J.B., Kasowski, M., Ursu, O., Spacek, D.V., Martin, A.R., Greenside, P., Srivas, R., Phanstiel, D.H., Pekowska, A., Heidari, N., Euskirchen, G., Huber, W., Pritchard, J.K., Bustamante, C.D., Steinmetz, L.M., Kundaje, A., Snyder, M., 2015. Genetic Control of Chromatin States in Humans Involves Local and Distal Chromosomal Interactions. Cell 162, 1051–1065. https://doi.org/10.1016/j.cell.2015.07.048

Guo, J.U., Su, Y., Zhong, C., Ming, G., Song, H., 2011. Hydroxylation of 5-Methylcytosine by TET1 Promotes Active DNA Demethylation in the Adult Brain. Cell 145, 423–434. https://doi.org/10.1016/j.cell.2011.03.022

Hannon, G.J., 2002. RNA interference. Nature 418, 244–251. https://doi.org/10.1038/418244a

Hark, A.T., Schoenherr, C.J., Katz, D.J., Ingram, R.S., Levorse, J.M., Tilghman, S.M., 2000. CTCF mediates methylation-sensitive enhancer-blocking activity at the H19/Igf2 locus. Nature 405, 486–489. https://doi.org/10.1038/35013106

Hatefi, Y., Hanstein, W.G., 1974. [77] Destabilization of membranes with chaotropic ions, in: Methods in Enzymology, Biomembranes Part A. Academic Press, pp. 770–790. https://doi.org/10.1016/0076-6879(74)31080-4

Héberlé, É., Bardet, A.F., 2019a. Sensitivity of transcription factors to DNA methylation. Essays Biochem 63, 727–741. https://doi.org/10.1042/EBC20190033

Herman, J.G., Baylin, S.B., 2003. Gene Silencing in Cancer in Association with Promoter Hypermethylation. N Engl J Med 349, 2042–2054. https://doi.org/10.1056/NEJMra023075

Hollenberg, N.K., 2001. A genome-wide search for susceptibility loci to human essential hypertension. Curr Hypertens Rep 3, 7–8.

Holmes, K., Williams, C.M., Chapman, E.A., Cross, M.J., 2010. Detection of siRNA induced mRNA silencing by RT-qPCR: considerations for experimental design. BMC Res Notes 3, 53. https://doi.org/10.1186/1756-0500-3-53

Hon, G.C., Song, C.X., Du, T., Jin, F., Selvaraj, S., Lee, A.Y., Yen, C.-A., Ye, Z., Mao, S.Q., Wang, B.A., Kuan, S., Edsall, L.E., Zhao, B.S., Xu, G.L., He, C., Ren, B., 2014. 5mC oxidation by Tet2 modulates enhancer activity and timing of transcriptome reprogramming during differentiation. Mol Cell 56, 286–297. https://doi.org/10.1016/j.molcel.2014.08.026

Imbeaud, S., Graudens, E., Boulanger, V., Barlet, X., Zaborski, P., Eveno, E., Mueller, O., Schroeder, A., Auffray, C., 2005. Towards standardization of RNA quality assessment using user-independent classifiers of microcapillary electrophoresis traces. Nucleic Acids Res 33, e56. https://doi.org/10.1093/nar/gni054

Issa, L.L., Leong, G.M., Eisman, J.A., 1998. Molecular mechanism of vitamin D receptor action. Inflamm. res. 47, 451–475. https://doi.org/10.1007/s000110050360

Jacobsen, L.B., Calvin, S.A., Lobenhofer, E.K., 2009. Transcriptional effects of transfection: the potential for misinterpretation of gene expression data generated from transiently transfected cells. BioTechniques 47, 617–624. https://doi.org/10.2144/000113132

JC Fleet, PL Kovalenko, Y Li, J Smolinski, C Spees, JG Yu, JM Thomas-Ahner, M Cui, A Neme, C Carlberg, 2019. Vitamin D signaling suppresses early prostate carcinogenesis in TgAPT121 mice. Cancer Prevention Research 12, 343–356.

Jeziorska, D.M., Murray, R.J.S., Gobbi, M.D., Gaentzsch, R., Garrick, D., Ayyub, H., Chen, T., Li, E., Telenius, J., Lynch, M., Graham, B., Smith, A.J.H., Lund, J.N., Hughes, J.R., Higgs, D.R., Tufarelli, C., 2017. DNA methylation of intragenic CpG islands depends on their transcriptional activity during differentiation and disease. PNAS 114, E7526–E7535. https://doi.org/10.1073/pnas.1703087114

Jones, G., Vriezen, D., Lohnes, D., Palda, V., Edwards, N.S., 1987. Side-chain hydroxylation of vitamin D3 and its physiological implications. Steroids 49, 29–53. https://doi.org/10.1016/0039-128X(87)90078-X

Judd, S.E., Nanes, M.S., Ziegler, T.R., Wilson, P.W.F., Tangpricha, V., 2008. Optimal vitamin D status attenuates the age-associated increase in systolic blood pressure in white Americans: results from the third National Health and Nutrition Examination Survey. Am J Clin Nutr 87, 136–141. https://doi.org/10.1093/ajcn/87.1.136

Kazmi, N., Elliott, H.R., Burrows, K., Tillin, T., Hughes, A.D., Chaturvedi, N., Gaunt, T.R., Relton, C.L., 2020. Associations between high blood pressure and DNA methylation. PLOS ONE 15, e0227728. https://doi.org/10.1371/journal.pone.0227728

Kearney, P.M., Whelton, M., Reynolds, K., Muntner, P., Whelton, P.K., He, J., 2005. Global burden of hypertension: analysis of worldwide data. The Lancet 365, 217–223. https://doi.org/10.1016/S0140-6736(05)17741-1

Khan, A., Fornes, O., Stigliani, A., Gheorghe, M., Castro-Mondragon, J.A., van der Lee, R., Bessy, A., Chèneby, J., Kulkarni, S.R., Tan, G., Baranasic, D., Arenillas, D.J., Sandelin, A., Vandepoele, K., Lenhard, B., Ballester, B., Wasserman, W.W., Parcy, F., Mathelier, A., 2018. JASPAR 2018: update of the open-access database of transcription factor binding profiles and its web framework. Nucleic Acids Research 46, D260–D266. https://doi.org/10.1093/nar/gkx1126

Kheiri, B., Abdalla, A., Osman, M., Ahmed, S., Hassan, M., Bachuwa, G., 2018. Vitamin D deficiency and risk of cardiovascular diseases: a narrative review. Clinical Hypertension 24, 9. https://doi.org/10.1186/s40885-018-0094-4

Kim, J., Kollhoff, A., Bergmann, A., Stubbs, L., 2003. Methylation-sensitive binding of transcription factor YY1 to an insulator sequence within the paternally expressed imprinted gene, Peg3. Human Molecular Genetics. https://doi.org/10.1093/hmg/ddg028

Knight, B.S., Sunn, N., Pennell, C.E., Adamson, S.L., Lye, S.J., 2009. Developmental regulation of cardiovascular function is dependent on both genotype and environment. American Journal of Physiology-Heart and Circulatory Physiology 297, H2234–H2241. https://doi.org/10.1152/ajpheart.01338.2008

Kumar, R., 1984. Metabolism of 1,25-dihydroxyvitamin D3. Physiological Reviews 64, 478–504. https://doi.org/10.1152/physrev.1984.64.2.478

Kunutsor, S.K., Apekey, T.A., Steur, M., 2013. Vitamin D and risk of future hypertension: metaanalysis of 283,537 participants. Eur J Epidemiol 28, 205–221. https://doi.org/10.1007/s10654-013-9790-2

Lai, G.-R., Lee, Y.-F., Yan, S.-J., Ting, H.-J., 2020. Active vitamin D induces gene-specific hypomethylation in prostate cancer cells developing vitamin D resistance. American Journal of Physiology-Cell Physiology 318, C836–C847. https://doi.org/10.1152/ajpcell.00522.2019

Lang, J.A., Ying, L.H., Morris, B.J., Sigmund, C.D., 1996. Transcriptional and posttranscriptional mechanisms regulate human renin gene expression in Calu-6 cells. Am. J. Physiol. 271, F94100. https://doi.org/10.1152/ajprenal.1996.271.1.F94

Lanier, L.L., Warner, N.L., 1981. Paraformaldehyde fixation of hematopoietic cells for quantitative flow cytometry (FACS) analysis. Journal of Immunological Methods 47, 25–30. https://doi.org/10.1016/0022-1759(81)90253-2

Lee, S.-M., Lee, J., Noh, K.-M., Choi, W.-Y., Jeon, S., Oh, G.T., Kim-Ha, J., Jin, Y., Cho, S.-W., Kim, Y.-J., 2017. Intragenic CpG islands play important roles in bivalent chromatin assembly of developmental genes. PNAS 114, E1885–E1894. https://doi.org/10.1073/pnas.1613300114

Legarth, C.; Grimm, D.; Krüger, M.; Infanger, M.; Wehland, M. Potential Beneficial Effects of Vitamin D in Coronary Artery Disease. *Nutrients* **2020**, *12*, 99. https://doi.org/10.3390/nu12010099

Lerman, L.O., Kurtz, T.W., Touyz, R.M., Ellison, D.H., Chade, A.R., Crowley, S.D., Mattson, D.L., Mullins, J.J., Osborn, J., Eirin, A., Reckelhoff, J.F., Iadecola, C., Coffman, T.M., 2019. Animal Models of Hypertension: A Scientific Statement From the American Heart Association. Hypertension (Dallas, Tex. : 1979). https://doi.org/10.1161/HYP.0000000000000090

Levine, M., Cattoglio, C., Tjian, R., 2014. Looping back to leap forward: Transcription enters a new era. Cell. https://doi.org/10.1016/j.cell.2014.02.009

Lewis, E.J., Hunsicker, L.G., Bain, R.P., Rohde, R.D., 1993. The Effect of AngiotensinConverting-Enzyme Inhibition on Diabetic Nephropathy. New England Journal of Medicine 329, 1456–1462. https://doi.org/10.1056/NEJM199311113292004

Li, M.-P., Hu, Y.-D., Hu, X.-L., Zhang, Y.-J., Yang, Y.-L., Jiang, C., Tang, J., Chen, X.-P., 2016. MiRNAs and miRNA Polymorphisms Modify Drug Response. International Journal of Environmental Research and Public Health 13, 1096. https://doi.org/10.3390/ijerph13111096

Li, Y., Tollefsbol, T.O., 2011. DNA methylation detection: Bisulfite genomic sequencing analysis. Methods Mol Biol 791, 11–21. https://doi.org/10.1007/978-1-61779-316-5_2

Li, Y.C., Kong, J., Wei, M., Chen, Z.-F., Liu, S.Q., Cao, L.-P., 2002. 1,25-Dihydroxyvitamin D3 is a negative endocrine regulator of the renin-angiotensin system. Journal of Clinical Investigation 110, 229–238. https://doi.org/10.1172/jci15219

Li, Z., Cai, X., Cai, C.-L., Wang, J., Zhang, W., Petersen, B.E., Yang, F.-C., Xu, M., 2011. Deletion of Tet2 in mice leads to dysregulated hematopoietic stem cells and subsequent development of myeloid malignancies. Blood 118, 4509–4518. https://doi.org/10.1182/blood-2010-12325241

Lieberman-Aiden, E., van Berkum, N.L., Williams, L., Imakaev, M., Ragoczy, T., Telling, A., Amit, I., Lajoie, B.R., Sabo, P.J., Dorschner, M.O., Sandstrom, R., Bernstein, B., Bender, M.A., Groudine, M., Gnirke, A., Stamatoyannopoulos, J., Mirny, L.A., Lander, E.S., Dekker, J., 2009.

Comprehensive mapping of long range interactions reveals folding principles of the human genome. Science 326, 289–293. https://doi.org/10.1126/science.1181369

Lincoln, C.K., Gabridge, M.G., 1998. Cell culture contamination: sources, consequences, prevention, and elimination. Methods Cell Biol 57, 49–65. https://doi.org/10.1016/s0091679x(08)61571-x

Liu, P.T., Stenger, S., Li, H., Wenzel, L., Tan, B.H., Krutzik, S.R., Ochoa, M.T., Schauber, J., Wu, K., Meinken, C., Kamen, D.L., Wagner, M., Bals, R., Steinmeyer, A., Zügel, U., Gallo, R.L., Eisenberg, D., Hewison, M., Hollis, B.W., Adams, J.S., Bloom, B.R., Modlin, R.L., 2006. Toll-like receptor triggering of a vitamin D-mediated human antimicrobial response. Science 311, 1770–1773. https://doi.org/10.1126/science.1123933

Livak, K.J., Schmittgen, T.D., 2001. Analysis of Relative Gene Expression Data Using Real-Time Quantitative PCR and the 2−ΔΔCT Method. Methods 25, 402–408. https://doi.org/10.1006/meth.2001.1262

Lois Y. Matsuoka, Lorraine Ide, Jacobo Wortsman, Julia A. Maclaughlin, Michael F. Holick, Sunscreens Suppress Cutaneous Vitamin D_3 Synthesis, *The Journal of Clinical Endocrinology & Metabolism*, Volume 64, Issue 6, 1 June 1987, Pages 1165–1168, https://doi.org/10.1210/jcem-64-6-1165

Lonn E M, Yusuf S, Jha P, Montague T J, Teo K K, Benedict C R, Pitt B, 1994. Emerging role of angiotensin-converting enzyme inhibitors in cardiac and vascular protection. Circulation 90, 2056–2069. https://doi.org/10.1161/01.CIR.90.4.2056

Lu, F., Liu, Y., Jiang, L., Yamaguchi, S., Zhang, Y., 2014. Role of Tet proteins in enhancer activity and telomere elongation. Genes Dev 28, 2103–2119. https://doi.org/10.1101/gad.248005.114

Mahé, E.A., Madigou, T., Sérandour, A.A., Bizot, M., Avner, S., Chalmel, F., Palierne, G., Métivier, R., Salbert, G., 2017. Cytosine modifications modulate the chromatin architecture of transcriptional enhancers. Genome Res 27, 947–958. https://doi.org/10.1101/gr.211466.116

Makin, G., Lohnes, D., Byford, V., Ray, R., Jones, G., 1989. Target cell metabolism of 1,25dihydroxyvitamin D3 to calcitroic acid. Evidence for a pathway in kidney and bone involving 24-oxidation. Biochemical Journal 262, 173–180. https://doi.org/10.1042/bj2620173

Malluche, H.H., Mawad, H., Koszewski, N.J., 2002. Update on vitamin D and its newer analogues: Actions and rationale for treatment in chronic renal failure. Kidney International 62, 367–374. https://doi.org/10.1046/j.1523-1755.2002.00450.x

Mardis, E., McCombie, W.R., 2017. Library Quantification: Fluorometric Quantitation of Double-Stranded or Single-Stranded DNA Samples Using the Qubit System. Cold Spring Harb Protoc 2017, pdb.prot094730. https://doi.org/10.1101/pdb.prot094730

Martinez, M.F., Martini, A.G., Sequeira-Lopez, M.L.S., Gomez, R.A., 2020. Ctcf is required for renin expression and maintenance of the structural integrity of the kidney. Clinical science (London, England : 1979) 134, 1763–1774. https://doi.org/10.1042/CS20200184

Martinez, R., Soliz, P., Mujica, O.J., Reveiz, L., Campbell, N.R. and Ordunez, P., 2020. The slowdown in the reduction rate of premature mortality from cardiovascular diseases puts the Americas at risk of achieving SDG 3.4: A population trend analysis of 37 countries from 1990 to 2017. *The Journal of Clinical Hypertension*, *22*(8), pp.1296-1309.

Maurano, M.T., Wang, H., John, S., Shafer, A., Canfield, T., Lee, K., Stamatoyannopoulos, J.A., 2015. Role of DNA Methylation in Modulating Transcription Factor Occupancy. Cell Reports 12, 1184–1195. https://doi.org/10.1016/j.celrep.2015.07.024

Meyer, Goetsch, Pike, 2012. VDR/RXR and TCF4/beta-catenin cistromes in colonic cells of colorectal tumor origin: impact on c-FOS and c-MYC gene expression. Molecular Endocrinology 26, 37–51.

McKinnon, K.M., 2018. Flow Cytometry: An Overview. Curr Protoc Immunol 120, 5.1.1-5.1.11. https://doi.org/10.1002/cpim.40

Melzak, K.A., Sherwood, C.S., Turner, R.F.B., Haynes, C.A., 1996. Driving Forces for DNA Adsorption to Silica in Perchlorate Solutions. Journal of Colloid and Interface Science 181, 635–644. https://doi.org/10.1006/jcis.1996.0421

Meyer, V., Saccone, D.S., Tugizimana, F., Asani, F.F., Jeffery, T.J., Bornman, L., 2017. Methylation of the Vitamin D Receptor (VDR) Gene, Together with Genetic Variation, Race, and Environment Influence the Signaling Efficacy of the Toll-Like Receptor 2/1-VDR Pathway. Front Immunol 8. https://doi.org/10.3389/fimmu.2017.01048

Mikeska, T., Dobrovic, A., 2009. Validation of a primer optimisation matrix to improve the performance of reverse transcription – quantitative real-time PCR assays. BMC Research Notes 2, 112. https://doi.org/10.1186/1756-0500-2-112

Mills, K. T., Stefanescu, A., & He, J. (2020). The global epidemiology of hypertension. Nature reviews. Nephrology, *16*(4), 223–237. https://doi.org/10.1038/s41581-019-0244-2

Miranda, T.B., Jones, P.A., 2007. DNA methylation: the nuts and bolts of repression. J. Cell. Physiol. 213, 384–390. https://doi.org/10.1002/jcp.21224

Moore, L.D., Le, T., Fan, G., 2013. DNA Methylation and Its Basic Function. Neuropsychopharmacol 38, 23–38. https://doi.org/10.1038/npp.2012.112

Norman, A.W., 2006. Minireview: vitamin D receptor: new assignments for an already busy receptor. Endocrinology 147, 5542–5548.

Nurminen, V., Neme, A., Seuter, S., Carlberg, C., 2018. The impact of the vitamin D-modulated epigenome on VDR target gene regulation. Biochimica et Biophysica Acta (BBA) - Gene Regulatory Mechanisms 1861, 697–705. https://doi.org/10.1016/j.bbagrm.2018.05.006

Odom, D.T., Dowell, R.D., Jacobsen, E.S., Gordon, W., Danford, T.W., MacIsaac, K.D., Rolfe, P.A., Conboy, C.M., Gifford, D.K., Fraenkel, E., 2007. Tissue-specific transcriptional regulation has diverged significantly between human and mouse. Nature Genetics 39, 730–732. https://doi.org/10.1038/ng2047

Ohyama, Y., Ozono, K., Uchida, M., Yoshimura, M., Shinki, T., Suda, T., Yamamoto, O., 1996. Functional Assessment of Two Vitamin D-responsive Elements in the Rat 25-Hydroxyvitamin D3 24-Hydroxylase Gene*. Journal of Biological Chemistry 271, 30381–30385. https://doi.org/10.1074/jbc.271.48.30381

O'Keefe, E.P., 2021. siRNAs and shRNAs: Tools for Protein Knockdown by Gene Silencing. Materials and Methods.

P Tuoresmäki, S Väisänen, A Neme, S Heikkinen, C Carlberg, 2014. Patterns of genome-wide VDR locations. PLoS ONE 9, e96105.

Pan Li, Gross Kenneth W., 2005. Transcriptional Regulation of Renin. Hypertension 45, 3–8. https://doi.org/10.1161/01.HYP.0000149717.55920.45

Patel, R.S., Masi, S., Taddei, S., 2017. Understanding the role of genetics in hypertension. European Heart Journal 38, 2309–2312. https://doi.org/10.1093/eurheartj/ehx273

Penefsky, H.S., Tzagoloff, A., 1971. [19] Extraction of water-soluble enzymes and proteins from membranes, in: Methods in Enzymology, Enzyme Purification and Related Techniques. Academic Press, pp. 204–219. https://doi.org/10.1016/0076-6879(71)22021-8

Petronis, A., 2010. Epigenetics as a unifying principle in the aetiology of complex traits and diseases. Nature 465, 721–727. https://doi.org/10.1038/nature09230

Petrovic, N., Black, T.A., Fabian, J.R., Kane, C., Jones, C.A., Loudon, J.A., Abonia, J.P., Sigmund, C.D., Gross, K.W., 1996. Role of Proximal Promoter Elements in Regulation of Renin Gene Transcription. J. Biol. Chem. 271, 22499–22505. https://doi.org/10.1074/jbc.271.37.22499

Phillips, J.E., Corces, V.G., 2009. CTCF: Master Weaver of the Genome. Cell. https://doi.org/10.1016/j.cell.2009.06.001

Pilz, S., Tomaschitz, A., Ritz, E., Pieber, T.R., 2009. Vitamin D status and arterial hypertension: a systematic review. Nature Reviews Cardiology 6, 621–630. https://doi.org/10.1038/nrcardio.2009.135

Pittas, A.G., Chung, M., Trikalinos, T., Mitri, J., Brendel, M., Patel, K., Lichtenstein, A.H., Lau, J., Balk, E.M., 2010. Systematic Review: Vitamin D and Cardiometabolic Outcomes. Ann Intern Med 152, 307–314. https://doi.org/10.7326/0003-4819-152-5-201003020-00009

Plum, L.A., DeLuca, H.F., 2010. Vitamin D, disease and therapeutic opportunities. Nature Reviews Drug Discovery 9, 941–955. https://doi.org/10.1038/nrd3318

Pombo, A., Dillon, N., 2015. Three-dimensional genome architecture: players and mechanisms. Nat Rev Mol Cell Biol 16, 245–257. https://doi.org/10.1038/nrm3965

Portela, A., Esteller, M., 2010. Epigenetic modifications and human disease. Nat Biotechnol 28, 1057–1068. https://doi.org/10.1038/nbt.1685

Quandt K, Frech K, Karas H, Wingender E, Werner T (1995) MatInd and MatInspector: new fast and versatile tools for detection of consensus matches in nucleotide sequence data. Nucleic Acids Res. 23, 4878-84

Raines, R.T., 1998. Ribonuclease a. Chemical reviews 98, 1045–1066.

Rashid, M., Coombs, K.M., 2019. Serum-reduced media impacts on cell viability and protein expression in human lung epithelial cells. J Cell Physiol 234, 7718–7724. https://doi.org/10.1002/jcp.27890

Rasmussen, K.D., Berest, I., Keβler, S., Nishimura, K., Simón-Carrasco, L., Vassiliou, G.S., Pedersen, M.T., Christensen, J., Zaugg, J.B., Helin, K., 2019. TET2 binding to enhancers facilitates transcription factor recruitment in hematopoietic cells. Genome Res 29, 564–575. https://doi.org/10.1101/gr.239277.118

Razin, S., Yogev, D., Naot, Y., 1998. Molecular Biology and Pathogenicity of Mycoplasmas. Microbiol Mol Biol Rev 62, 1094–1156.

Resnick, L.M., 1994. Calciotropic hormones in salt-sensitive essential hypertension: 1,25dihydroxyvitamin D and parathyroid hypertensive factor. J Hypertens Suppl 12, S3-9.

Resnick, L.M., 1986. Calcium-Regulating Hormones in Essential Hypertension: Relation to Plasma Renin Activity and Sodium Metabolism. Ann Intern Med 105, 649. https://doi.org/10.7326/0003-4819-105-5-649

Rhein, M., Hagemeier, L., Klintschar, M., Muschler, M., Bleich, S., Frieling, H., 2015. DNA methylation results depend on DNA integrity – role of post mortem interval. Frontiers in Genetics 6, 182. https://doi.org/10.3389/fgene.2015.00182

Robinson, R.F., Batisky, D.L., Hayes, J.R., Nahata, M.C., Mahan, J.D., 2005. Significance of Heritability in Primary and Secondary Pediatric Hypertension. Am J Hypertens 18, 917–921. https://doi.org/10.1016/j.amjhyper.2005.01.010

Rostand, S.G., 1997. Ultraviolet light may contribute to geographic and racial blood pressure differences. Hypertension 30, 150–156. https://doi.org/10.1161/01.hyp.30.2.150

Rottem, S., Barile, M.F., 1993. Beware of mycoplasmas. Trends in Biotechnology 11, 143–151. https://doi.org/10.1016/0167-7799(93)90089-R

S Heikkinen, S Väisänen, P Pehkonen, S Seuter, V Benes, C Carlberg, 2011. Nuclear hormone 1α,25-dihydroxyvitamin D3 elicits a genome-wide shift in the locations of VDR chromatin occupancy. Nucleic Acids Research 39, 9181–9193.

Sati, S., Cavalli, G., 2017. Chromosome conformation capture technologies and their impact in understanding genome function. Chromosoma 126, 33–44. https://doi.org/10.1007/s00412-016-0593-6

Saxonov, S., Berg, P., Brutlag, D.L., 2006. A genome-wide analysis of CpG dinucleotides in the human genome distinguishes two distinct classes of promoters. Proc. Natl. Acad. Sci. U.S.A. 103, 1412–1417. https://doi.org/10.1073/pnas.0510310103

Scourzic, L., Mouly, E., Bernard, O.A., 2015. TET proteins and the control of cytosine demethylation in cancer. Genome Med 7, 9. https://doi.org/10.1186/s13073-015-0134-6

Scragg, R., Sowers, M., Bell, C., 2007. Serum 25-hydroxyvitamin D, ethnicity, and blood pressure in the Third National Health and Nutrition Examination Survey. Am. J. Hypertens. 20, 713–719. https://doi.org/10.1016/j.amjhyper.2007.01.017

Seuter, S., Pehkonen, P., Heikkinen, S., Carlberg, C., 2013. Dynamics of 1α,25dihydroxyvitamin D3-dependent chromatin accessibility of early vitamin D receptor target genes. Biochimica et Biophysica Acta (BBA) - Gene Regulatory Mechanisms 1829, 1266–1275. https://doi.org/10.1016/j.bbagrm.2013.10.003

Sigmund, C.D., Okuyama, K., Ingelfinger, J., Jones, C.A., Mullins, J.J., Kane, C., Kim, U., Wu, C.Z., Kenny, L., Rustum, Y., 1990. Isolation and characterization of renin-expressing cell lines from transgenic mice containing a renin-promoter viral oncogene fusion construct. J. Biol. Chem. 265, 19916–19922.

Singal, R., Ginder, G.D., 1999. DNA methylation. Blood 93, 4059–4070.

Southgate, L., Machado, R.D., Gräf, S., Morrell, N.W., 2020. Molecular genetic framework underlying pulmonary arterial hypertension. Nature Reviews Cardiology 17, 85–95. https://doi.org/10.1038/s41569-019-0242-x

Steckelings, U.M., Rompe, F., Kaschina, E., Unger, T., 2009. The evolving story of the RAAS in hypertension, diabetes and CV disease – moving from macrovascular to microvascular targets. Fundamental & Clinical Pharmacology 23, 693–703. https://doi.org/10.1111/j.14728206.2009.00780.x

Stoll, S., Wang, C., Qiu, H., 2018. DNA Methylation and Histone Modification in Hypertension. Int J Mol Sci 19. https://doi.org/10.3390/ijms19041174

Tabacova, S., Little, R., Tsong, Y., Vega, A., Kimmel, C.A., 2003. Adverse pregnancy outcomes associated with maternal enalapril antihypertensive treatment. Pharmacoepidemiology and Drug Safety 12, 633–646. https://doi.org/10.1002/pds.796

The International Consortium of Blood Pressure (ICBP) 1000G Analyses, The CHD Exome+ Consortium, The ExomeBP Consortium, The T2D-GENES Consortium, The GoT2DGenes Consortium, The Cohorts for Heart and Ageing Research in Genome Epidemiology (CHARGE) BP Exome Consortium, The International Genomics of Blood Pressure (iGEN-BP) Consortium, The UK Biobank CardioMetabolic Consortium BP working group, Warren, H.R., Evangelou, E., Cabrera, C.P., Gao, H., Ren, M., Mifsud, B., Ntalla, I., Surendran, P., Liu, C., Cook, J.P., Kraja, A.T., Drenos, F., Loh, M., Verweij, N., Marten, J., Karaman, I., Lepe, M.P.S., O'Reilly, P.F., Knight, J., Snieder, H., Kato, N., He, J., Tai, E.S., Said, M.A., Porteous, D., Alver, M., Poulter, N.,

Farrall, M., Gansevoort, R.T., Padmanabhan, S., Mägi, R., Stanton, A., Connell, J., Bakker, S.J.L., Metspalu, A., Shields, D.C., Thom, S., Brown, M., Sever, P., Esko, T., Hayward, C., van der Harst, P., Saleheen, D., Chowdhury, R., Chambers, J.C., Chasman, D.I., Chakravarti, A., Newton-Cheh, C., Lindgren, C.M., Levy, D., Kooner, J.S., Keavney, B., Tomaszewski, M., Samani, N.J., Howson, J.M.M., Tobin, M.D., Munroe, P.B., Ehret, G.B., Wain, L.V., 2017. Genome-wide association analysis identifies novel blood pressure loci and offers biological insights into cardiovascular risk. Nat Genet 49, 403–415. https://doi.org/10.1038/ng.3768

Tobler, A., Miller, C.W., Norman, A.W., Koeffler, H.P., 1988. 1,25-Dihydroxyvitamin D3 modulates the expression of a lymphokine (granulocyte-macrophage colony-stimulating factor) posttranscriptionally. J Clin Invest 81, 1819–1823. https://doi.org/10.1172/JCI113525

Tomaschitz, A., Pilz, S., Ritz, E., Grammer, T., Drechsler, C., Boehm, B.O., März, W., 2010. Independent association between 1,25-dihydroxyvitamin D, 25-hydroxyvitamin D and the renin-angiotensin system: The Ludwigshafen Risk and Cardiovascular Health (LURIC) study. Clin Chim Acta 411, 1354–1360. https://doi.org/10.1016/j.cca.2010.05.037

Tripkovic, L., Lambert, H., Hart, K., Smith, C.P., Bucca, G., Penson, S., Chope, G., Hyppönen, E., Berry, J., Vieth, R., Lanham-New, S., 2012. Comparison of vitamin D2 and vitamin D3 supplementation in raising serum 25-hydroxyvitamin D status: a systematic review and metaanalysis. Am J Clin Nutr 95, 1357–1364. https://doi.org/10.3945/ajcn.111.031070

Untergasser A, Cutcutache I, Koressaar T, Ye J, Faircloth BC, Remm M and Rozen SG. Primer3 new capabilities and interfaces. Nucleic Acids Res. 2012 Aug 1;40(15):e115.

Ushiki, A., Matsuzaki, H., Fukamizu, A., Tanimoto, K., 2018. Homeostatic Response of Mouse renin Gene Transcription in a Hypertensive Environment Is Mediated by a Novel 5' Enhancer . Molecular and Cellular Biology 38. https://doi.org/10.1128/mcb.00566-17

Vaidya, A., Williams, J.S., 2012. The relationship between vitamin D and the renin-angiotensin system in the pathophysiology of hypertension, kidney disease, and diabetes. Metabolism 61, 450–458. https://doi.org/10.1016/j.metabol.2011.09.007

Vandesompele, J., De Preter, K., Pattyn, F., Poppe, B., Van Roy, N., De Paepe, A., Speleman, F., 2002. Accurate normalization of real-time quantitative RT-PCR data by geometric averaging of multiple internal control genes. Genome Biol 3, research0034.1research0034.11.

Vimaleswaran, K.S., Cavadino, A., Berry, D.J., Jorde, R., Dieffenbach, A.K., Lu, C., Alves, A.C., Heerspink, H.J.L., Tikkanen, E., Eriksson, J., Wong, A., Mangino, M., Jablonski, K.A., Nolte, I.M., Houston, D.K., Ahluwalia, T.S., van der Most, P.J., Pasko, D., Zgaga, L., Thiering, E., Vitart, V., Fraser, R.M., Huffman, J.E., de Boer, R.A., Schöttker, B., Saum, K.-U., McCarthy, M.I., Dupuis, J., Herzig, K.-H., Sebert, S., Pouta, A., Laitinen, J., Kleber, M.E., Navis, G., Lorentzon, M., Jameson, K., Arden, N., Cooper, J.A., Acharya, J., Hardy, R., Raitakari, O., Ripatti, S., Billings, L.K., Lahti, J., Osmond, C., Penninx, B.W., Rejnmark, L., Lohman, K.K., Paternoster, L., Stolk, R.P., Hernandez, D.G., Byberg, L., Hagström, E., Melhus, H., Ingelsson, E., Mellström, D., Ljunggren, Ö., Tzoulaki, I., McLachlan, S., Theodoratou, E., Tiesler, C.M.T., Jula, A., Navarro,

P., Wright, A.F., Polasek, O., Hayward, C., Wilson, J.F., Rudan, I., Salomaa, V., Heinrich, J., Campbell, H., Price, J.F., Karlsson, M., Lind, L., Michaëlsson, K., Bandinelli, S., Frayling, T.M., Hartman, C.A., Sørensen, T.I.A., Kritchevsky, S.B., Langdahl, B.L., Eriksson, J.G., Florez, J.C., Spector, T.D., Lehtimäki, T., Kuh, D., Humphries, S.E., Cooper, C., Ohlsson, C., März, W., de Borst, M.H., Kumari, M., Kivimaki, M., Wang, T.J., Power, C., Brenner, H., Grimnes, G., van der Harst, P., Snieder, H., Hingorani, A.D., Pilz, S., Whittaker, J.C., Järvelin, M.-R., Hyppönen, E., 2014. Association of vitamin D status with arterial blood pressure and hypertension risk: a mendelian randomisation study. Lancet Diabetes Endocrinol 2, 719–729. https://doi.org/10.1016/S2213-8587(14)70113-5

von Scheidt, M., Zhao, Y., Kurt, Z., Pan, C., Zeng, L., Yang, X., Schunkert, H., Lusis, A.J., 2017. Applications and Limitations of Mouse Models for Understanding Human Atherosclerosis. Cell Metabolism. https://doi.org/10.1016/j.cmet.2016.11.001

Wallenstein, E.J., Barminko, J., Schloss, R.S., Yarmush, M.L., 2010. Serum Starvation Improves Transient Transfection Efficiency in Differentiating Embryonic Stem Cells. Biotechnol Prog 26, 1714–1723. https://doi.org/10.1002/btpr.472

Wandai, M.E., Norris, S.A., Aagaard-Hansen, J., Manda, S.O., 2020. Geographical influence on the distribution of the prevalence of hypertension in South Africa : a multilevel analysis: research. Cardiovascular Journal of Africa 31, 47–54. https://doi.org/10.5830/CVJA-2019-047

Wang, L., Manson, J.E., Song, Y., Sesso, H.D., 2010. Systematic Review: Vitamin D and Calcium Supplementation in Prevention of Cardiovascular Events. Ann Intern Med 152, 315–323. https://doi.org/10.7326/0003-4819-152-5-201003020-00010

Wang, Y., Leung, F.C.C., 2004. An evaluation of new criteria for CpG islands in the human genome as gene markers. Bioinformatics 20, 1170–1177. https://doi.org/10.1093/bioinformatics/bth059

Warnecke, P.M., Stirzaker, C., Melki, J.R., Millar, D.S., Paul, C.L., Clark, S.J., 1997. Detection and measurement of PCR bias in quantitative methylation analysis of bisulfite-treated DNA. Nucleic Acids Res 25, 4422–4426.

Waterston, R.H., Lindblad-Toh, K., Birney, E., Rogers, J., Abril, J.F., Agarwal, P., Agarwala, R., Ainscough, R., Alexandersson, M., An, P., Antonarakis, S.E., Attwood, J., Baertsch, R., Bailey,

J., Barlow, K., Beck, S., Berry, E., Birren, B., Bloom, T., Bork, P., Botcherby, M., Bray, N., Brent, M.R., Brown, D.G., Brown, S.D., Bult, C., Burton, J., Butler, J., Campbell, R.D., Carninci, P., Cawley, S., Chiaromonte, F., Chinwalla, A.T., Church, D.M., Clamp, M., Clee, C., Collins, F.S., Cook, L.L., Copley, R.R., Coulson, A., Couronne, O., Cuff, J., Curwen, V., Cutts, T., Daly, M., David, R., Davies, J., Delehaunty, K.D., Deri, J., Dermitzakis, E.T., Dewey, C., Dickens, N.J., Diekhans, M., Dodge, S., Dubchak, I., Dunn, D.M., Eddy, S.R., Elnitski, L., Emes, R.D., Eswara, P., Eyras, E., Felsenfeld, A., Fewell, G.A., Flicek, P., Foley, K., Frankel, W.N., Fulton, L.A., Fulton, R.S., Furey, T.S., Gage, D., Gibbs, R.A., Glusman, G., Gnerre, S., Goldman, N., Goodstadt, L., Grafham, D., Graves, T.A., Green, E.D., Gregory, S., Guigó, R., Guyer, M., Hardison, R.C., Haussler, D., Hayashizaki, Y., LaHillier, D.W., Hinrichs, A., Hlavina, W., Holzer, T., Hsu, F., Hua,

A., Hubbard, T., Hunt, A., Jackson, I., Jaffe, D.B., Johnson, L.S., Jones, M., Jones, T.A., Joy, A., Kamal, M., Karlsson, E.K., Karolchik, D., Kasprzyk, A., Kawai, J., Keibler, E., Kells, C., Kent, W.J., Kirby, A., Kolbe, D.L., Korf, I., Kucherlapati, R.S., Kulbokas, E.J., Kulp, D., Landers, T., Leger, J.P., Leonard, S., Letunic, I., Levine, R., Li, J., Li, M., Lloyd, C., Lucas, S., Ma, B., Maglott, D.R., Mardis, E.R., Matthews, L., Mauceli, E., Mayer, J.H., McCarthy, M., McCombie, W.R., McLaren, S., McLay, K., McPherson, J.D., Meldrim, J., Meredith, B., Mesirov, J.P., Miller, W., Miner, T.L., Mongin, E., Montgomery, K.T., Morgan, M., Mott, R., Mullikin, J.C., Muzny, D.M., Nash, W.E., Nelson, J.O., Nhan, M.N., Nicol, R., Ning, Z., Nusbaum, C., O'Connor, M.J., Okazaki, Y., Oliver, K., Overton-Larty, E., Pachter, L., Parra, G., Pepin, K.H., Peterson, J., Pevzner, P., Plumb, R., Pohl, C.S., Poliakov, A., Ponce, T.C., Ponting, C.P., Potter, S., Quail, M., Reymond, A., Roe, B.A., Roskin, K.M., Rubin, E.M., Rust, A.G., Santos, R., Sapojnikov, V., Schultz, B., Schultz, J., Schwartz, M.S., Schwartz, S., Scott, C., Seaman, S., Searle, S., Sharpe, T., Sheridan, A., Shownkeen, R., Sims, S., Singer, J.B., Slater, G., Smit, A., Smith, D.R., Spencer, B., Stabenau, A., Stange-Thomann, N., Sugnet, C., Suyama, M., Tesler, G., Thompson, J., Torrents, D., Trevaskis, E., Tromp, J., Ucla, C., Ureta-Vidal, A., Vinson, J.P., von Niederhausern, A.C., Wade, C.M., Wall, M., Weber, R.J., Weiss, R.B., Wendl, M.C., West, A.P., Wetterstrand, K., Wheeler, R., Whelan, S., Wierzbowski, J., Willey, D., Williams, S., Wilson, R.K., Winter, E., Worley, K.C., Wyman, D., Yang, S., Yang, S.P., Zdobnov, E.M., Zody, M.C., Lander, E.S., 2002. Initial sequencing and comparative analysis of the mouse genome. Nature 420, 520–562. https://doi.org/10.1038/nature01262

Weeres, M.A., Robien, K., Ahn, Y.-O., Neulen, M.-L., Bergerson, R., Miller, J.S., Verneris, M.R., 2014. The Effects of 1,25 Dihydroxyvitamin D3 ($1,25(OH)_2D_3$) on In Vitro Human Natural Killer Cell DevelopmentFrom Hematopoietic Stem Cells. J Immunol 193, 3456–3462. https://doi.org/10.4049/jimmunol.1400698

West, A.G., Fraser, P., 2005. Remote control of gene transcription. Hum Mol Genet 14 Spec No 1, R101-111. https://doi.org/10.1093/hmg/ddi104

Witham, M.D., Nadir, M.A., Struthers, A.D., 2009. Effect of vitamin D on blood pressure: a systematic review and meta-analysis. Journal of Hypertension 27, 1948–1954. https://doi.org/10.1097/HJH.0b013e32832f075b

Wu, S.H., Ho, S.C., Zhong, L., 2010. Effects of vitamin D supplementation on blood pressure. South Med J 103, 729–737. https://doi.org/10.1097/SMJ.0b013e3181e6d389

Yadava, P., Gibbs, M., Castro, C., Hughes, J.A., 2007. Effect of Lyophilization and Freezethawing on the Stability of siRNA-liposome Complexes. AAPS PharmSciTech 9, 335–341. https://doi.org/10.1208/s12249-007-9000-1

Yamazaki, J., Jelinek, J., Lu, Y., Cesaroni, M., Madzo, J., Neumann, F., He, R., Taby, R., Vasanthakumar, A., Macrae, T., Ostler, K.R., Kantarjian, H.M., Liang, S., Estecio, M.R., Godley, L.A., Issa, J.-P.J., 2015. TET2 Mutations Affect Non-CpG Island DNA Methylation at Enhancers and Transcription Factor-Binding Sites in Chronic Myelomonocytic Leukemia. Cancer Res 75, 2833–2843. https://doi.org/10.1158/0008-5472.CAN-14-0739

Yan, W., Chen, D., Schumacher, J., Durantini, D., Engelhorn, J., Chen, M., Carles, C.C., Kaufmann, K., 2019. Dynamic control of enhancer activity drives stage-specific gene expression during flower morphogenesis. Nat Commun 10, 1705. https://doi.org/10.1038/s41467-019-09513-2

Yuan, W., Pan, W., Kong, J., Zheng, W., Szeto, F.L., Wong, K.E., Cohen, R., Klopot, A., Zhang, Z., Yan, C.L., 2007. 1,25-Dihydroxyvitamin D3 suppresses renin gene transcription by blocking the activity of the cyclic AMP response element in the renin gene promoter. Journal of Biological Chemistry 282, 29821–29830. https://doi.org/10.1074/jbc.M705495200

Yue, F., Cheng, Y., Breschi, A., Vierstra, J., Wu, W., Ryba, T., Sandstrom, R., Ma, Z., Davis, C., Pope, B.D., Shen, Y., Pervouchine, D.D., Djebali, S., Thurman, R.E., Kaul, R., Rynes, E., Kirilusha, A., Marinov, G.K., Williams, B.A., Trout, D., Amrhein, H., Fisher-Aylor, K., Antoshechkin, I., DeSalvo, G., See, L.H., Fastuca, M., Drenkow, J., Zaleski, C., Dobin, A., Prieto, P., Lagarde, J., Bussotti, G., Tanzer, A., Denas, O., Li, K., Bender, M.A., Zhang, M., Byron, R., Groudine, M.T., McCleary, D., Pham, L., Ye, Z., Kuan, S., Edsall, L., Wu, Y.C., Rasmussen, M.D., Bansal, M.S., Kellis, M., Keller, C.A., Morrissey, C.S., Mishra, T., Jain, D., Dogan, N., Harris, R.S., Cayting, P., Kawli, T., Boyle, A.P., Euskirchen, G., Kundaje, A., Lin, S., Lin, Y., Jansen, C., Malladi, V.S., Cline, M.S., Erickson, D.T., Kirkup, V.M., Learned, K., Sloan, C.A., Rosenbloom, K.R., De Sousa, B.L., Beal, K., Pignatelli, M., Flicek, P., Lian, J., Kahveci, T., Lee, D., Kent, W.J., Santos, M.R., Herrero, J., Notredame, C., Johnson, A., Vong, S., Lee, K., Bates, D., Neri, F., Diegel, M., Canfield, T., Sabo, P.J., Wilken, M.S., Reh, T.A., Giste, E., Shafer, A., Kutyavin, T., Haugen, E., Dunn, D., Reynolds, A.P., Neph, S., Humbert, R., Hansen, R.S., De Bruijn, M., Selleri, L., Rudensky, A., Josefowicz, S., Samstein, R., Eichler, E.E., Orkin, S.H., Levasseur, D., Papayannopoulou, T., Chang, K.H., Skoultchi, A., Gosh, S., Disteche, C., Treuting, P., Wang, Y., Weiss, M.J., Blobel, G.A., Cao, X., Zhong, S., Wang, T., Good, P.J., Lowdon, R.F., Adams, L.B., Zhou, X.Q., Pazin, M.J., Feingold, E.A., Wold, B., Taylor, J., Mortazavi, A., Weissman, S.M., Stamatoyannopoulos, J.A., Snyder, M.P., Guigo, R., Gingeras, T.R., Gilbert, D.M., Hardison, R.C., Beer, M.A., Ren, B., 2014. A comparative encyclopedia of DNA elements in the mouse genome. Nature 515, 355–364. https://doi.org/10.1038/nature13992

Zhang, H., Zhang, X., Clark, E., Mulcahey, M., Huang, S., Shi, Y.G., 2010. TET1 is a DNA-binding protein that modulates DNA methylation and gene transcription via hydroxylation of 5methylcytosine. Cell Res 20, 1390–1393. https://doi.org/10.1038/cr.2010.156

Zhang, Y., Li, S., Zhuo, F., Wang, H., Geng, X., Xu, B., Yin, L., Sun, H., Yan, X., 2021. Additive Effects of VDBP and 1,25$(OH)_2D_3$ on the Viability and Apoptosis of Rheumatoid Arthritis Synovial Fibroblasts. Frontiers in Endocrinology 11, 1090. https://doi.org/10.3389/fendo.2020.583229

Zhang, Y., Moran, A.E., 2017. Trends in the Prevalence, Awareness, Treatment, and Control of Hypertension Among Young Adults in the United States, 1999 to 2014. Hypertension 70, 736–742. https://doi.org/10.1161/HYPERTENSIONAHA.117.09801

Zheng, J., Rao, D.C., Shi, G., 2015. An update on genome-wide association studies of hypertension. Appl Inform 2, 10. https://doi.org/10.1186/s40535-015-0013-7

Zhou, Q., Gedrich, R.W., Engel, D.A., 1995. Transcriptional repression of the c-fos gene by YY1 is mediated by a direct interaction with ATF/CREB. Journal of virology 69, 4323–4330. https://doi.org/10.1128/jvi.69.7.4323-4330.1995

Zhou, X., Davis, D.R., Sigmund, C.D., 2006. The human renin kidney enhancer is required to maintain base-line renin expression but is dispensable for tissue-specific, cell-specific, and regulated expression. Journal of Biological Chemistry 281, 35296–35304. https://doi.org/10.1074/jbc.M608055200

Zhu, H., Wang, X., Shi, H., Su, S., Harshfield, G.A., Gutin, B., Snieder, H., Dong, Y., 2013. A Genome-Wide Methylation Study of Severe Vitamin D Deficiency in African American Adolescents. The Journal of Pediatrics 162, 1004-1009.e1. https://doi.org/10.1016/j.jpeds.2012.10.059

Zierold, C., Darwish, H.M., DeLuca, H.F., 1994. Identification of a vitamin D-response element in the rat calcidiol (25-hydroxyvitamin D3) 24-hydroxylase gene. PNAS 91, 900–902. https://doi.org/10.1073/pnas.91.3.900

Zittermann, A., Frisch, S., Berthold, H.K., Götting, C., Kuhn, J., Kleesiek, K., Stehle, P., Koertke, H. and Koerfer, R., 2009. Vitamin D supplementation enhances the beneficial effects of weight loss on cardiovascular disease risk markers. *The American journal of clinical nutrition*, *89*(5), pp.1321-1327.

Zwart, S.R., Parsons, H., Kimlin, M., Innis, S.M., Locke, J.P., Smith, S.M., 2013. A 250 μg/week dose of vitamin D was as effective as a 50 μg/d dose in healthy adults, but a regimen of four weekly followed by monthly doses of 1250 μg raised the risk of hypercalciuria. British Journal of Nutrition 110, 1866–1872. https://doi.org/10.1017/S000711451300113X

Web resources

Kennedy, S. (2021) *"How DNA Extraction Kits Work in the Lab."* Available at : https://bitesizebio.com/25018/how-dna-extraction-kits-work-in-the-lab/ (Acessessed: 5 September 2021)

Thermofisher (2022) "Factors Influencing Transfection Efficiency." Available at: https://www.thermofisher.com/za/en/home/references/gibco-cell-culture-basics/transfection-basics/factors-influencing-transfection-efficiency.html (Accessed: 21 February 2022).

World health organisation (2013) "*A Global Brief on Hypertension*". Available online: http://apps.who.int/iris/bitstream/10665/79059/1/WHO_DCO_WHD_2013.2_eng.p df (Accessed: 30 October 2021).

World health organisation (2021) Hypertension. "Key Facts." Available at: https://www.who.int/news-room/fact-sheets/detail/hypertension (Accessed : 16 June 2020)

World Health Organization (2018) Geneva Noncommunicable diseases country profiles 2018 Available from: https://www.who.int/publications/i/item/9789241514620 (Accessed on: 5 June 2022).